

**DETERMINATION OF WOUND ROLL STRUCTURE
USING ACOUSTIC TIME OF FLIGHT
MEASUREMENT**

By

RONALD P. SWANSON

Bachelor of Science

University of Nebraska

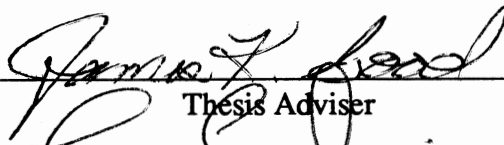
Lincoln, Nebraska

1985

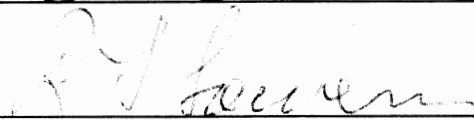
Submitted to the Faculty of the
Graduate School of the
Oklahoma State University
in partial fulfillment of
the requirements for
the Degree of
MASTER OF SCIENCE
December, 1991

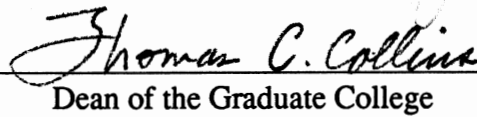
DETERMINATION OF WOUND ROLL STRUCTURE
USING ACOUSTIC TIME OF FLIGHT
MEASUREMENT

Thesis Approved:



Thesis Adviser





Dean of the Graduate College

ACKNOWLEDGMENTS

I would like to thank Dr. J. Keith Good and Dr. Richard Lowery for their guidance and assistance. I also would like to thank everyone involved with the Web Handling Research Center, which provided a unique opportunity to research this project and broaden my knowledge of web handling and engineering. I also would like to thank J. David Pfeiffer for initiating this work in 1966 and for his insights and assistance.

My special thanks go to my wife Deb, for her patience and understanding during my nine months of absence and, evenings and weekends of near absence doing coursework and preparing this thesis.

I also would like to express my thanks to 3M Company, especially my supervisor Yvonne Cadwallader and managers Robert Nelson and Shuzo Fuchigami who provided the opportunity and support required to complete this project.

TABLE OF CONTENTS

Chapter	Page
I. INTRODUCTION	1
II. LITERATURE SURVEY	3
III. WOUND ROLL STRUCTURE	6
Fundamentals	6
Present Measurement Methods	8
IV. STACK TESTS	11
Radial Modulus Stack Tests	11
Effect of Radial Pressure on Density	15
Theoretical Speed of Sound	16
Wave Generation	17
Speed of Sound Measurement	19
Wave Attenuation	25
Coupling	27
V. ACOUSTIC ROLL MEASUREMENTS	28
Wave Reception	28
Roll Time of Flight Measurement	29
Ray Theory and Cylindrical Geometry	31
VI. DETERMINATION OF ROLL STRUCTURE	32
Hakiel's Winding Model	33
The Hoop Stress Outer Boundary Condition	37
Roll Structure Algorithm	39
VII. VERIFICATION	44
FSR and Pull Tab Measurement	44
Wound Roll Test Results	45
VIII. RESULTS AND CONCLUSION	54
Future Research	54
Future Development	55

Chapter	Page
REFERENCES	56
APPENDICES	58
APPENDIX A - STACK TEST PROCEDURES	59
APPENDIX B - MATERIAL PROPERTY DATA	68
APPENDIX C - ACOUSTIC GAGE PROGRAM (LabVIEW 2)	70
APPENDIX D - ACOUSTIC GAGE PROGRAM (Quick BASIC)	88
APPENDIX E - WEB HANDLING CONFERENCE PAPER	106
APPENDIX F - WEB HANDLING CONFERENCE VISUALS	116

LIST OF TABLES

Table	Page
I. Wound Roll Test Results	47
II. Material Property Data	69

LIST OF FIGURES

Figure	Page
1. Roll Stress Equilibrium	7
2. Stress versus Strain for Linear Elastic Material (Steel)	12
3. Stress versus Strain for Non-Linear Material (Paper Stack)	12
4. Instron 8500 with Extensometer and PC for Data Collection	13
5. E_r vs. Radial Pressure with Polynomial Regression	14
6. Density vs. Radial Pressure for a PET Stack	15
7. Density vs. Radial Pressure for a Paper Stack	16
8. The Mechanical Pulser	19
9. Instron Setup for Time of Flight Measurements	20
10. Kynar Sensor with Leads Attached	20
11. High Frequency Attenuation with Time	21
12. Signals with High Frequency Attenuation	21
13. Signals from Two Closely Spaced Sensors	22
14. Cross-correlation of Signals in Figure 13	23
15. Actual vs. Theoretical Speed of Sound	23
16. Rho-c Impedance of PET vs. Radial Pressure	25
17. Attenuation Calculation	26
18. Time of Flight Fixture	29
19. Time of Flight Signals	30
20. Ray Focusing	31
21. Adding Hoop #1	35
22. Adding Hoop #2	36

Figure	Page
23. Adding Hoop #3	37
24. Reduction in Tension at the Outer Boundary	39
25. Acoustic Gage Flow Chart	40
26. TOF Front Panel	42
27. Hakiel Front Panel	43
28. Acoustic Gage Front Panel	43
29. Test Roll #1 (Left)	48
30. Test Roll #1 (Right)	48
31. Test Roll #2 (Left)	49
32. Test Roll #2 (Right)	49
33. Test Roll #3 (Left)	50
34. Test Roll #3 (Right)	50
35. Test Roll #4 (Left)	51
36. Test Roll #4 (Right)	51
37. Test Roll #5 (Left)	52
38. Test Roll #5 (Right)	52
39. Test Roll #6 (Left)	53
40. Test Roll #6 (Right)	53
41. Stress versus Strain for Linear Elastic Material (Steel)	61
42. Stress versus Strain for Nonlinear Material (Paper Stack)	61
43. Instron 8500 with Extensometer and PC for Data Collection	62
44. Instron 8500 Machine Stiffness Curve	64
45. Derivative Plot of Different Order Polynomials	66
46. Spreadsheet Setup to Calculate E_r with Linear Regression	67
47. Example of E_r vs Pressure with Linear Regression	67

NOMENCLATURE

A	Constant
B	Constant
C	Constant
c	Speed of Sound (in. / second)
CID	Core Inside Diameter (in.)
COD	Core Outside Diameter (in.)
d	Diameter (in.)
E	Elastic Modulus (psi)
E _c	Elastic Modulus of the Core Material (psi)
E _r	Modulus in the Radial Direction (psi)
E _t	Modulus in the Tangential Direction (psi)
FSR	Force Sensing Resistor
f	Frequency (Hz)
g^2	E_t / E_r Modulus Ratio
h	Caliper or Grid Spacing (in.)
K ₁	Constant in Pfeiffer's Radial Modulus Regression
K ₂	Constant in Pfeiffer's Radial Modulus Regression
L	Length (in.)
OD	Roll Outside Diameter (in.)
P	Radial Pressure (Negative Stress in the Radial Direction) (psi)
P _i	Incident Complex Pressure Amplitude
P _r	Reflected Complex Pressure Amplitude
P _t	Transmitted Complex Pressure Amplitude

PTF	Pull Tab Force (lbs)
PET	Polyester Film
R	Resistance (Ohms)
r	Radius (in.)
r1	Impedance (lbs / in ² s)
r2	Impedance (lbs / in ² s)
T	Tension (Stress in the Tangential Direction) (psi)
t	Time (seconds)
Ti	Intensity Transmission Coefficient
T _w	Winding Tension (Freespan Stress at the Roll Tangent Point) (psi)
T.O.F.	Time of Flight (seconds)
u	Radial Displacement (in.)
V	Velocity (in. / second)
v _r	Poisson's Ratio in Radial Direction
v _t	Poisson's Ratio in Tangential Direction
ε	Strain (in. / in.)
ε _r	Radial Strain (in. / in.)
ε _t	Tangential Strain (in. / in.)
θ	Angle in Cylindrical Coordinates (Radians)
ρ	Density (lbs / in ³)
σ _r	Stress in the Radial Direction (psi)
σ _t	Stress in the Tangential Direction (psi)

CHAPTER I

INTRODUCTION

Roll structure measurement is presently done with destructive and intrusive measuring devices, such as Force Sensing Resistors (FSR) [1] or with specially instrumented winders. These methods are generally limited to research and development applications. Prior to this project, there was no method of non-destructively determining the internal stresses, or roll structure, with unknown winding conditions.

This thesis presents a measurement technique, the Acoustic Roll Structure Gage, that uses acoustic time of flight (T.O.F.) measurements to determine roll structure, an extension of the work done by J. David Pfeiffer [2] and alluded to by L. Eriksson [3] and D. R. Roisum [4]. A measurement is made of the time required for an acoustic wave to travel through the roll. This time of flight measurement is used as an extra degree of freedom in a winding model such as Z. Hakiel's [5] to replace an unknown or questionable model input, such as radial modulus or winding tension. The roll structure is determined by iterating the model input until the calculated time of flight matches the measured time of flight. This measurement technique is called the Acoustic Gage.

The Acoustic Gage was verified by comparison with two other independent methods, FSR's [1] and pull tabs [4]. Each method was used to map the radial pressures in the left and right sides of six different wound rolls. The Acoustic Gage agreed with two other independent roll structure measurement tools, all of which were much lower radial pressure than predicted by winding models. The results cast doubt on the validity of the hoop stress equation as an outer boundary condition for wound roll models.

This thesis discusses pertinent literature, roll structure fundamentals, preliminary experiments and, acoustic and wave propagation topics. The equipment and procedures for time of flight measurements in wound rolls, including the method of determining roll structure from time of flight measurements are presented.

CHAPTER II

LITERATURE SURVEY

The use of waves to measure material properties is widely documented, but three authors have done work specifically with stacks of web and wound rolls; Pfeiffer, Habeger, and Rhee [2, 6-11]. Pfeiffer's August 1966 paper "Internal Pressures in a Wound Roll of Paper" was the foundation upon which this project was built. Pfeiffer begins by describing the stack modulus (E_r) with an early form of his power law regression for the constants K_1 and K_2 .

$$\sigma_r = K_1 e^{(K_2 \epsilon)} \quad (1)$$

The stack modulus (E_r) is the slope of the stress-strain curve and can be found, as a function of pressure, by differentiating equation 1.

$$E_r = \frac{d \sigma_r}{d \epsilon} = K_2 K_1 e^{(K_2 \epsilon)} = K_2 \sigma_r \quad (2)$$

K_2 is therefore identical to the C_1 or slope term of the polynomial regression for E_r as a function of radial pressure. Wave speed should follow the relationship for solid body wave mechanics.

$$c = \sqrt{\frac{E_r}{\rho}} = \sqrt{\frac{K_2 \sigma_r}{\rho}} \quad (3)$$

This relationship was confirmed by Pfeiffer with a stack test in a hydraulic press. Three capacitors were used, one as a pulser and two as receivers. The pulser capacitor was slowly charged and quickly discharged to initiate the wave. A receiver capacitor indicated wave passage with a change in circuit voltage and time was measured with an oscilloscope.

The same process was used to determine wound roll pressures. The pulser capacitor was wound around the core and a paper roll wound over the capacitor. A phonograph needle was used to determine wave arrival at numerous radial points on the edge of the roll.

The wave's time of flight as a function of radius and equations 2 and 3 can then be used to map the radial pressure in the roll as a function of radial position. Pfeiffer then tried to use the radial pressure profile to determine the wound in tension profile. He realized that wound in tension and the first derivative of the radial stress were related, but was missing the radial stress term ($-\sigma_r$) in what is commonly called the equilibrium equation in cylindrical coordinates.

$$\sigma_t - \sigma_r - r \frac{d\sigma_r}{dr} = 0 \quad (4)$$

Pfeiffer did not employ the advantages of winding models and their associated equations and boundary conditions, although several existed, including Altmann and Trampusch [12,13]. The measurement method was also intrusive, destructive and could not be used to determine cross web profiles of radial pressure.

Rhee [11] developed a method of determining the modulus of elasticity of a stack using FSR sensors. Rhee's result confirmed Pfeiffer's power law relationship and discussed measurement problems. Habeger's work [6 - 10] in ultrasonics focuses on material properties measurement and sensor construction.

Wound roll structure authors include Altmann, Tramposch, Pfeiffer, Hakiel, Yagoda and Roisum [12,13,14, 5,15, 4]. These authors have given qualitative and quantitative insights into roll structure. Hakiel's [5] model was used for this project because it was considered the most rigorous and elegant.

Many sources were used in the areas of acoustics, ultrasonics and wave propagation [16-23]. Some of the most valuable literature was the discussion of group velocities and forerunners [17].

Roll structure measurement methods presently in the literature and used in industry can be grouped in four categories; surface measurements, intrusive and destructive measurements, instrumented winders and qualitative measurements. There are several references that discuss present roll structure measurement tools [1, 2, 5], and a summary has been given by Roisum [4]. Measurement tools will be discussed further in Chapters 3 and 7.

A summary of this project titled "Determination of Wound Roll Structure Using Acoustic Time of Flight Measurements", was presented at the First International Conference on Web Handling, Stillwater, Oklahoma, May 1991 [25]. The paper is included as Appendix E and the Conference visuals are included in Appendix F.

CHAPTER III

WOUND ROLL STRUCTURE

Wound roll structure has been quantitatively discussed by Altmann, Tramposch, Pfeiffer, Hakiel and Yagoda [12,13,14,5,15]. These individual references discuss their respective models including equations, boundary conditions and assumptions. Roisum [4] summarizes and compares these models, along with a discussion of roll structure measurement tools. This paper will not attempt to reiterate these papers, but will provide information that is critical to this project. Hakiel's model was used extensively for this work and will be detailed in Chapter 6.

Fundamentals

Wound rolls are difficult to analyze because of their material properties and geometry. Wound rolls are often made of paper or plastic web. Their material properties often exhibit viscoelasticity and nonlinearity. This problem is magnified when hundreds or thousands of layers are wound with entrapped air and rough surfaces. The material properties are significantly different (orthotropic) across the stack, versus through the stack. The usual approach to solving this largely geometrical problem is to assume a solid body with orthotropic and/or nonlinear material properties. These nonlinearities limit the use of the principle of superposition and greatly increase the complexity of the analysis.

Winding models use equilibrium, constitutive and compatibility equations to obtain a second order differential equation. The equilibrium equation can be derived by examining the stresses acting on a small element, in cylindrical coordinates. There could poten-

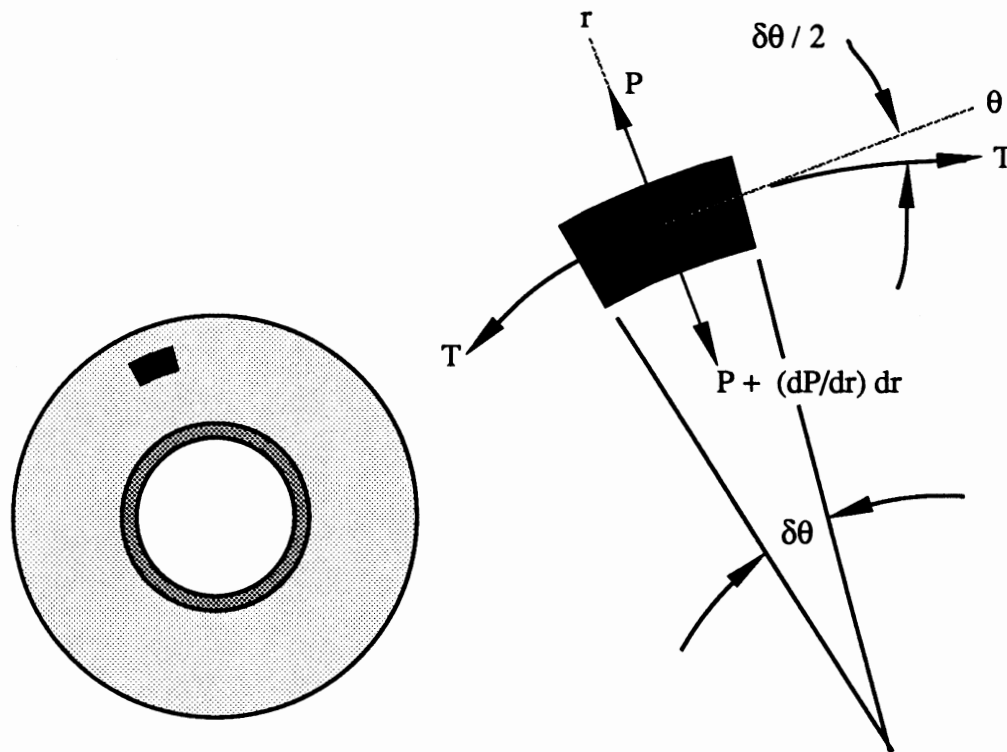


Figure 1. Roll Stress Equilibrium Equation

tially be three normal stresses and three shearing stresses acting on the faces of this element. It is generally assumed that all the shear stresses and the axial (Z) stresses are zero. This leaves only two normal stresses, radial (σ_r or P) and tangential (σ_θ or T). Negative radial stress ($-\sigma_r$) is usually defined as positive radial pressure (P).

The axes of a cylindrical element are not orthogonal, as shown in Figure 1. The forces must be balanced, therefore the stresses are not independent of each other. Equation (5) is the equilibrium equation.

$$T + P + r(dP/dr) = 0 \quad (5)$$

This equation is very significant because if we know the roll pressure as a function of radius, we can calculate the residual or wound in tension. All winding models use this equilibrium equation.

The equilibrium equation is based upon Newton's second law, and the only assumptions are that the shear stresses are negligible. The constitutive equation doesn't have as strong a foundation. The constitutive equation is derived from Hooke's law and Maxwell's relation. Hooke's law is probably a good assumption in the tangential direction, but a poor assumption in the radial direction. Maxwell relates orthotropic modulus and Poisson's ratios using energy principles. This relationship may also be questionable with a laminate structure having a very low Poisson's ratio.

The compatibility equation requires that there are no gaps or voids in the roll and that no adjacent laps occupy the same space. These three equations are combined to form a second order differential equation. A second order differential equation requires two boundary conditions for solution. The first is at the core, where radial deformation of the inside of the first wound on layer is equated to the radial deformation of the outside of the core. The second boundary condition is usually the hoop stress equation applied to the inside of the outside lap. Hakiel's model was used extensively in this work and the complete derivation will be given in Chapter 6.

Present Measurement Methods

The roll structure measurement tools used in industry today can be placed in four categories. These categories are surface measurements, intrusive and destructive devices, instrumented winders and qualitative tests. Many roll structure measurement tools are discussed by Roisum [4].

Surface measurement tools use various methods to characterize the "hardness" of the outer surface of the roll. This is usually done by striking the roll and measuring the deceleration or loss in energy. These devices are easy to use and can provide relative

crossweb information. The data from these devices can often be correlated to certain defects. Surface measurement methods do not yield stresses in engineering units, and the depth from which information is obtained is questionable. Examples include the Rhometer and Schmidt Hammer [2, 4].

Intrusive and destructive devices are thin pressure sensors that are wound into the roll to determine the pressure at various locations. They can often be calibrated in engineering units. These thin pressure transducers can be difficult to calibrate and use. Stress concentrations, can cause extraneous results for materials with low anisotropy ratios (E_t/E_r). The intrusive devices, are destructive in nature, and are therefore generally restricted to the laboratory. They can not be used for quality control of input material or output product. Examples of these include FSR's [1], pull tabs [4], pressure sensitive films, the Smith Needle, capacitive devices, strain gage hubs and other thin pressure transducers. FSR's and pull tab's will be further discussed in Chapter 7.

Instrumented winders accurately measure the incoming web speed and roll rotational velocity along with other factors to determine roll structure. These methods can give a stress profile in engineering units. Instrumented winders usually must measure quantities that are very small, such as strain or density changes. This usually limits their use to relatively soft materials with high anisotropy ratios (E_t/E_r). This measurement method requires very accurate, sophisticated and expensive equipment. The use of instrumented winders is generally limited to the laboratory. An example of an instrumented winder roll structure measurement tool is the density analyzer [4].

Qualitative measurement methods include the thumb test, the backtender's friend [4] and many other tests in which the winder operator's years of experience can be used to "feel" the quality or structure of the roll. Although these tests are often invaluable when it comes to short term goals of getting product out the door, they are of little value in process development or fundamental process understanding.

Each of these tests have certain advantages and disadvantages, but none of these existing tests can take a wound roll and non-destructively measure the stresses occurring in that roll. This would be very useful in process development and quality control, as well as incoming material inspections. The Acoustic Gage presented herein can fill this void in wound roll structure measurement.

CHAPTER IV

STACK TESTS

When this project started, there were many questions to be answered about laminate structures and wave travel. Many of these questions could best be answered with a material testing machine in stack rather than roll form. These questions included properties of laminate structures, application of solid body wave theory, coupling, attenuation, wave generation and reception. This chapter will discuss the stack test procedures, along with the test results and conclusions.

Radial Modulus Stack Tests

The radial modulus of a material, E_r , is a critical variable in the winding process. The largely geometrical problems of a laminate stacks, are usually handled with material property data in solid body mechanics. Therefore the radial modulus is a combination of many factors such as air entrainment, surface roughness and coatings. These factors combine to form an elastic modulus in the radial direction which is usually non-linear. Non-linear material properties create difficulty in modeling and therefore difficulty in understanding wound roll structure.

Most engineering materials, such as steel, are linear elastic. This means that if we tested a steel specimen in a material testing machine, and plot of stress versus strain, it will form a straight line as shown in Figure 2. The slope of this line will be the elastic or Young's modulus.

A web stack on the other hand exhibits nonlinear stress-strain characteristics when subjected to normal compression. The entrained air and surface asperities cause the curve to be more like a parabola, as shown in Figure 3.

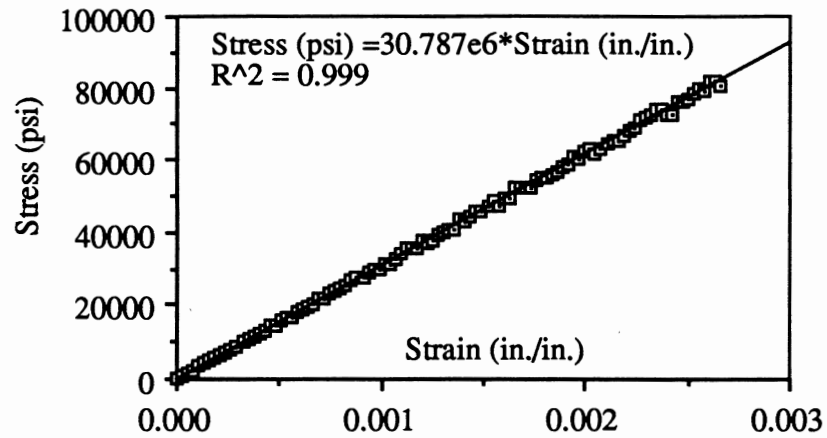


Figure 2. Stress versus Strain for Linear Elastic Material (Steel)

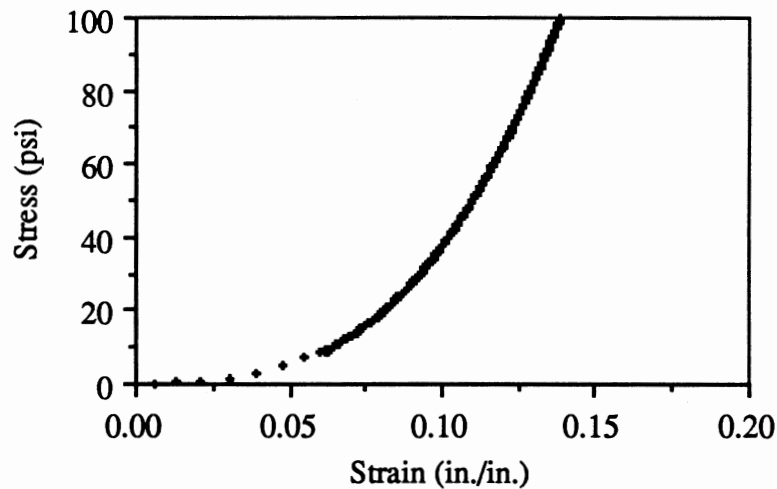


Figure 3. Stress versus Strain for Nonlinear Material (Paper Stack)

Measuring the radial modulus is very difficult. Therefore an assumption has been made that a stack test (flat geometry) is equivalent to the cylindrical geometry.

A Instron 8500 material testing system, as shown in Figure 4, was employed to determine stack modulus. The Instron consists of a load cell, platens, actuator and data collection system. A strain extensometer is also highly recommended.

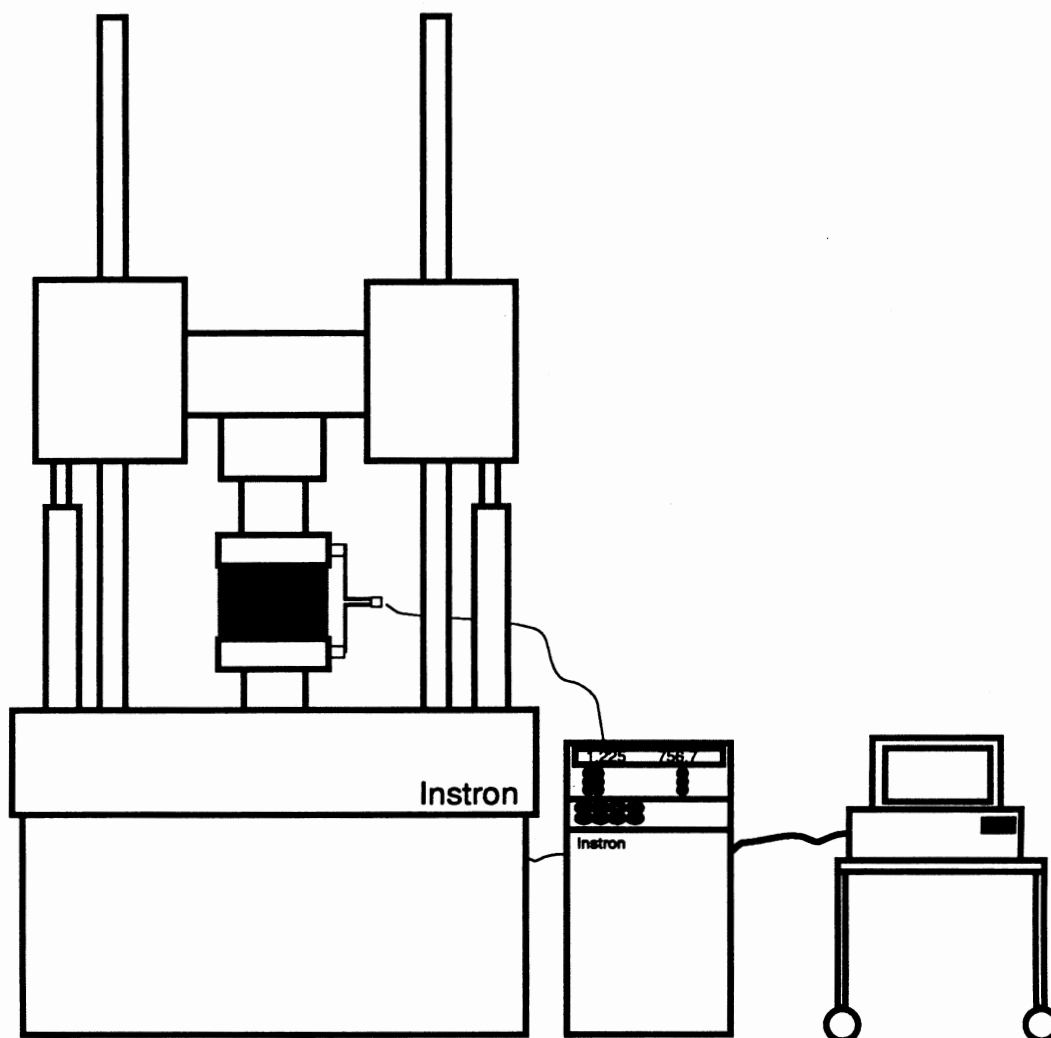


Figure 4. Instron 8500 with Extensometer and PC for Data Collection

Stress versus strain data, such as in Figure 3, were taken for many materials. The slope of this line is the radial modulus E_r , which was calculated as a function of radial pressure. Figure 5 shows the radial modulus versus radial pressure with polynomial regression. A detailed procedure for radial modulus testing is given in Appendix A and a catalog of material properties, including E_r , is given in Appendix B.

Radial modulus, as a function of radial pressure, can be described in many ways. Hakiel's model could use any mathematical function, but a polynomial is most common

and convenient. One of the difficulties involved in determining a material's radial modulus function is defining zero strain. The stress versus strain curve for web stacks asymptotically approaches the strain axis at zero pressure, as shown in Figure 3. This creates two problems, defining zero strain, and sometimes causing the constant of the polynomial regression to be negative. Fortunately, the outer boundary conditions of most winding models neglects to account for the strain of the first layer and, therefore, the low pressure E_r curve has little effect on predicted roll pressure.

The dominate term of the E_r polynomial regression is usually the first order (slope) term. Therefore, many materials could be described by just the slope term with only small deviations in predicted radial pressure. This makes it very simple to compare the "radial stiffness" of different materials by comparing the slope terms of the E_r polynomial regression.

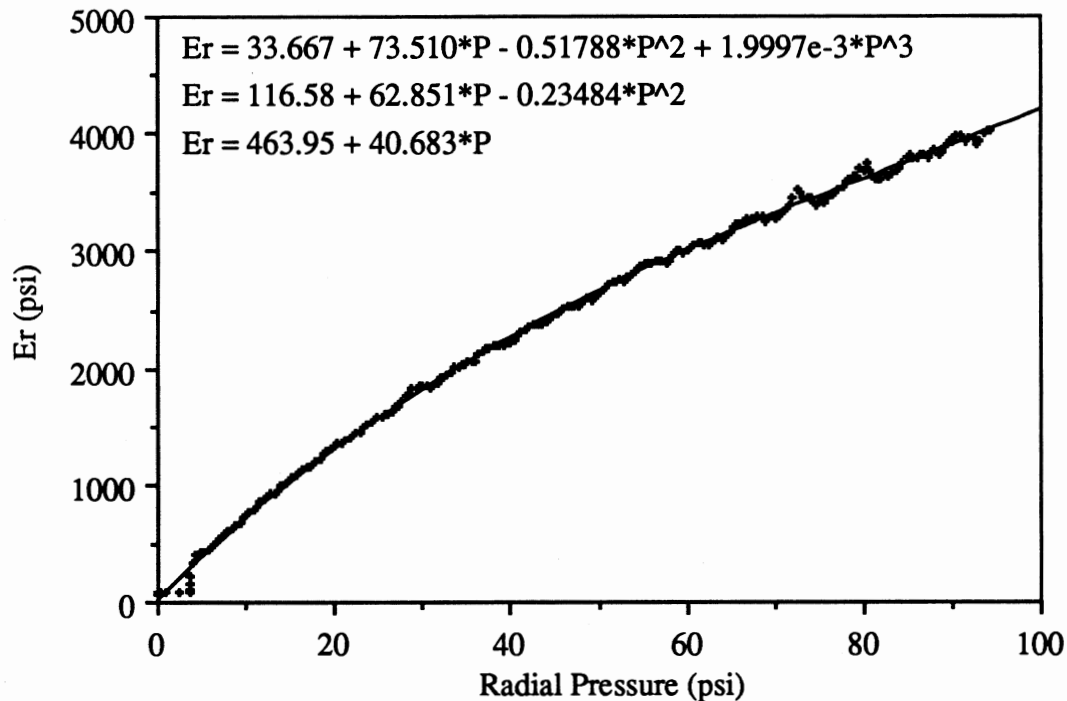


Figure 5. E_r vs. Radial Pressure with Polynomial Regression

The Effect of Radial Pressure on Density

The theoretical speed of sound, in a solid, is the square root of a characteristic restoring force divided by the square root of the density. Therefore, the density of the stack is critical to this project. The density of the material was determined by measuring mass, sample area and stack height. The percent strain in stack height is approximately equal to the percent change in volume because of the low Poisson's ratio. Figure 6 and 7 show the density of polyester (PET) and paper could be considered constant with a small error percentage. This assumption can be made for most webs. This is also an indication of the precision required by online density analyzers to infer pressure accurately.

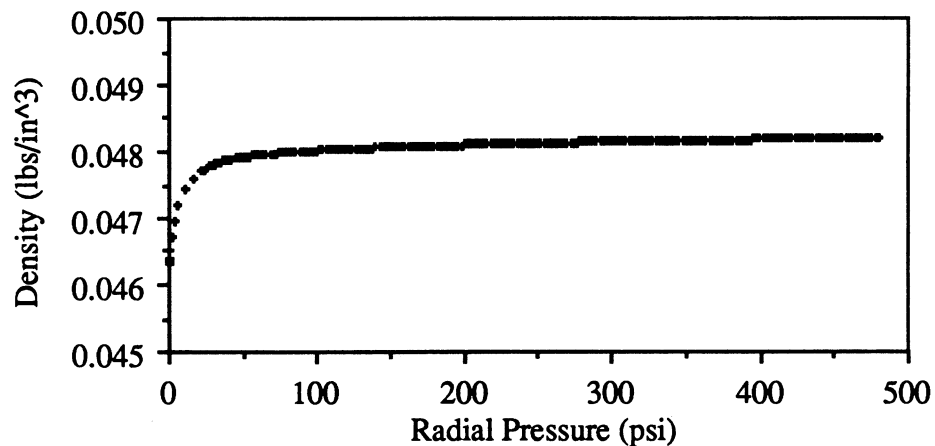


Figure 6. Density vs. Radial Pressure for a PET Stack

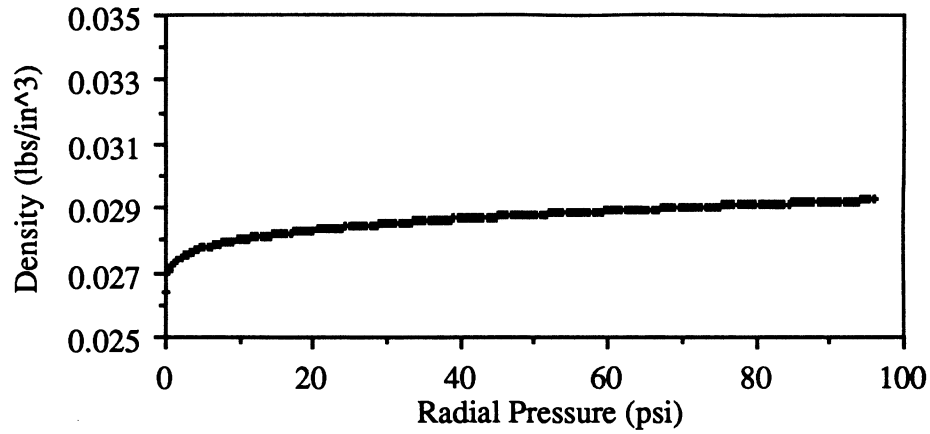


Figure 7. Density vs. Radial Pressure for a Paper Stack

Theoretical Speed of Sound

The simplest model for determining the speed of sound from the measured E_r and density data is to use the thin bar approximation. This method assumes that plane sections remain plane and that there is no shear. Most winding models make similar assumption. The theoretical speed of sound of a one dimensional wave in a solid is given by equation (6), where E is Young's modulus for a bar (one dimensional longitudinal wave) or the bulk modulus for multi-dimensional waves [16]. The stack test data was used to determine the theoretical speed of sound, by replacing E with E_r as a function of pressure and using a constant density ρ in equation (7).

$$c = \sqrt{\frac{E}{\rho}} \quad (6)$$

$$c = \sqrt{\frac{E_r(P)}{\rho}} \quad (7)$$

Wave Generation

Initial efforts into wave generation concentrated on commercial ultrasonic equipment typically used for non-destructive testing (NDT). This equipment has high frequency and wide bandwidth, which is advantageous for time of flight measurements. Commercial equipment works very well on steel and composites, where coupling fluids and high contact pressures are not considered destructive or intrusive, but this is not the case with wound rolls. A test of a pair of Panametrics¹ 1/2 inch, 1 Mhz transducers showed that 25 psi was required to dry couple a signal through a 0.38 inch stack of polyester film. Frequency analysis of the received signal revealed all frequency components above 300 kHz had been completely attenuated. This test showed that excessive intrusive coupling pressure was required to transmit a signal through a web stack that is a small fraction of the typical wound roll stack heights encountered in most wound rolls. The test also revealed that the bandwidth advantage of the commercial systems is nullified by the high frequency attenuation of the material. An attempt was then made to build a piezo pulser that had approximately 100 times the energy of the commercial systems, but lacked the commercial systems bandwidth. This system was only a marginal improvement over the commercial systems.

Rhee [11] also concluded the attenuation in web stacks is too high for commercial ultrasonic equipment. He switched to a simple method of hitting the stack with a hammer and sensing the wave with a FSR. This technique produced acceptable results. The hammer can apply tremendous energy to the wave and easily overcome the attenuation problems. A tap with a half pound hammer, as used by Rhee, would be about 1 joule of energy. The trouble with this method is that the frequency is very low and determining the actual arrival of a low frequency wave is much more difficult and less accurate than a broad band wave.

¹Panametrics Inc., Waltham, Massachusetts

A pulser was needed to initiate a wave capable of coupling and traveling through a large roll. This pulser would need the energy of a hammer blow which would be about 10,000 times the energy of commercial NDT equipment. This pulser must not only have high energy, but also bandwidth that will fully exploit the frequency transmission capability of the wound roll.

A mechanical pulser, shown in Figure 8, was developed that released about 1 joule of energy in 3.3 ms (300 kHz). This was done by using a form of Hopkinson pressure bar [22]. A short bar (projectile) is shot at known velocity into a longer bar (pressure bar). The impact creates a pressure wave, of magnitude described by equation (8), and duration described by equation (9). The wave travels down the pressure bar and into the roll. Figure 8 is a cross sectional view of the mechanical pulser. The mechanical pulser produces high frequency, wide bandwidth waves capable of traveling through large rolls.

The pulser consists of a barrel, short bar and a pressure bar. It is important that the pressure bar be more than twice as long as the short bar. This constraint ensures that the short bar has rebounded from the impact before the wave has reached the end of the pressure bar. The wave period is therefore independent of the properties of the wound roll surface. Air vents allow the projectile to travel at high velocity and prevents the pressure bar from acting as a pneumatic cylinder. The spring allows the pressure bar to be coupled to the roll with light contact pressure.

$$P = \rho c V \quad (8)$$

$$t = \frac{2L}{c} \quad (9)$$

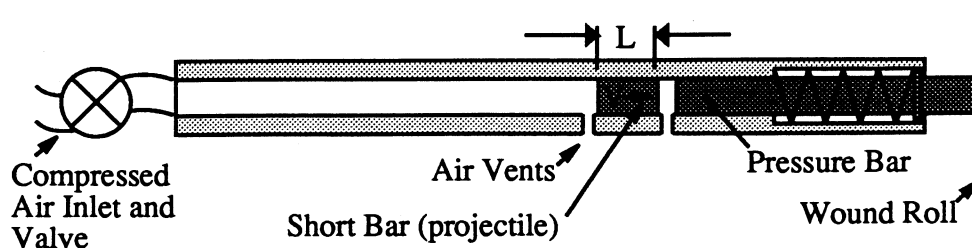


Figure 8. The Mechanical Pulser

The pulser is used to initiate a wave by first tipping the pulser back allowing the projectile to slide to the inlet end of the tube. The pressure bar was pressed against the roll with very light spring pressure. The pneumatic valve was fired causing the projectile to be shot into the pressure bar, initiating the pressure wave that travels down the pressure bar and into the roll.

Speed of Sound Measurement

Once a broad band wave of sufficient intensity could be generated, the next step was to determine if this theory, based on solid body mechanics, would be valid for a laminate structure with variable modulus. A box was made that could be placed on the lower platen of the Instron. The top of the box had a plunger that could be struck with the mechanical pulser and couple the wave to the stack. Two Kynar² (polyvinylidene fluoride) film strips were used as sensors to observe the wave as it passed two positions in the test stack. The Instron could be used to control pressure, as shown in Figure 9. The other equipment required for this measurement included an oscilloscope, analog amplifiers and filters.

²Kynar is a registered trademark of Atochem North America, Inc.

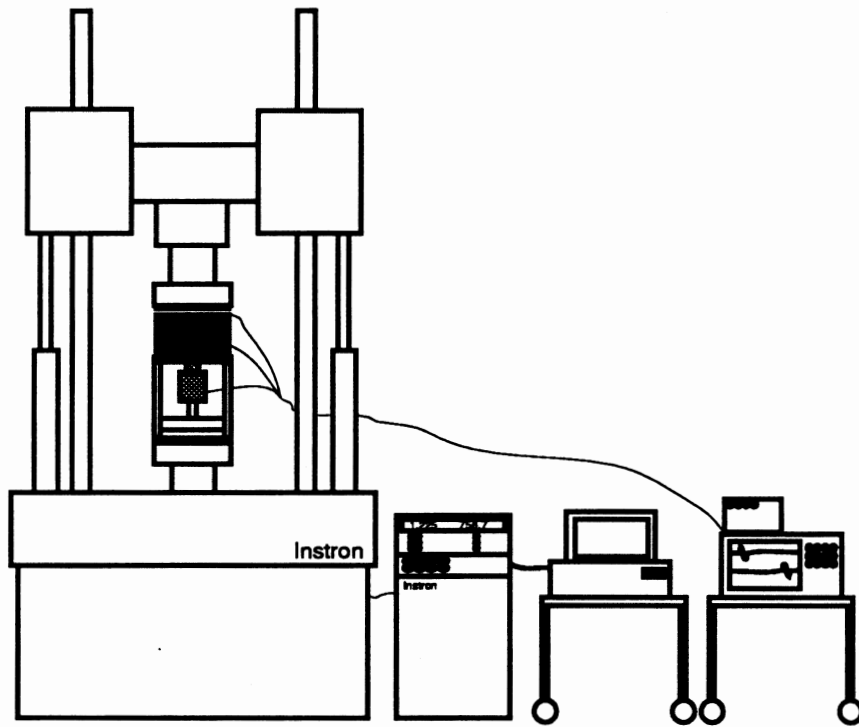


Figure 9. Instron Setup for Time of Flight Measurements

Kynar is a polymeric piezoelectric film that is commonly used in the ultrasonic industry. The Kynar film has electrodes on the top and bottom surfaces, which consist of metal vapor coating. Leads were connected to the Kynar by soldering wires to small pieces of copper tape with conductive adhesive. The leads were stuck to the top and bottom of the Kynar forming a very thin sensor, as shown in Figure 10.



Figure 10. Kynar Sensor with Leads Attached

Initially the leading edges of the signals were used to determine the time of flight between the two sensors. This technique produced wave velocities well in excess of those predicted by equation (7). It was later determined that this technique is not valid due to the existence of forerunners and high frequency attenuation [17]. Forerunners are small waves that travel ahead of the main energy packet, at speeds in excess of the group velocity. Figure 11 shows a very simplistic example of a wave with it's high frequency components attenuated with time.

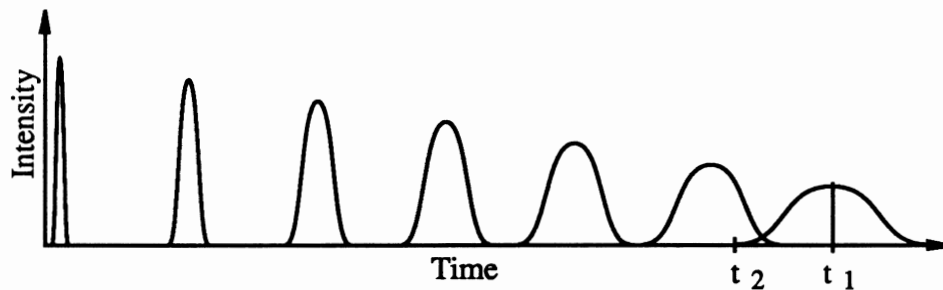


Figure 11. High Frequency Attenuation with Time

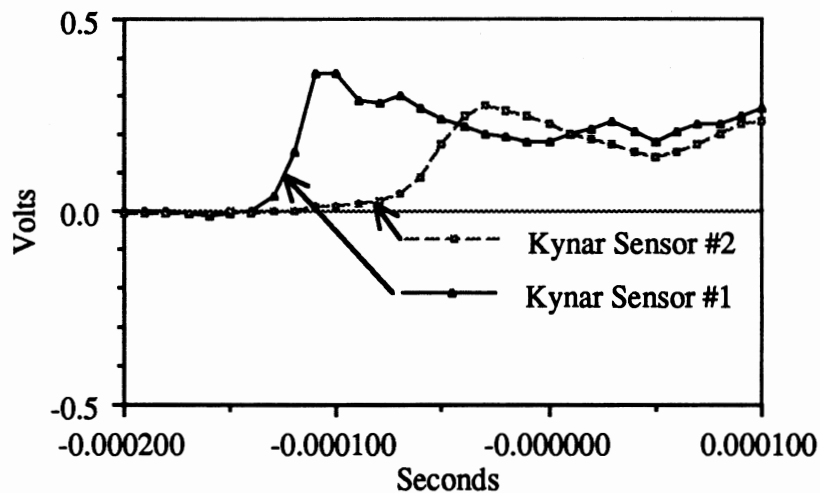


Figure 12. Signals with High Frequency Attenuation

If the leading edge (t_2) of the wave is used, the wave would appear to be traveling much faster than if t_1 was used. The time t_1 is a much better indicator of the actual time of flight. This phenomenon can be seen in Figure 12. Note how the wave has spread out. Using the leading edge of this wave would give very fast, and misleading wave velocity.

The best technique to measure wave speed was to place the two sensors relatively close together and to use cross correlation to determine the time of flight. The sensors were placed relatively close to minimize the wave shape change due to frequency dependent velocity and attenuation. The decrease in accuracy caused by close spacing was more than offset by the accuracy increase from cross correlation. An example of the output from the two Kynar sensors is shown in Figure 13. An example of the cross correlation output of the Figure 13 signals, is shown in Figure 14.

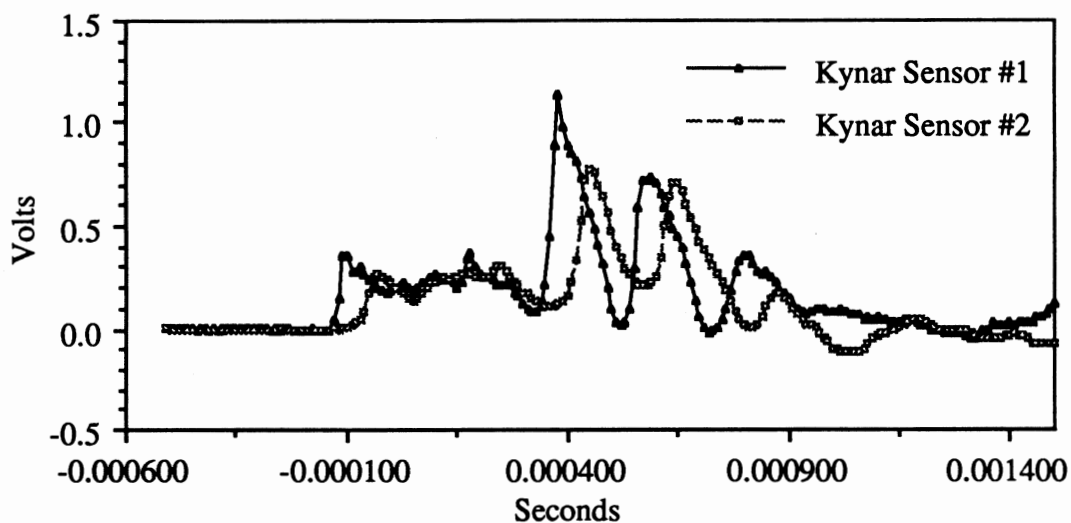


Figure 13. Signals from Two Closely Spaced Sensors

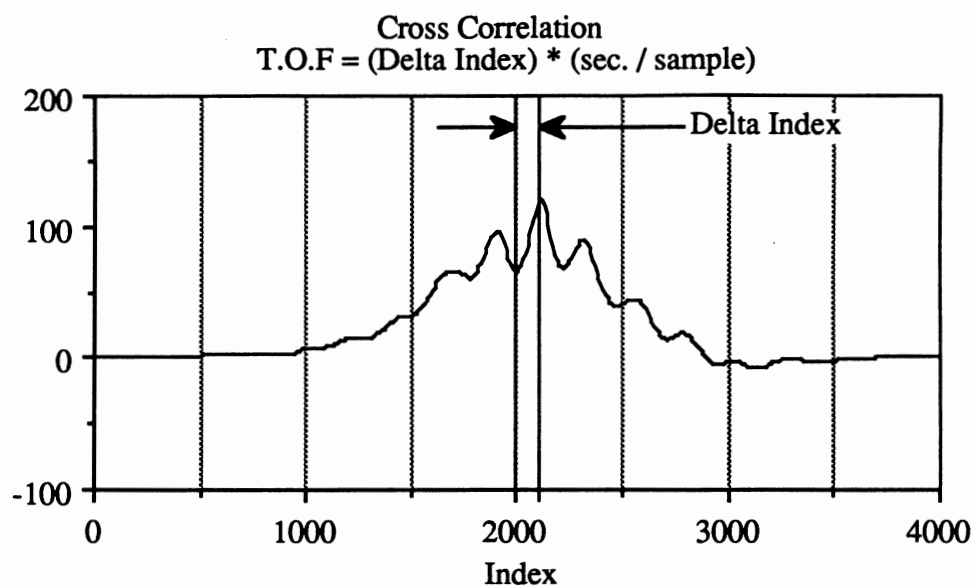


Figure 14. Cross-correlation of Signals in Figure 13

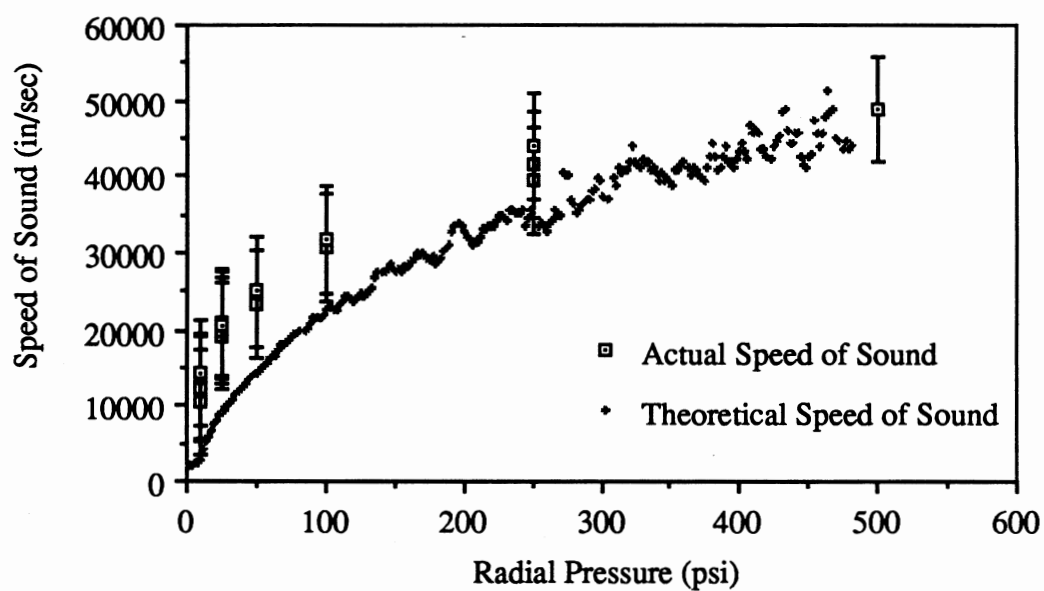


Figure 15. Actual vs. Theoretical Speed of Sound

Figure 15 shows the results of measured speed of sound tests and the theoretical speed of sound, as calculated by equation (7). The shape of the curve is good, but the results deviate at the low pressure end of the graph. This may be due to measurement difficulty and deviation from theory at low pressures, where stacks act less like solid bodies. At low pressure, there is still a significant amount of entrapped air, and the actual speed of sound at zero pressure may be approaching the speed of sound in air, 13,500 in./s and not zero as predicted.

The results of this test showed three conclusions; a) That equation (7) is valid for a laminate structure with variable modulus. b) There are difficulties involved in time of flight measurements with waves traveling through highly attenuating non-linear materials. c) There are potential problems with solid body wave mechanics at low pressure.

Both Pfeiffer [2] and Rhee [11] used a power law regression to describe wave speed as a function of pressure as shown in equation (10). This can easily be done by performing a linear regression on the logarithm of the speed of sound versus the logarithm of pressure. The constants A and B are the intercept and slope of this regression. The slope, B, should be 0.5 (square root) according to equation (7). Pfeiffer determined B for paper to be 0.36 and Rhee found paper to be 0.45, and film to be 0.62. The discrepancy between these values and equation (7) is probably due to the interaction between the slope "B" and the intercept "A" when regressing over a relatively small range. A significant second or third order term in the polynomial regression would also cause B to deviate from 0.5 .

$$c = A * P^B \quad (10)$$

Wave Attenuation

Wave attenuation in a laminate is very important to this project. It has already been stated that the attenuation is high, especially at low pressures and high frequencies. A calculation was done to determine the attenuation through an air gap, in a effort to investigate the effects of entrapped air. Figure 16 shows the rho-c impedance of a PET stack versus pressure. Figure 17 is the calculations that show that the attenuation is very high at an air gap.

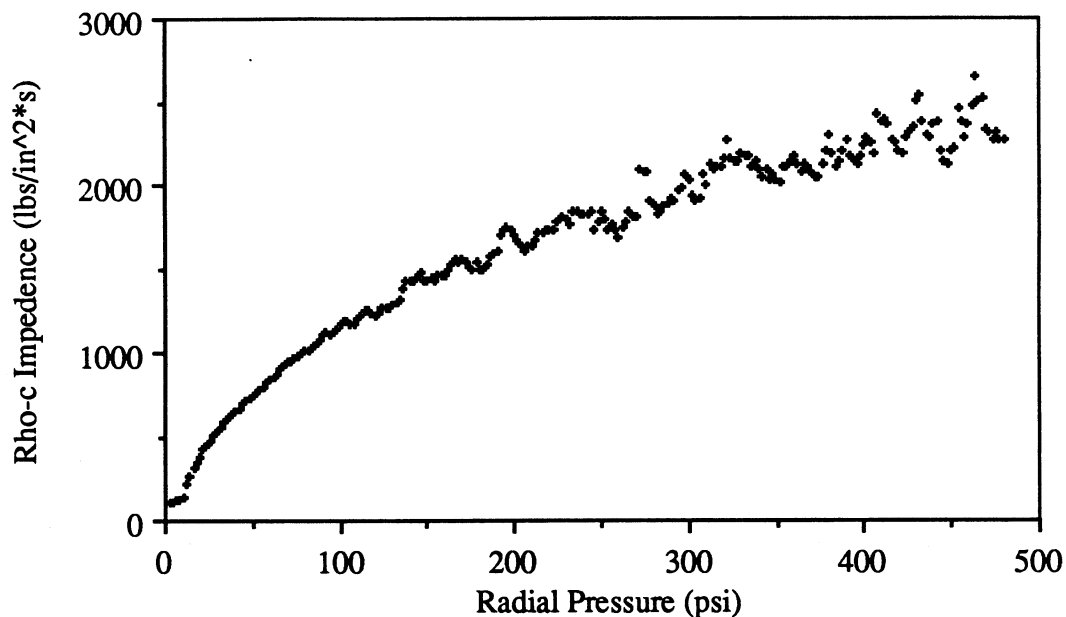


Figure 16. Rho-c Impedance of PET vs. Radial Pressure

A test was preformed to determine the signal attenuation through both film and paper. The signal attenuation was determined by placing two sensors in a stack at several different pressures and distances and recording a wave as it passed. The attenuation,

expressed in dB, was calculated as ten times the common logarithm of the ratio of peak signal strengths. The results of these tests were fit with a simple regression, as shown in equations (11) and (12).

The Intensity Transmission Coefficient (Ti)
for this situation is:

$$r1 \text{ (PET @ 100 psi)} = 1000 \text{ lbs/in}^2 \cdot s$$

$$r2 \text{ (Air)} = .59 \text{ lbs/in}^2 \cdot s$$

$$Ti = 4 \frac{\frac{r1}{r2}}{\left[1 + \frac{r1}{r2}\right]^2} = .0023$$

$$\text{dB} = 10 \log(Ti) = -26.4$$

The attenuation between a PET air interface is -26.4 dB.

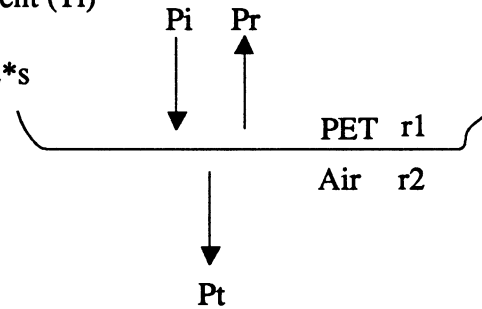


Figure 17. Attenuation Calculation [16]

$$\text{Paper dB / inch} = -4.5 + .016 * \text{Radial Pressure (psi)} \quad (11)$$

$$\text{Film dB / inch} = -8.0 + .013 * \text{Radial Pressure (psi)} \quad (12)$$

This measured attenuation is very high, but much less than predicted by the calculations shown in Figure 17. The measured values show attenuation decreasing with increasing pressure, contrary to that predicted by Figures 16 and 17. This calculation is strong evidence the wave travels only through the contact areas and not through the air gaps.

Equations (11) and (12) show the high attenuation in laminate stacks. At pressures commonly found in wound rolls, the signal will lose more than half of its strength for every inch of travel.

Coupling

References [6], [16] and [23] explain the coupling of a piston transducer. In order for power to be efficiently transmitted from the piston, the real part of the complex impedance must be maximized and the reactive part must be minimized. This happens when the piston diameter is greater than or equal to two times the speed of sound in the media divided by π times the frequency, as shown in equation (13). If the speed of sound is low, the diameter can be small. If the frequency is high, the diameter can be small.

$$d \geq 2 c / \pi f \quad (13)$$

The speed of sound in PET will always be less than 50,000 inches per second, as shown in Figure 15, and the frequency in the 300,000 Hz range. This would yield a transducer diameter of 0.106 inch. Therefore, we can efficiently couple high frequencies with a very small pulser.

Equation (13) shows that the diameter of the pulser acts as a high pass filter. A small diameter pulser would couple higher frequency wave components. This would increase the accuracy of the time of flight measurements. Equation (8) shows that the pressure intensity of the wave is not a function of the pulser diameter or the projectile length. Therefore, it would be advantageous to design a pulser with a pressure bar as small as 0.106 inches in diameter.

CHAPTER V

ACOUSTIC ROLL MEASUREMENTS

The stack tests answered many questions about wave propagation through laminate structures. The tests also provided valuable information about wave generation, reception and signal processing. With these questions answered, the emphasis was then shifted from the stack to roll geometry.

Wave Reception

The stack tests showed that the mechanical pulser was capable of generating a wave in the laminate stack, and that Kynar was capable of receiving that signal. Frequency analysis showed these signal frequencies to be all under 300,000 Hz. Most of the received signals were under 30,000 Hz. These signals can easily be detected with commercially available accelerometer equipment. The accelerometer used for this work was a PCB³ 302A with a PCB 480D06 amplifier. This sensor has a published frequency range of .7 to 10,000 Hz and is specially designed for low phase shift. This frequency range refers to the linear output range, actual frequencies of to 300,000 Hz have been recorded. The output of this accelerometer is very similar to a Panametrics ultrasonic receiver with a frequency response up to 1,000,000 Hz. The amplifier is battery powered and has a 1, 10, 100 selectable gain.

A fixture was made to align the pulser and accelerometer. The pulser was held against the roll with light spring pressure and the accelerometer was hand held firmly against the inside of the core. This fixture is shown in Figure 18.

³PCB Piezotronics, Inc., Depew, New York

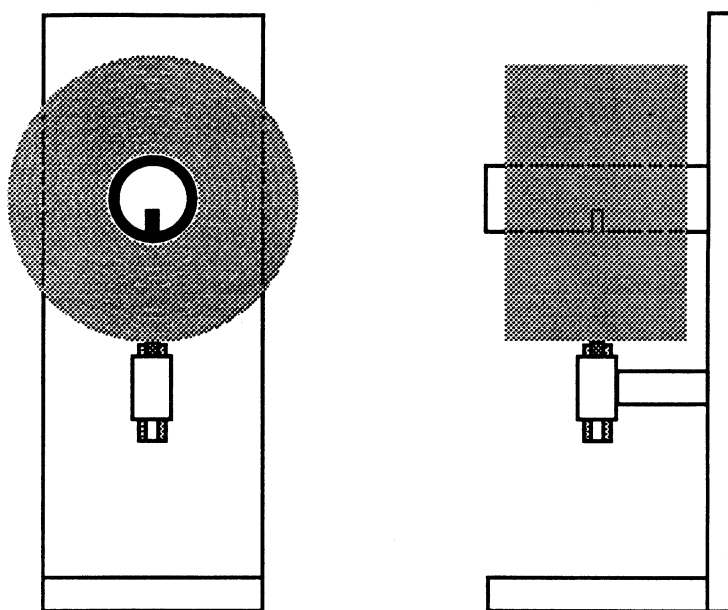


Figure 18. Time of Flight Fixture

Roll Time of Flight Measurement

To determine the time of flight through the roll, the wave must be initiated and received at known times. Unlike the stack test, cross correlation cannot be used because of the extreme differences in wave shape between initiation and reception. A simple technique to determine the initiation time of the wave is to place a Kynar film sensor between the pulser pressure bar and the roll. When the pulser is fired, the Kynar produces a voltage signal as the wave travels from the pressure bar through the Kynar and into the roll. The signal from the Kynar sensor can go directly into an oscilloscope. This signal is very clean and has an amplitude of several volts. The scope is DC coupled and triggered at a level above the noise, and below the peak amplitude of the signal. The actual trigger level is not important because of the extremely fast rise time of the signal. Recall that the total theoretical pulse duration is only $3.3 \mu\text{s}$ as compared to time of flights ranging from hundreds to thousands of microseconds.

The determination of the exact time the wave has been received is very difficult because of the low frequency and small bandwidth of the wave. Many references were consulted about this problem [17, 21, 23]. There are several references discussing the problem, but a satisfactory solution was not found in the literature. The stack tests showed that the leading edge of the wave cannot be used because of the forerunners. The technique that worked best was to pick the first major peak. These peaks are generally in the 10,000 to 30,000 Hz frequency range. High frequency components riding on this wave can cause the peak picking algorithm to have a large test to test variability. The problem was easily fixed with a low pass filter. The cut-off frequency is selected above the frequency of the main wave but below the high frequency components. In all the cases tested, this algorithm produced reasonable time of flight values. Figure 19 shows two examples of normalized signals.

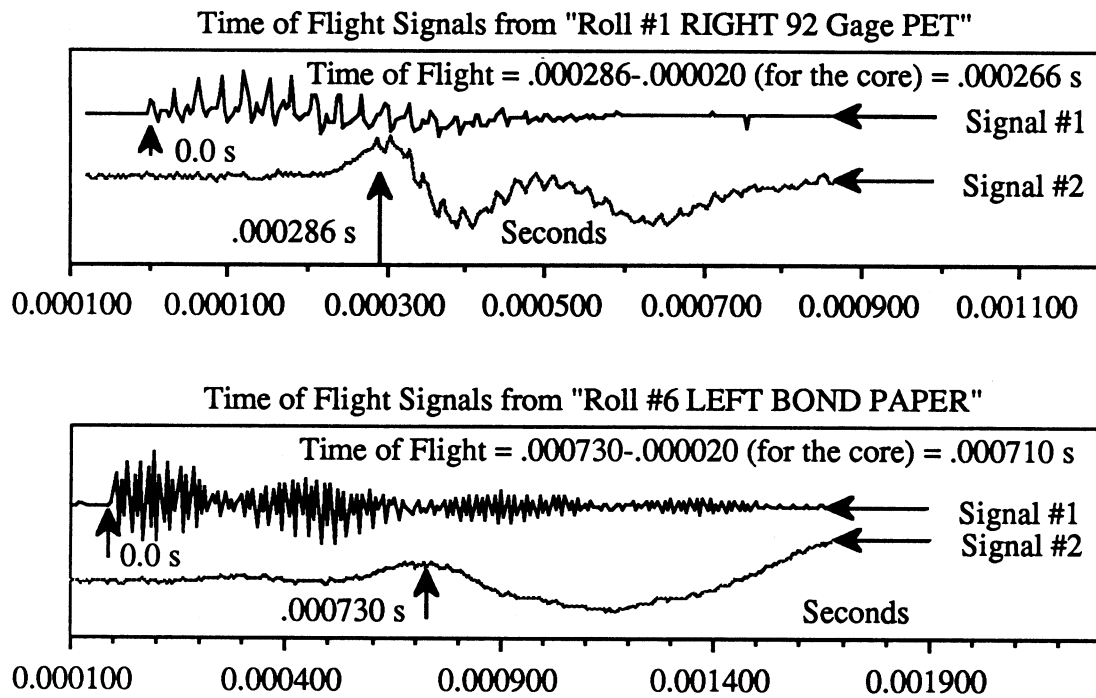


Figure 19. Time of Flight Signals

Ray Theory and Cylindrical Geometry

Reference [20] discusses what happens when waves travel through media with a gradient in the sound velocity. The conclusion was that the ray of the wave is always bent toward the region of low velocity. The speed of sound in a roll will usually be slower at the outside diameter than the core, due to the pressure distribution inherent to wound rolls. This will cause a wave initiated at the outside diameter to scatter toward the core and a wave initiated at the core to be focused toward the outside diameter, as shown in Figure 20. Therefore it would be preferable to have the pulser at the core and the receiver at the outside diameter.

Designing a mechanical pulser that fits inside a small core is not easy. The projectile and the pressure bar must be large enough in diameter to efficiently couple to the core, as discussed in Chapter 4. The projectile must be about one and one half diameters long to avoid binding in the barrel, and the pressure bar must be more than twice as long as the projectile. The barrel must also be long enough to allow the projectile to accelerate to a velocity that will create a sufficiently intense wave, as described in equation (8). Because of these design problems an outside pulser was initially used for this project.

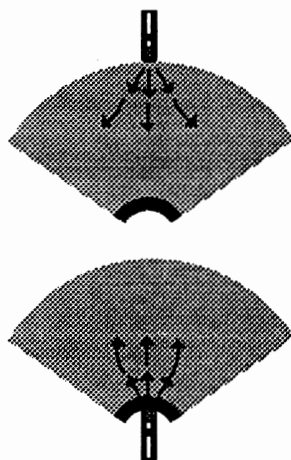


Figure 20. Ray Focusing

CHAPTER VI

DETERMINATION OF WOUND ROLL STRUCTURE

The previous chapters have discussed the technology, equipment and procedures required to make time of flight measurements in wound rolls. The time of flight measurements themselves are a valuable roll hardness measurement. T.O.F. is inversely proportional to the square root of the average roll pressure. This measurement can be used to evaluate wound roll hardness, similar to the Rhometer⁴. The Rhometer does not yield stress in engineering units, but has been successfully correlated to many "hard-soft" type wound roll defects. T.O.F. measurements can be used to predict defects in a similar fashion, but this would not fully utilize all the information available in the T.O.F. measurement.

The goal of this project was to map the stresses in a wound roll. The preliminary algorithm to transform T.O.F. into a stress map consisted of using T.O.F. and equation (6) to calculate a constant or average value for E_r . This constant E_r value would be used in a linear anisotropic model such as Altmann [12] or Yagoda [15] to generate a radial pressure profile.

This algorithm had two flaws. First, E_r is a pressure dependent material property that could be more accurately described as a function of pressure from a stack test, than as an average value from a T.O.F. measurement. Secondly, this algorithm requires that the winding tension be known. Winding tension is the only independent model input, all other model inputs are either geometrical or a material property. If the winding tension was always known, the roll pressure could be modeled without T.O.F. data.

⁴ Rhometer is a registered trademark of the Beloit Corporation

Hakiel's winding model requires 13 model inputs to predict the radial pressure profile. The T.O.F. measurement adds an additional constraint to this model. Therefore, one of the 13 inputs must be changed from an independent to a dependent variable, to avoid over constraining the model. Any of the 13 inputs could be used, but from the discussion of the previous paragraphs, it is evident that winding tension is the logical choice. This was confirmed by experiment and will be discussed in Chapter 7.

To fully understand the roll structure algorithm, we must first understand the model that is used. Hakiel's model and his outer boundary condition are discussed in the next sections.

Hakiel's Winding Model

Hakiel's winding model [5] is a nonlinear orthotropic hoop model that has the following properties or assumptions:

1. It is a stress, not a displacement based model.
2. The model is essentially one dimensional, assuming pressure varies only with radius.
3. The roll is modeled as a series of concentric hoops. Each hoop or cylinder is linear elastic in the circumferential direction and nonlinear elastic in the radial direction.
4. The assumption of plane-stress has been made.
5. The roll is built by adding successive hoops. During the addition of a new hoop, the previous hoops are assumed to have constant linear elastic orthotropic properties and the incremental addition of stress on each hoop can be added with the principle of superposition.

The basic equations include the equilibrium equation (14), the linear orthotropic constitutive equations (15) and (16), and the strain energy constraint equation (17). These equations were combined to form a second order linear differential equation in terms of radial stress (18). This second order equation requires two boundary conditions, one at the core and one at the outside of the roll.

$$r \frac{d\sigma_r}{dr} + \sigma_r - \sigma_t = 0 \quad (14)$$

$$\epsilon_r = \frac{1}{E_r} \sigma_r - \frac{\nu_{rt}}{E_t} \sigma_t \quad (15)$$

$$\epsilon_t = \frac{1}{E_t} \sigma_t - \frac{\nu_{tr}}{E_r} \sigma_r \quad (16)$$

$$\frac{\nu_{tr}}{E_r} = \frac{\nu_{rt}}{E_t} \quad (17)$$

$$r^2 \frac{d^2\sigma_r}{dr^2} + 3r \frac{d\sigma_r}{dr} - (g^2 - 1) \sigma_r = 0 \quad (18)$$

$$\left. \frac{\partial(\delta P)}{\partial r} \right|_{r=1} = \left(\frac{E_t}{E_c} - 1 + \nu \right) \delta P \Big|_{r=1} \quad (19)$$

$$P = \frac{T_w * h}{r} \quad (20)$$

The core boundary condition (19) is a relationship that states that the pressure and radial deflection of the outside of the core, node #1, must equal the pressure and radial deflection of the inside of the first lap, which is also node #1. The outer boundary condition is a static pressure equal to the radial pressure predicted by the hoop stress equation (20) on the next lap to be added. The outer boundary discussion will continue in the next section.

The model algorithm is best described as the incremental addition of successive hoops starting at the core. The outside of the core is subjected to a static pressure as calculated by the hoop stress equation (20) as shown in Figure 21. The "h" in this model refers to the finite difference grid size and not necessarily the web caliper. This is very important because the number of calculations and calculation time goes up geometrically with grid size. This model is surprisingly insensitive to grid spacing, as few as 30 grid points can often be used with no significant change in pressure levels. One hundred grid points seemed to be a good compromise between accuracy and computation time.

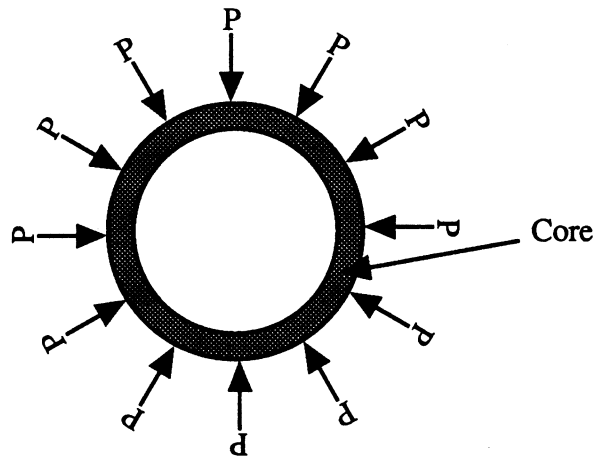


Figure 21. Adding Hoop #1

After the core has been subjected to the static pressure, the first hoop is applied having a circumferential stress equal the winding stress and a radial pressure on the inside equal to static pressure. The pressure at the core-web interface (grid node #1) is the static pressure. Next a static pressure, as predicted by equation (20), applied to hoop number two, is exerted on the core and hoop structure, as shown in Figure (22). The radial modulus of hoop number one is considered to be a constant linear elastic value equal to

the stack test value at the new pressure at node #1. The incremental pressure that this static pressure exerts on node #1 can be calculated using the finite difference technique on equation (18). The pressure on node #1 now becomes the sum of the original static pressure and the new incremental pressure. The second hoop is applied having a circumferential stress equal the winding stress and a radial pressure on the inside (node #2) equal the static pressure.

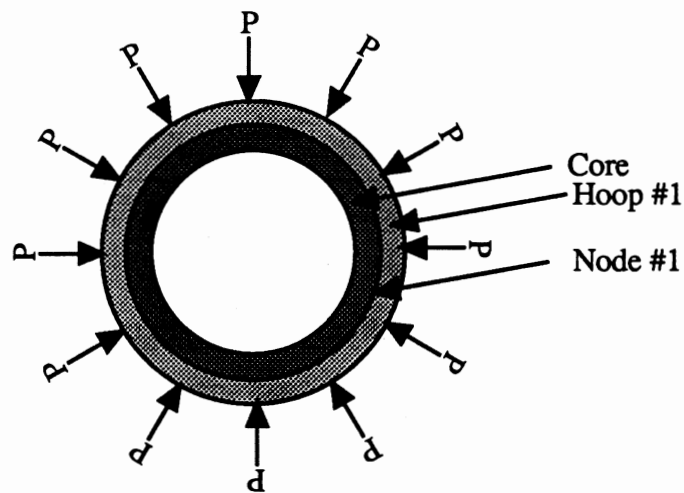


Figure 22. Adding Hoop #2

The computations continue when a static pressure, as predicted by equation (20), is applied to hoop number three, and must be reacted by the core and hoop structure, as shown in Figure (23). The radial modulus of hoop number one is considered to be a constant linear elastic value equal to the stack test value at the new pressure of node #1. The radial modulus of hoop number two is considered to be a constant linear elastic value, equal to the stack test value at the updated pressure at node #2. The incremental pressure that this static pressure exerts on node #1 and #2 can be calculated using the

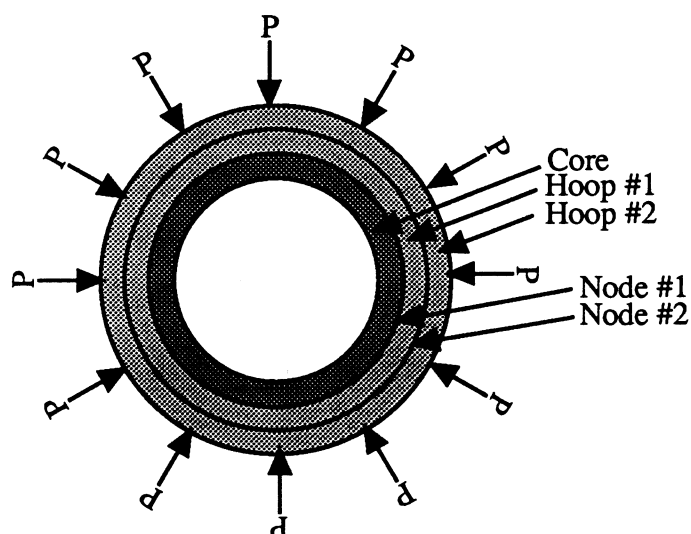


Figure 23. Adding Hoop #3

finite difference technique on equation (18). The pressure on node #1 and #2 now becomes the sum of the original pressure and the new incremental pressures. The third hoop is applied having a circumferential stress equal the winding stress and a radial pressure on the inside (node #3) equal the static pressure.

This process continues until all the hoops have been applied to the roll. The finite difference solution of equation (18) results in a tri-diagonal matrix which can be efficiently generated and solved with solution routine designed specifically to solve linear sets of tri-diagonal equations.

The Hoop Stress Outer Boundary Condition

Hakiel's model consistently predicts radial pressure levels that are higher than actually measured in center wound rolls. Chapter 7 will show the results of actual measurements versus Hakiel's model. Can the model have a fundamental error? Most winding models predict pressures that very similar to Hakiel's, all much higher than measured.

Pfeiffer's model [14] is formulated with a very different method than Hakiel, but produces similar results. All these models have one thing in common, some form of the hoop stress boundary condition in equation (21).

$$P = \frac{T_w * h}{r} \quad (21)$$

The previous section discussed how a new hoop is added to the wound roll model. A static pressure is applied to the existing hoop structure. The static pressure adds pressure to the existing nodes. Then the next hoop is snapped on having a circumferential stress equal to the winding stress. Hakiel's model is a stress model and never calculates displacements. Is this a good representation of the outside of a winding roll? It is more likely a upper limit, not accounting for losses in circumferential stress in the outer layer. If an elastic hoop was actually snapped on the existing hoop structure, the actual pressure at the interface would be less than predicted by (21) because the hoop would lose circumferential stress as the outside of the structure displaced under the applied pressure, as shown in Figure 24. This displacement could be quite large because of the extremely low stack modulus at low pressures and air entrainment. In the actual winding process, some of the tension loss could be replaced if the material was free to slide. The actual circumferential stress that should be used in place of T_w in equation (21) will be less than T_w and is probably friction related.

From the previous discussion it is evident that even if the winding tension T_w is accurately measured, the circumferential stress that should be used in equation (21) is not known. The winding tension of many rolls is unknown, such as a roll that is purchased as raw material. Winding tension is therefore the best model parameter to be used as a dependent instead of an independent variable, as discussed earlier in this chapter.

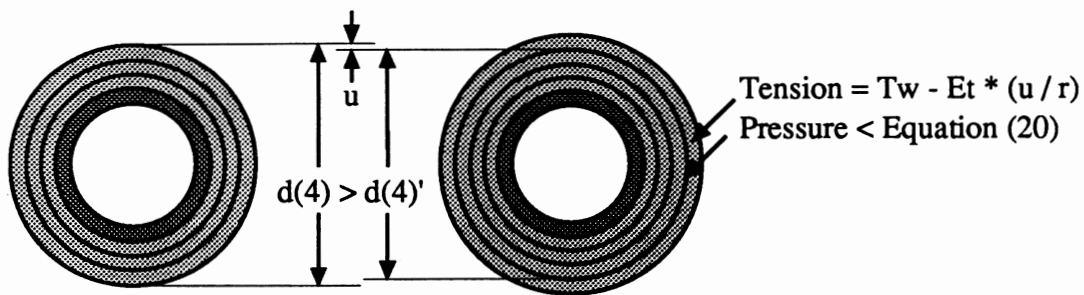


Figure 24. Reduction in Tension at the Outer Boundary

Roll Structure Algorithm

Hakiel's model requires 13 inputs to model a roll. The time of flight measurement is an extra input (redundant or indeterminate constraint) that can be used to replace an unknown or questionable model input. The previous sections explain why winding tension is the best choice.

The algorithm to determine the roll structure using acoustic time of flight measurements is as follows: The rolls geometry can be measured, material properties determined and the roll T.O.F. measured as discussed in Chapter V. A guess can be made of the winding tension, and the roll modeled. The model will produce a pressure profile that can be used with equation (7) to determine the speed of sound as a function of radius. The speed of sound as a function of radius can be integrated from the core to the outside of the roll to calculate the time of flight resulting from the initial guess. The difference between the calculated time of flight and the actual measured time of flight is then used to make a better guess at the winding tension. This iteration process is continued until the calculated time of flight converges with the actual measured time of flight. The data from the last iteration is the roll structure. This method is called the Acoustic Roll Structure Gage. Figure 25 is a program flow chart.

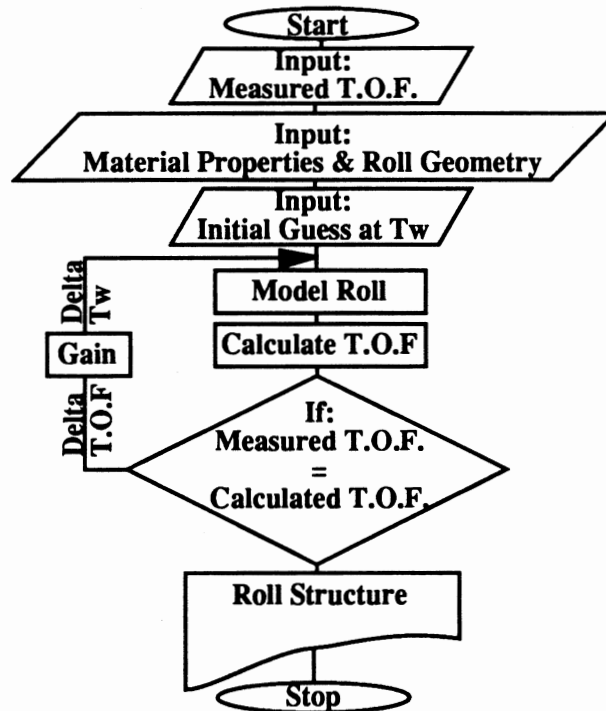


Figure 25. Acoustic Gage Flow Chart

An initial attempt to use a linear proportional-integral (PI) control algorithm on the iteration proved to be unstable. The gain would have to be carefully tuned for each roll. The solution often required numerous iterations of Hakiel's model to converge on the measured T.O.F. value. After reviewing the results of the winding model it was evident that the T.O.F. might be roughly estimated by a function which was inversely proportional to winding tension. A control algorithm exploiting the inverse relationship was implemented. After the T.O.F. was calculated from the initial guess, the tension guess and the resulting T.O.F. were regressed to the single degree of freedom inverse relationship shown in equation (22) to determine the constant C. The constant C and the measured T.O.F. were used to calculate the a better guess of the winding tension. The constant C is updated with every iteration. This method always converges in 3 to 6 iterations.

$$T_w = \frac{C}{TOF} \quad (21)$$

Another potential unknown or questionable model input is radial modulus. The time of flight measurement can be used with equation (6) to determine the average radial modulus. This constant modulus can be used in a model such as Altmann [12], Yagoda [15] or Hakiel [5] to determine roll structure. This method is called the Constant E_r Roll Structure Gage.

A computer program was written that reads the two signals from an oscilloscope. These two signals are processed, according to the criterion discussed earlier, to determine the measured time of flight. The program has two options: Constant E_r and Acoustic Gage. If the Constant E_r option is selected, the time of flight measurement is used to calculate an average E_r , which is used in the model to replace the stack test E_r function. The remaining model inputs, including T_w remain unchanged. The program then calculates the roll structure, plots the radial pressure distribution and files the data. If the Acoustic Gage option is invoked, an initial guess of T_w and the stack test E_r function is used to calculate the roll structure. This radial pressure and equation (6) is integrated to determine the calculated time of flight. The error between the measured time of flight and the calculated time of flight is used to make a better guess at T_w . This iteration process continues until the difference between the measured and calculated time of flight is less than 1 μ s. The roll structure data from the last iteration is plotted and the data written to a file.

The Acoustic gage program was written with a program called LabVIEW 2⁵. LabVIEW is a object oriented (iconic) programming tool used for data collection and analysis. The Hakiel's model subroutine was written in C and loaded into a LabVIEW 2 icon as a CIN (Code Interface Node). The front panels, wiring diagrams, Hakiel's C code

⁵National Instruments, Inc., Austin, Texas

and associated LabVIEW documentation is listed in Appendix C. A simplified version was also written in Microsoft Quick Basic and is listed in Appendix D.

A program written in LabVIEW 2 is virtual instrument. The program consists of a front panel with controls and displays and a wiring diagram that connects controls, displays and analysis icons. Figure 26 - 28 are the major front panels to the Acoustic Gage program.

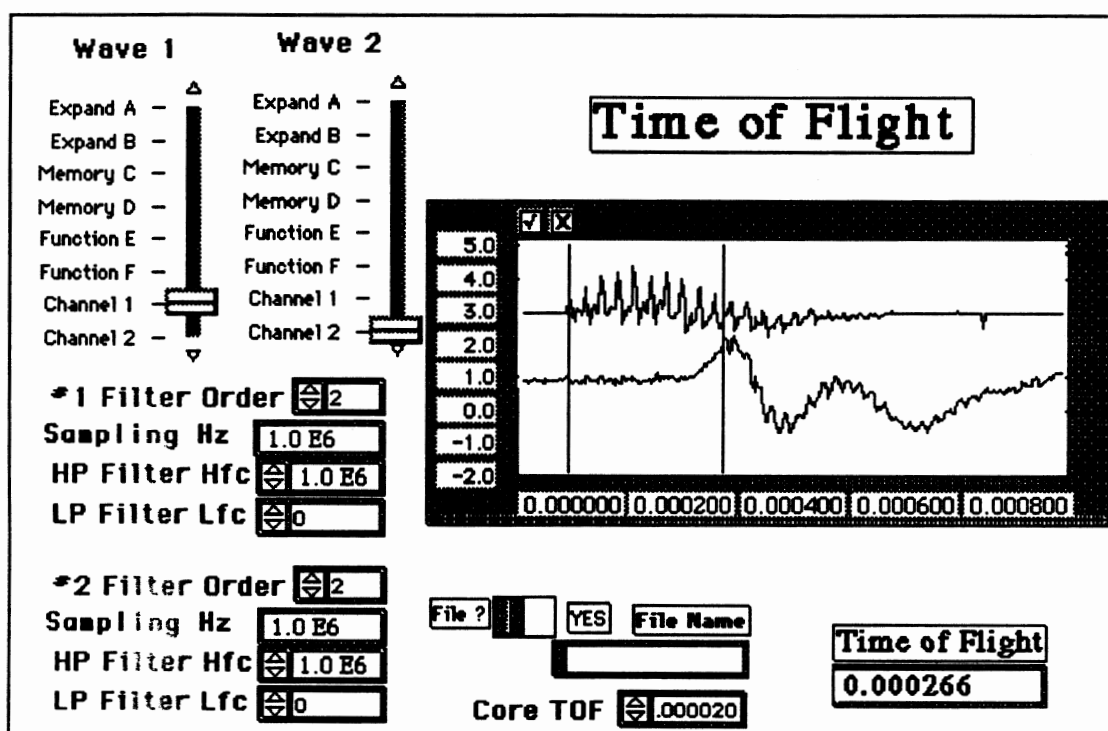


Figure 26. TOF Front Panel

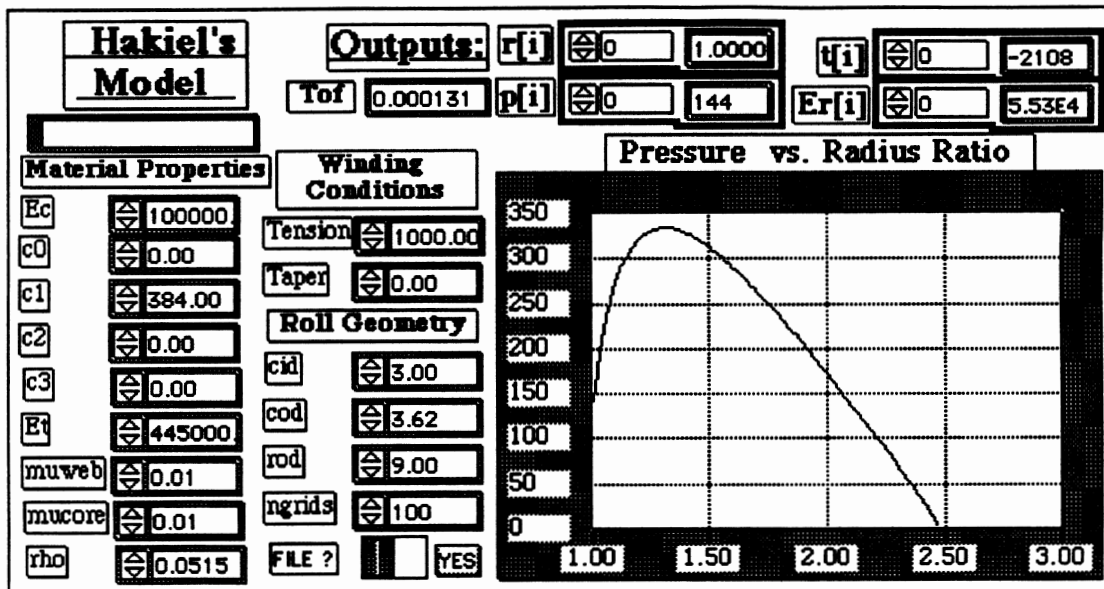


Figure 27. Hakiel Front Panel

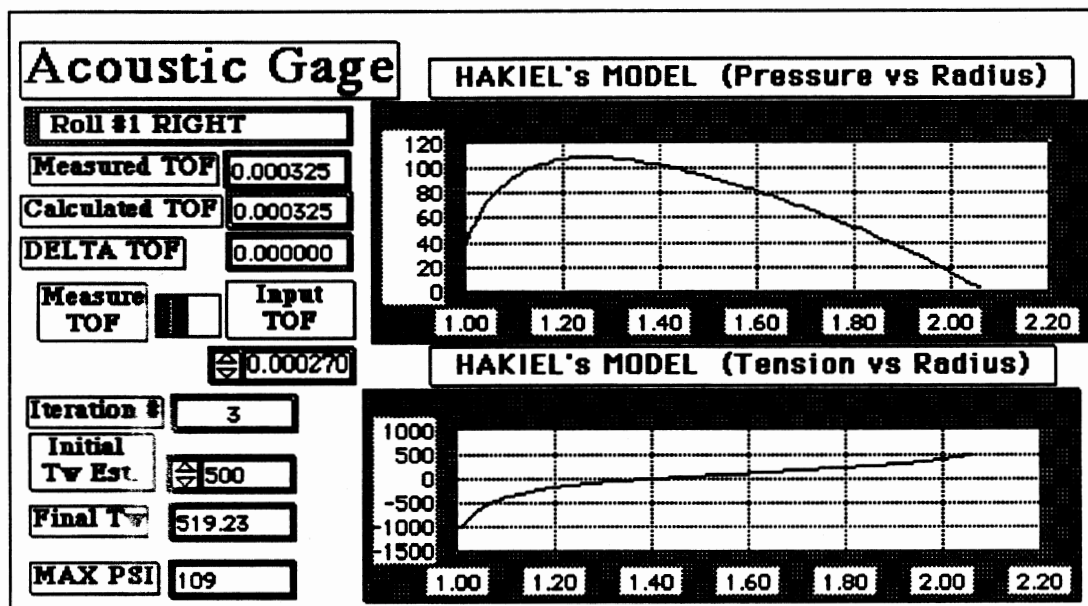


Figure 28. Acoustic Gage Front Panel

CHAPTER VII

VERIFICATION

Chapter III discussed present measurement methods that included two intrusive measurements FSRs and pull tabs. These two sensors were used to check the validity of this new measurement tool. Two different sensors were used to eliminate the possibility of gross measurement errors such as a bad calibration. Six test rolls were wound with FSRs and pull tabs. The FSR and pull tab data was compared to the Acoustic Gage Data for verification of measurement validity.

FSR and Pull Tab Measurement

FSRs [1, 24] have been established as a wound roll pressure sensor. These references discuss the difficulty in calibration. They produce best results when calibrated in a stack of the material for which it will be used, at a time approximately equal to the measurement time, in this case 20 minutes. This was done in a setup similar to that shown in Figure 4. The stack containing a FSR was placed in the Instron and the FSR resistance was measured as a function of pressure. The pressure versus resistance data was collected and regressed for paper and PET. Equations (23) and (24) express these relationships.

$$\text{Paper:} \quad P = 10^{(46.758 - 21.690 * \log(R) + 2.5306 * \log(R)^2)} \quad (23)$$

$$\text{PET:} \quad P = 10^{(87.753 - 43.929 * \log(R) + 5.5174 * \log(R)^2)} \quad (24)$$

Where $P \equiv$ Pressure (psi) and $R \equiv$ Resistance (Ohms)

Pull tabs [4] have also been established as a wound roll pressure sensor. Pull tabs can not measure crossweb radial pressure variations like a FSRs, but they also lack the calibration difficulties. Pull tabs are linear and insensitive to time and temperature. The pull tabs were made using of 1 mil thick, 0.5 inch wide and 4 inches long steel feeler gauge stock. A loop of filament tape was put at one end. The 2 tabs were placed end to end in a envelop made by lengthwise folding 2 inch by 6 inch brass shim stock. This sensor could now independently measure the left and right side of a 6 inch wide roll. The brass and steel sandwich create two contact surfaces of engineering materials. A hand-held force gage was used to determine the force required to initiate slippage of the steel feeler gage in the brass envelope. The tabs were placed in paper and film stacks which were compressed at known pressure in the Instron. The tabs were pulled to determine the pull tab force (PTF). The pressure and pull tab force were regressed to determine the calibration factor. Equations (25) and (26) express these relationships.

$$\text{Paper:} \quad P = 1.9066 * \text{PTF} \quad (25)$$

$$\text{PET:} \quad P = 1.9328 * \text{PTF} \quad (26)$$

Where $P \equiv$ Pressure (psi) and $\text{PTF} \equiv$ Pull Tab Force (lbs)

Wound Roll Test Results

The acoustic measurement techniques were verified by comparison of FSR and pull tabs data on six test rolls. The two direct pressure measurement methods and the two acoustic techniques were used to map the radial pressures in the left and right sides of six different wound rolls. The results of these measurements, along with Hakiel's model output, are given in Figures 29 - 40.

Table 1 and Figures 29 - 40 show excellent results were obtained with the Acoustic Gage when winding tension was used as a dependent variable. The Acoustic Gage predicted pressure averaged only 18 % deviation from average measured value. When the average radial modulus (Constant E_r), determined with time of flight measurements, was substituted for the stack test data the resulting radial pressure profile was similar to the original Hakiel's model output. The Constant E_r had an 148 % deviation from average measured value and Hakiel's model had 213 %. This suggests that the radial modulus determined with stack tests and the average modulus determine with T.O.F. measurements are similar. The excessive pressures predicted by winding models, the excellent results obtained by the Acoustic Gage, and the indication that stack tests produce accurate radial modulus data, cast doubt on the validity of the hoop stress boundary condition, as discussed in Chapter 6.

TABLE I
WOUND ROLL TEST RESULTS

Roll Mat'l	R/R	Measured Data (psi)				Analytical Results (psi)								
		FSRs and Pull Tabs				Within FSR & Pull Tab Measurements (Y/N)								
		Avg	Max	Min	Hakiel	% Err.	Y/N	Const	Er	% Err.	Y/N	Acoustic	% Err.	Y/N
1 L PET	1.1	68	115	35	237	249	N	219	222	N	141	107	N	
	1.5	120	204	50	322	168	N	285	138	N	187	56	Y	
	2.2	46	67	33	104	126	N	105	128	N	66	43	Y	
1 R PET	1.1	44	83	15	219	398	N	157	257	N	48	9	Y	
	1.5	36	66	14	322	794	N	200	456	N	62	72	Y	
	2.2	19	24	15	104	447	N	94	395	N	28	47	N	
2 L PET	1.1	82	92	68	219	167	N	191	133	N	99	21	N	
	1.5	89	135	70	322	262	N	261	193	N	137	54	N	
	2.2	51	73	30	104	104	N	102	100	N	51	0	Y	
2 R PET	1.1	55	62	47	219	298	N	87	58	N	48	-13	Y	
	1.5	56	67	39	322	475	N	111	98	N	62	11	Y	
	2.2	34	54	22	104	206	N	52	53	Y	28	-18	Y	
3 L PET	1.1	43	56	20	254	491	N	183	326	N	68	58	N	
	1.5	93	106	76	428	360	N	253	172	N	96	3	Y	
	2.5	53	76	33	216	308	N	175	230	N	61	15	Y	
3 R PET	1.1	56	72	40	254	354	N	164	193	N	48	-14	Y	
	1.5	47	58	37	428	811	N	215	357	N	63	34	N	
	2.5	47	62	40	216	360	N	160	240	N	43	-9	Y	
4 L News	1.1	41	56	23	60	46	N	64	56	N	41	0	Y	
	1.5	27	30	23	56	107	N	62	130	N	37	37	N	
	2.5	25	28	18	43	72	N	50	100	N	30	20	N	
4 R News	1.1	38	50	23	60	58	N	66	74	N	46	21	Y	
	1.5	25	27	21	56	124	N	64	156	N	43	72	N	
	2.5	28	22	33	43	54	N	51	82	N	33	18	N	
5 L News	1.1	62	73	51	112	81	N	102	65	N	53	-15	Y	
	1.5	62	81	46	109	76	N	100	61	N	49	-21	Y	
	2.5	35	55	22	74	111	N	78	123	N	38	9	Y	
5 R News	1.1	58	65	50	112	93	N	109	88	N	65	12	Y	
	1.5	67	86	51	109	63	N	108	61	N	61	-9	Y	
	2.5	32	42	24	74	131	N	81	153	N	46	44	N	
6 L Bond	1.1	24	36	14	28	17	Y	31	29	Y	20	-17	Y	
	1.5	19	22	15	25	32	N	29	53	N	18	-5	Y	
	2.5	13	17	9	19	46	N	24	85	N	14	8	Y	
6 R Bond	1.1	18	27	11	28	56	N	29	61	N	18	0	Y	
	1.5	12	14	7	25	108	N	28	133	N	16	33	N	
	2.5	15	18	13	19	27	N	23	53	N	12	-20	N	
AVERAGE						213	N=35 Y=1		148	N=34 Y=2		18	N=13 Y=23	

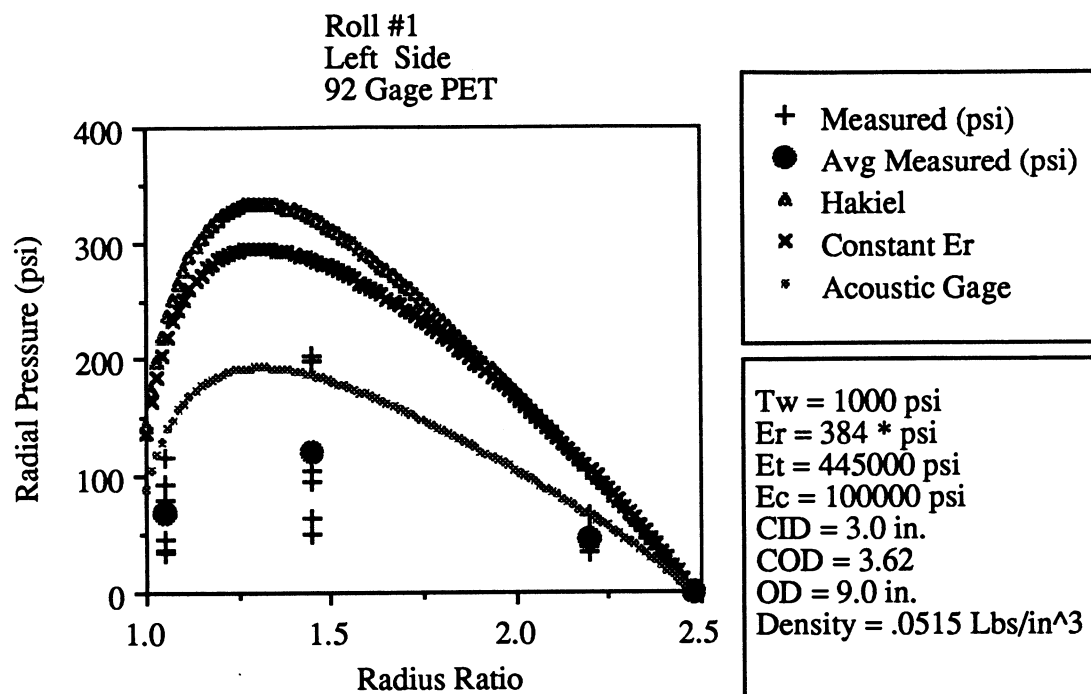


Figure 29. Test Roll #1 (Left)

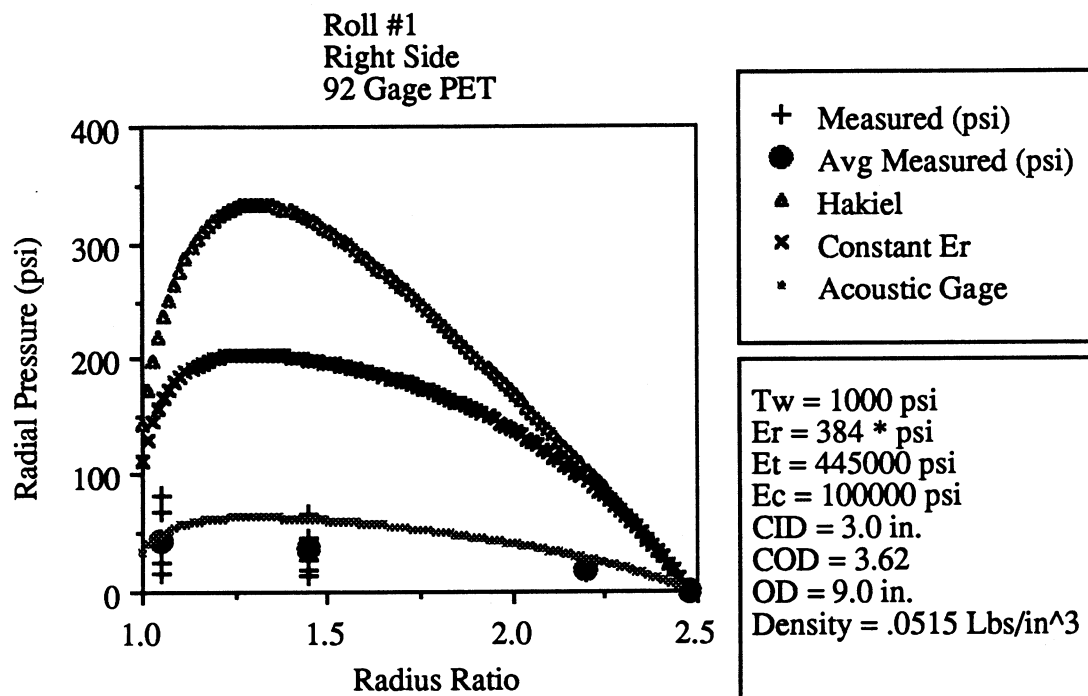


Figure 30. Test Roll #1 (Right)

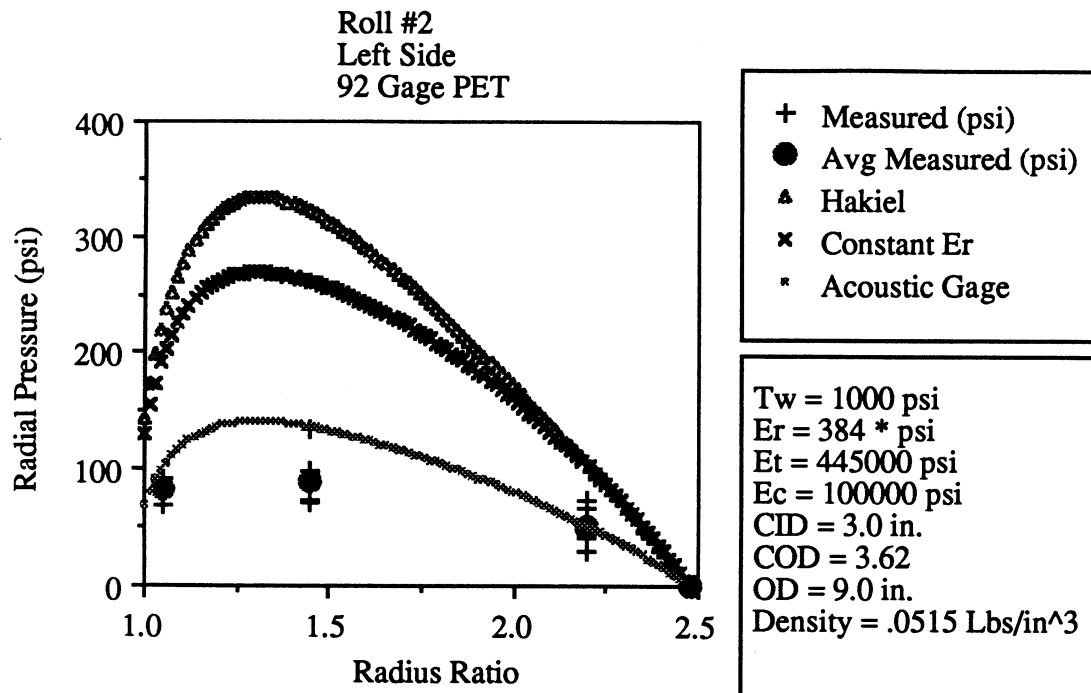


Figure 31. Test Roll #2 (Left)

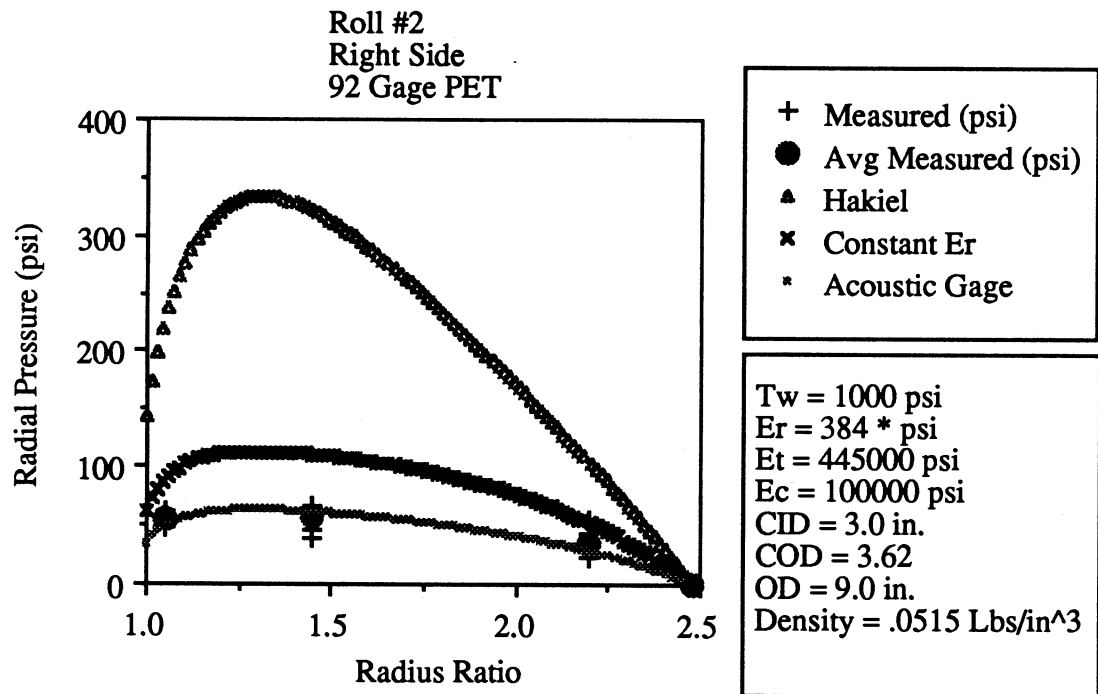


Figure 32. Test Roll #2 (Right)

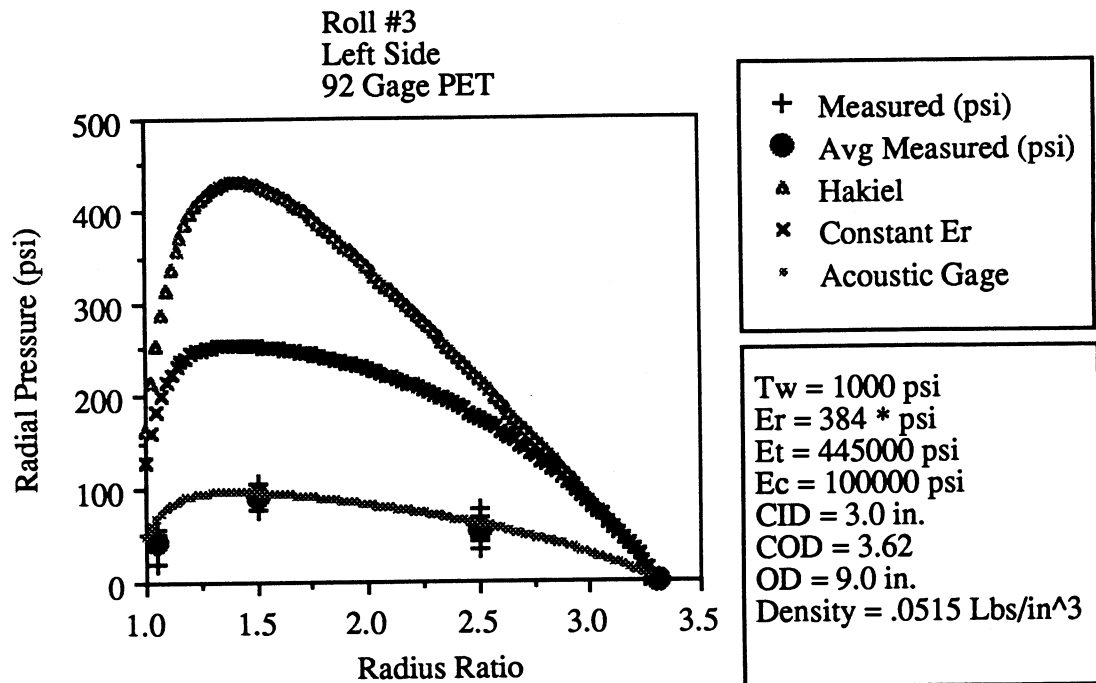


Figure 33. Test Roll #3 (Left)

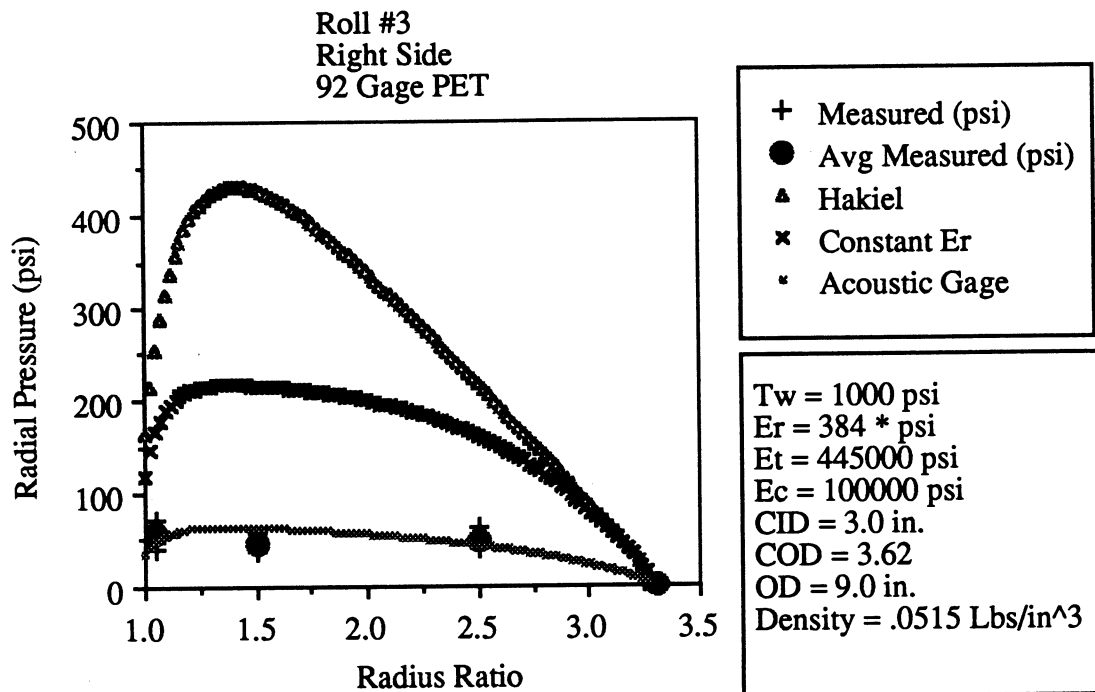


Figure 34. Test Roll #3 (Right)

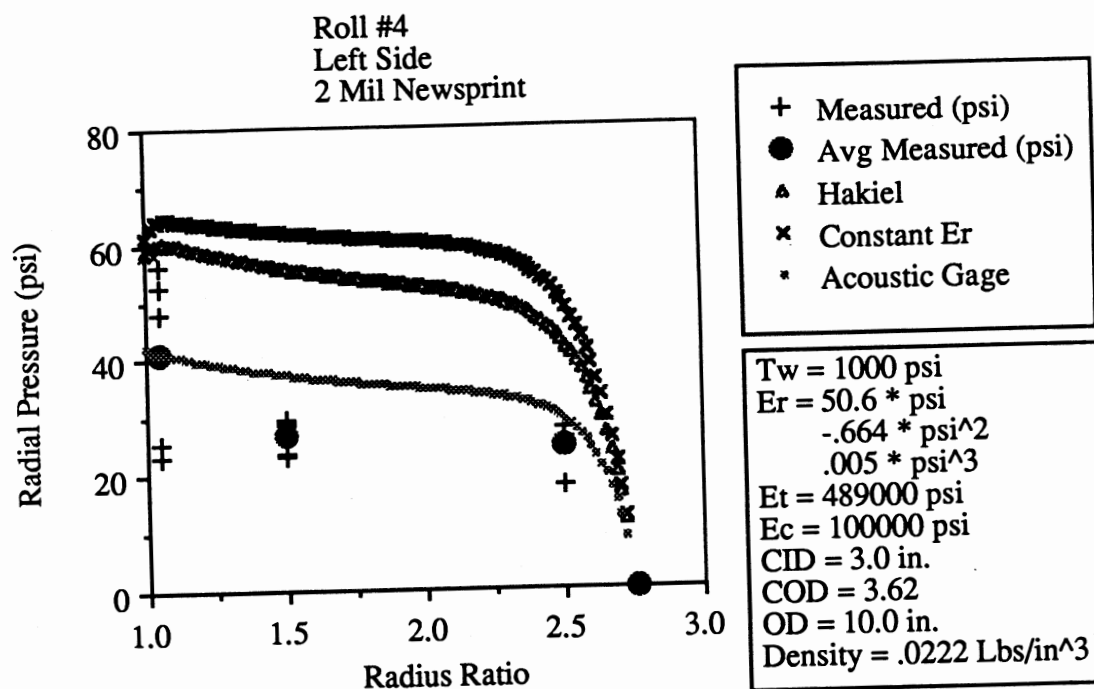


Figure 35. Test Roll #4 (Left)

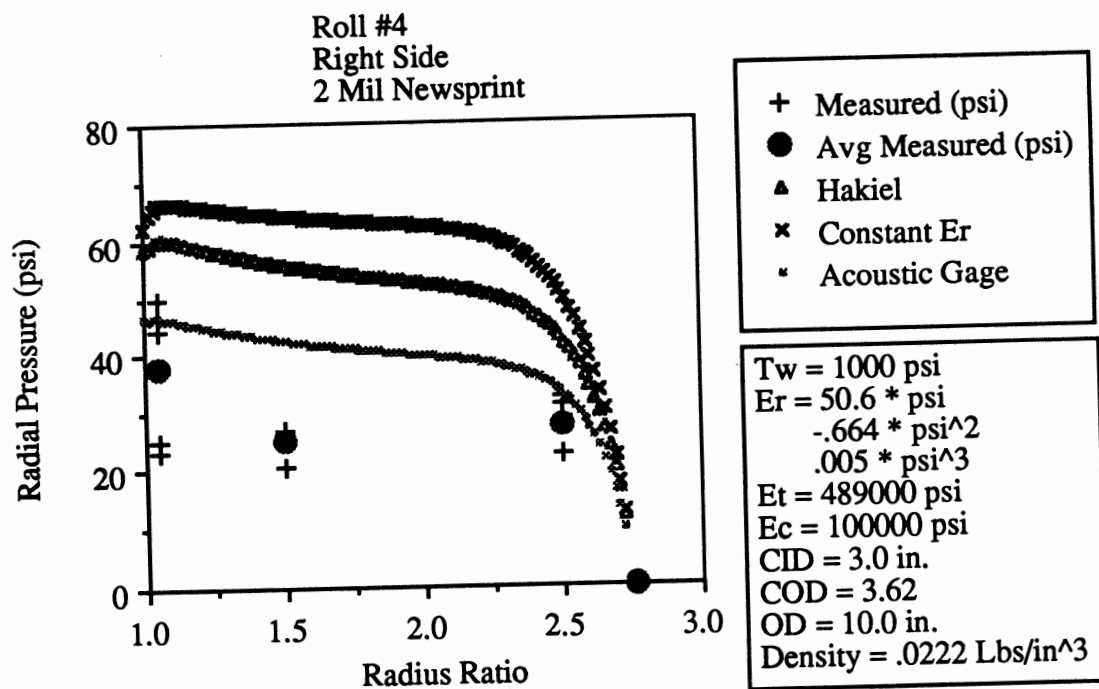


Figure 36. Test Roll #4 (Right)

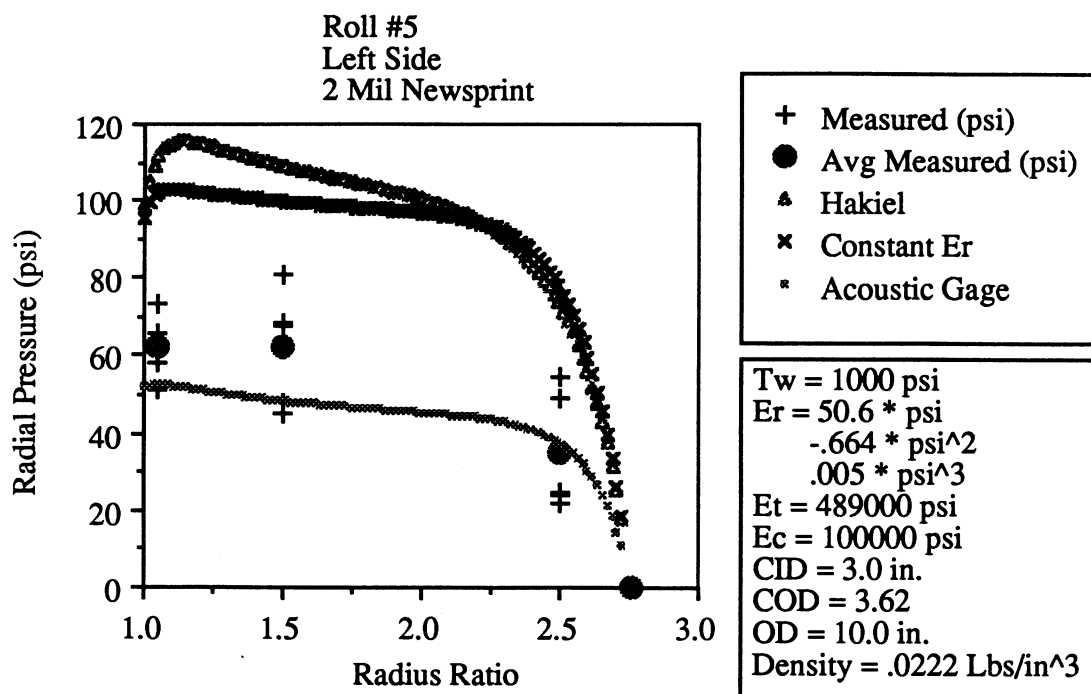


Figure 37. Test Roll #5 (Left)

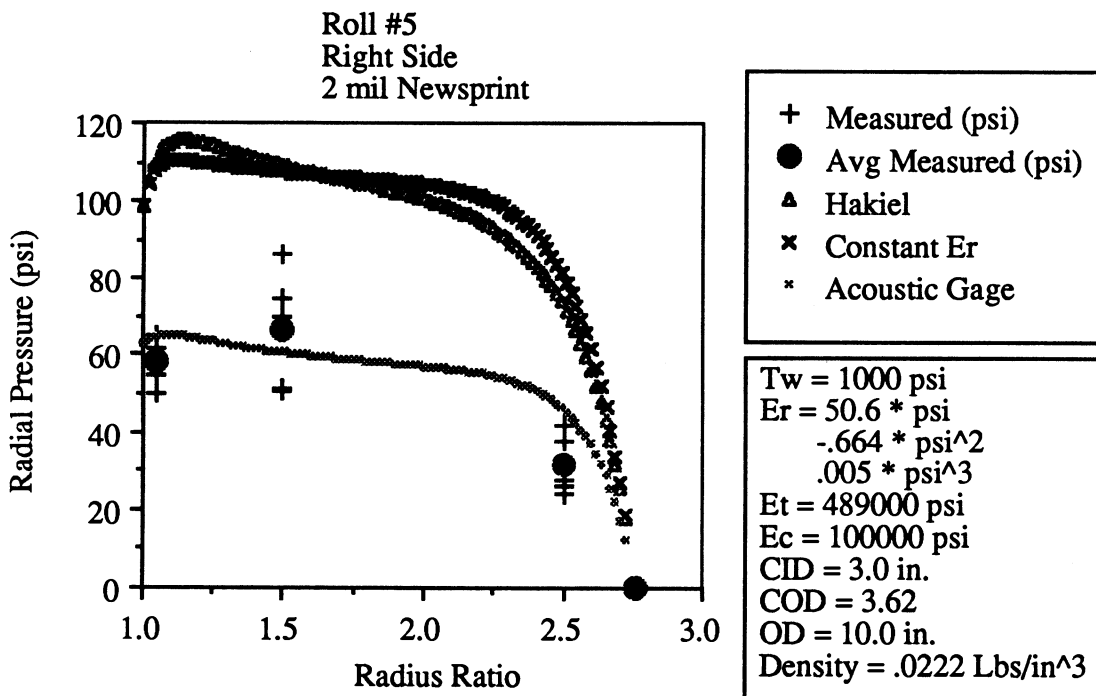


Figure 38. Test Roll #5 (Right)

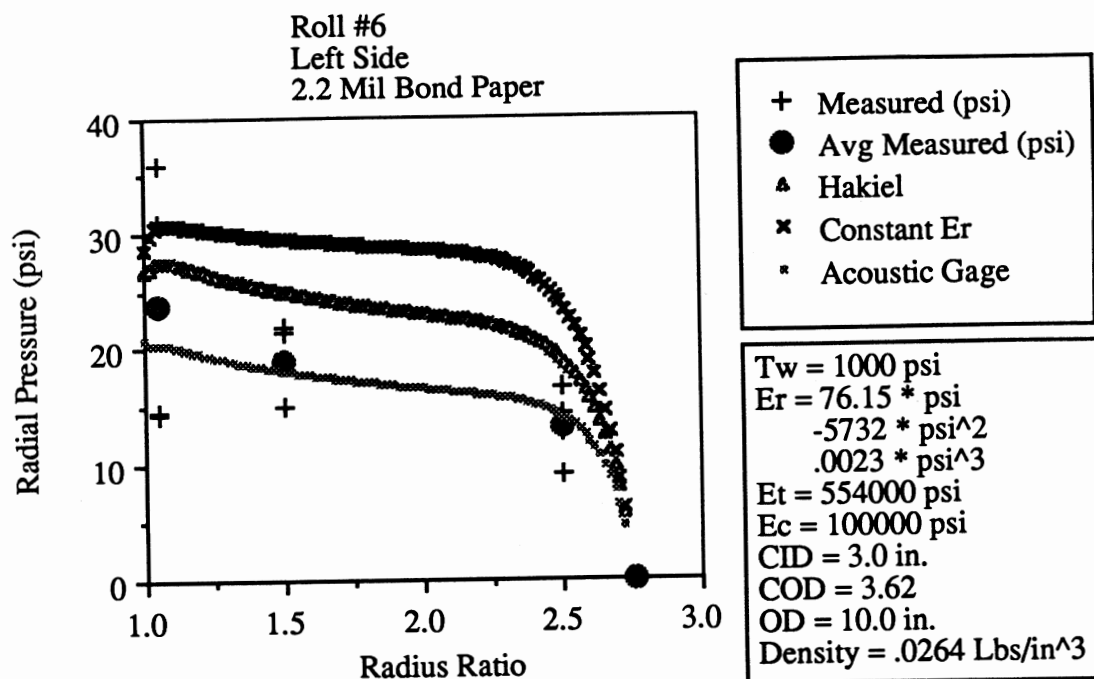


Figure 39. Test Roll #6 (Left)

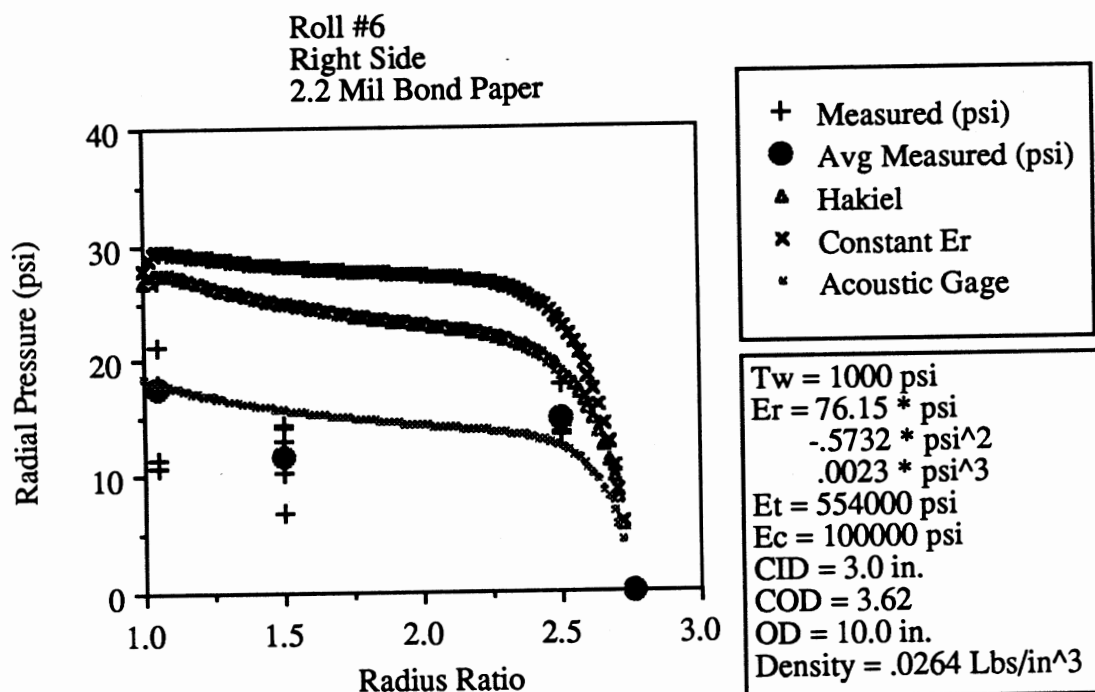


Figure 40. Test Roll #6 (Right)

CHAPTER VIII

RESULTS AND CONCLUSION

A new roll structure evaluation tool has been developed. This measurement technique uses time of flight measurements and existing winding models to determine roll structure. This method has several advantages over existing roll structure evaluation tools. These advantages include being non-destructive, non-intrusive and not requiring knowledge of the winding conditions.

Stack tests were done to determine material properties and confirm that solid body wave mechanics could be used to describe waves in laminates. A mechanical pulsar was developed that can generate a high energy, wide bandwidth wave in a wound roll. A time of flight measurement method was also developed. These components, including an existing winding model, were integrated into an algorithm to determine roll structure. This system is called the Acoustic Roll Structure Gage.

The Acoustic Gage results agreed with two other independent roll structure measurement tools, all of which were much lower than predicted by winding models. The results cast doubt on the validity of the hoop stress equation as an outer boundary condition for wound roll models.

Future Research

The Acoustic Gage went from an idea to a working unit in nine months. A large quantity of research was performed during this period. This research culminated in a working unit, but falls well short of a total understanding of all the potential pitfalls of this measurement tool. Several areas could be studied in more depth including:

1. The pressure determined by the Acoustic Gage is dependent on the stack test E_r function. This function was assumed to be independent of time, temperature, etcetera. This assumption should be researched to determine the effect of other variables. The results of this research would also be valuable to winding technology in general.
2. Figure 15 was used to substantiate the use of solid body wave equations with laminate structures with variable moduli. This assumption may break down under certain circumstances, such as very low pressures. This assumption should be investigated, and a more accurate theory developed.
3. The frequency dependence of wave velocity and attenuation, group velocities and forerunners should also be investigated in more depth.
4. Investigate the accuracy and repeatability of the measurements including signal to noise ratios for a wide variety of materials, including coated products, metals and fabrics.
5. Investigate methods of generating, coupling and receiving higher frequency signals.

Future Development

A new technology such as the Acoustic Gage requires a large amount of development to bring this lab scale model to a viable industrial measurement tool. This development includes the following:

1. Design and build appropriate fixtures.
2. Design and build a reliable pulser and receiver system.
3. Design and build signal processing equipment that can replace the expensive oscilloscope and computer system.
4. Develop a system that is capable of on-line measurement and control. This system might incorporate a non-contact displacement transducer instead of a contacting acceleration sensor system.

REFERENCES

1. Good, J. K., Fikes, W. R., "Predicting Internal Stresses in Center Wound Rolls with an Undriven Nip Roller", Tappi Journal, June 1991.
2. Pfeiffer, J. D. "Internal Pressures in a Wound Roll of Paper", Tappi Journal, Volume 49, No. 8, pp. 342 - 347, 1966.
3. Eriksson, L., "Deformations in Paper Rolls," Proceedings of the First Winding Technology Conference, Stockholm Sweden, pp. 195 - 212, 1987.
4. Roisum, D.R. "The Measurement of Web Stresses During Roll Winding." Ph.D Thesis, Department of Mechanical and Aerospace Engineering, Oklahoma State University, 1990.
5. Hakiel, Z. "Nonlinear Model for Wound Roll Stresses", Tappi Journal, Volume 70, No. 5, pp. 113 - 117, 1987.
6. Habeger, C.C., Wink, W.A., Van Zummeren, M.L., "Using Neoprene-faced, PVDF Transducers to Couple Ultrasound into Solids.", Journal of the Acoustic Society of America 84 (4), pp. 1388-1396, 1988.
7. Habeger, C.C. and Wink, W.A., "Development of a Double Element Pulse Echo, PVDF Transducer", Ultrasonics Volume 28 January, pp. 52-54, 1990.
8. Habeger, C.C., Mann R.W., Baum G.A., "Ultrasonic Plate Waves in Paper", Ultrasonics, pp. 57-62, March 1979.
9. Habeger, C.C., Wink, W.A., Van Zummeren, M.L., "Using a Robot-Based Instrument to Measure the In-Plane Ultrasonic Velocities of Paper", Tappi Journal, pp. 171-175, July 1989.
10. Habeger, C.C. "An Ultrasonic Technique for Testing the Orthotropic Symmetry of Polymeric Sheets by Measuring Their Elastic Shear Coupling Coefficients.", ASME, pp. 366-371, July 1990.
11. Rhee, Seun-Woo, "A Measurement Method for Determining Modulus of Elasticity of a Stack." Master Thesis, Department of Mechanical and Aerospace Engineering, Oklahoma State University, 1988.

12. Altmann, H. C. "Formulas for Computing the Stresses in Center-Wound Rolls." Tappi Journal, Volume 51, No. 4, pp. 176 - 179, April 1968.
13. Tramposh, H. "Relaxation of Internal Forces in a Wound Reel of Magnetic Tape." Journal of Applied Mechanics, volume 32, no. 4, Transactions of the ASME, no. 87, pp 865-873, December 1965.
14. Pfeiffer, J. D., "Prediction of Roll Defects from Roll structure Formulas." Tappi Journal, 70 (5), pp. 113-117, 1979.
15. Yagoda, H.P., "Resolution of a Core Problem in Wound Rolls." Transactions of ASME, Journal of Applied Mechanics, 47(12), pp. 847-854, 1980.
16. Kinsler, L. E., Frey, A. R., Coppens A. B., Sanders, J. V., Fundamentals of Acoustics, Third Edition, John Wiley & Sons, 1982.
17. Brillouin, Leon, Wave Propagation and Group Velocity, Academic Press, New York, 1960.
18. Brekhovskikh, L. M., Waves in Layered Media, Academic Press, (530.8 A652), 1960.
19. Brekhovskikh, L. M., Waves in Layered Media, Academic Press, Second Edition, (530.8 A652), 1980.
20. Ewing, M. W., Jardetzky, W. S. and Press, F., Elastic Waves in Layered Media, McGraw-Hill, (551.2 E95e), 1957.
21. Officer, C.B., Introduction to the Theory of Sound Transmission, McGraw-Hill, (534.2 032i), 1958.
22. Kolsky, H., Stress Waves in Solids, Dover Publications, Inc., New York, 1963.
23. Silk, M. G. Ultrasonic Transducers for Nondistinctive Testing, Adam Hilger Ltd, (620.11274 S584u), 1984.
24. Fikes, M., "The Use of Force Sensing Resistors to Measure Radial Interlayer Pressures in Wound Rolls." Master Thesis, Department of Mechanical and Aerospace Engineering, Oklahoma State University, 1990.
25. Swanson, R.P., "Determination of Wound Roll Structure Using Acoustic Time of Flight Measurements", The First International Conference on Web Handling, Stillwater, Oklahoma, May 1991.

APPENDICES

APPENDIX A

STACK TEST PROCEDURES

ABSTRACT

A procedure was developed to measure E_r as a function of radial pressure. The procedure outlines the necessary equipment, experimental steps and data analysis. The results of this procedure on several different materials was tabulated in Appendix B. Slight variations in this procedure and the associated advantages and disadvantages were discussed.

BACKGROUND

The radial modulus of a material is a very critical variable in the winding process. The radial modulus of a material is a combination of many factors such as air entrainment, surface roughness and coatings. These factors combine to form an elastic modulus in the radial direction that are usually nonlinear. Nonlinear material properties create difficulty in modeling and therefore difficulty in understanding wound roll structure.

Most engineering materials, such as steel, are linear elastic. This means that if we tested a steel specimen in a material testing machine, and plotted stress vs. strain it would form a straight line as shown in Figure 41. The slope of this line will be the elastic or Young's modulus. A stack of web on the other hand does not form a straight line. The entrained air and surface asperities cause the curve to be more like a parabola as shown in Figure 42.

Measuring the radial modulus is very difficult. Therefore the assumption that a stack test (flat geometry) is equivalent to the cylindrical geometry has been made.

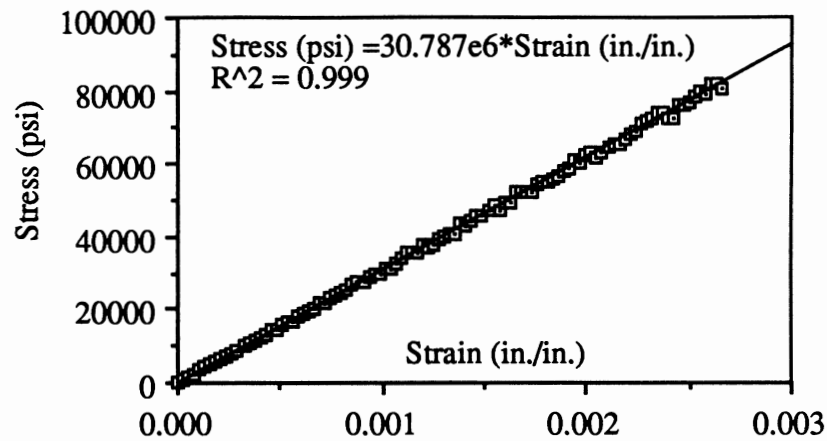


Figure 41. Stress versus Strain for Linear Elastic Material (Steel)

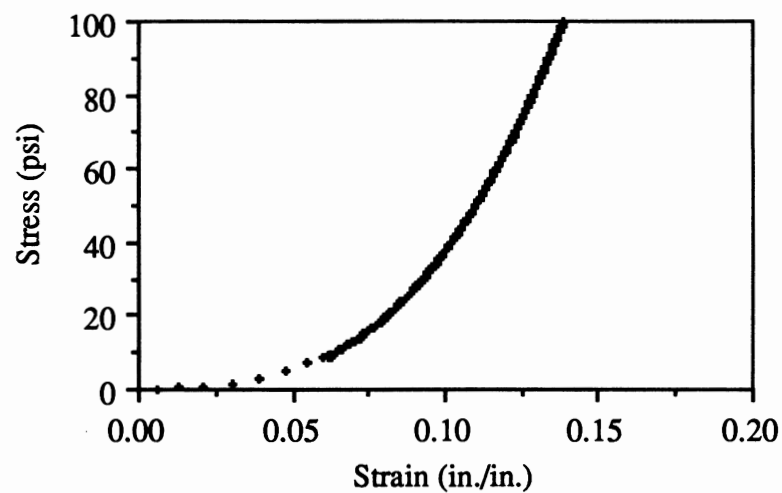


Figure 42. Stress versus Strain for Non-Linear Material (Paper Stack)

APPARATUS

A material testing system such as and Instron 8500 (Figure 43) must be used to determine stack modulus. The Instron consists of a load cell, platens, actuator and data collection system. An extensometer is also highly recommended.

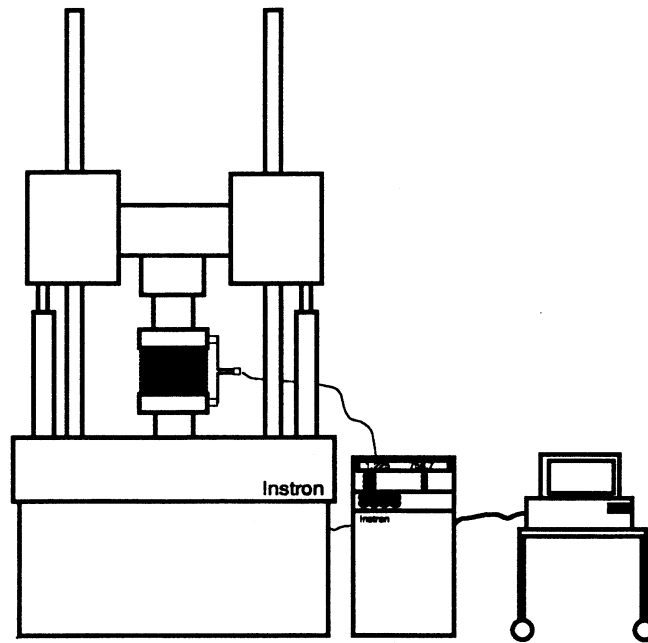


Figure 43. Instron 8500 with Extensometer and PC for Data Collection

PROCEDURE

This procedure assumes you are using an Instron 8500, the procedure on other systems will vary slightly.

Sample Preparation

A material stack of a known area must be prepared. This can be done in one of two ways, carefully cut the sample smaller than the platens with very square sides, or have the sample larger than the platens on all sides and use the area of the platens as the test area. Both methods have advantages and disadvantages, and I suggest doing whichever is easier.

The stack must be thick enough to produce strains that can easily be measured. Soft materials, such as paper, do not need to be as thick as harder materials such as PET. I suggest stack heights in the one to 4 inch range.

Some materials such as paper, can be cut and stacked with relative ease, while other materials are more troublesome. One method that works very well on nonadhesive products is to slab the material off a stock roll. Place the neatly stacked, slabs on a thin board or thick cardboard and cut the slabs to length on a band saw. The friction of the band saw will weld the edges of polymeric stacks, making a very easy to handle unit. This stack must be bigger than the platens so this edge will not affect the results.

Adhesive samples can be made by carefully winding adhesive products on to a specially made flat core. A flat low stress sample can be cut from the resulting flat sides of the roll.

Machine Setup

Turn on the machine and associated equipment. The machine will go through an internal test. When the test is complete, calibrate the load cell using the auto calibration menu. Set the appropriate load limits and actions. Move the actuator to zero. Carefully move the upper platen down just touching the actuator platen or a gage spacer between the two platens. Lock the crosshead. Now you have a reference to determine the original height of the stack at zero load.

Lower the actuator platen and insert the stack. Manually raise the actuator platen until contact results in a slight change in the load cell readout.

If you are going to use an extensometer use rubber bands to attach it to the special fixtures on the platens. Calibrate the extensometer with the auto calibrate function. Set the appropriate limits and actions. It is highly recommended that you use an extensometer for strain measurement instead of the actuator position. There are two reasons for this first the extensometer has one hundred times the resolution of the actuator and secondly because the actuator does not account for machine deflection which can be significant with large sample areas and high forces as shown in Figure 44.

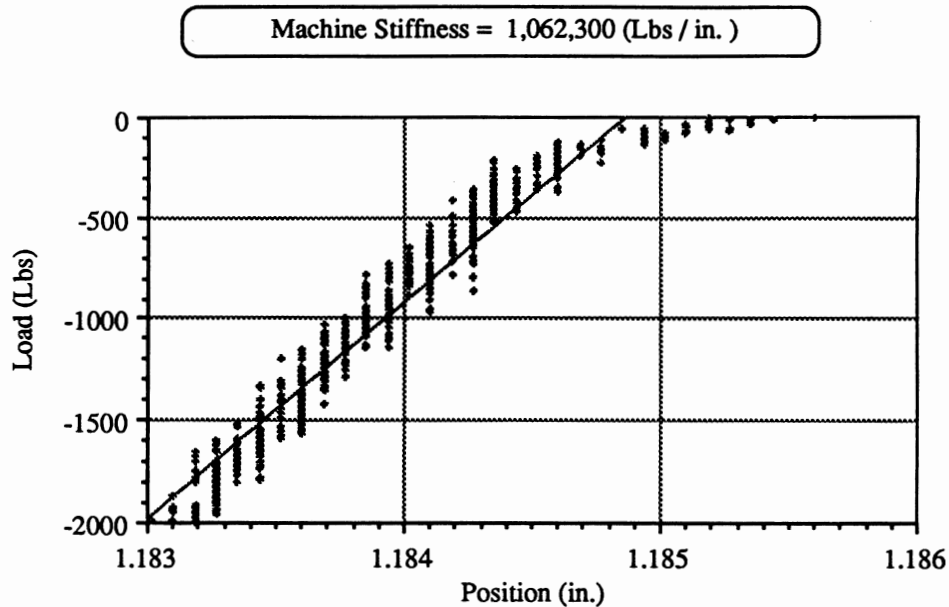


Figure 44. Instron 8500 Machine Stiffness Curve

The machine must now be put in either load or position control. Both methods have advantages and disadvantages. Load control increases the load at a constant rate. This gives data with very even load spacing, which is advantageous when the data is to be regressed with stress as the independent variable. Unfortunately it doesn't give many data points on the very low pressure range. Position control increases the position at a constant rate. This gives data with very even strain spacing, which is advantageous when the data is to be regressed with strain as the independent variable. Unfortunately it doesn't give many data points on the very high pressure range. The decision on which method to use should be based on the final use of the data.

Next a waveform must be setup. A waveform is the action of the machine during the test. An example could be a load ramp the goes from zero to 1000 lbs. at the rate of 100 Lbs. per second. Again the different waveforms have different advantages and the choice of waveform should be based on the final use of the data. The waveform used to collect the data in Appendix A was the loading side of a cyclic triangle load waveform.

Data Collection

The Inston comes with software for automatic execution and data collection. The software is for IBM and compatible systems and is written in Microsoft QuickBasic. The interfacing is done with IEEE-488.

The software is a set of programs that do different tasks. The most commonly used programs are "COLLRAMP.BAS" and "COLLCYCL.BAS", which start a console setup ramp or cycle waveform and collect data. Note that the collramp program will not start a cyclic waveform and visa versa. The program prompts for the type of data to collect and collection rate. The program collects user specified load, position and strain data at rates up to 10 milliseconds per sample. The program starts the waveform, and starts collecting data when the remote button on the console is pressed and stops when the user presses esc. The data pairs are then written in ASCII format to the user specified file. The data is given as a percent of full scale.

DATA ANALYSIS

Modulus is the slope (derivative) of the stress strain curve. Finding the derivative of digital data can be tricky and can potentially produce huge errors.

There are several ways to calculate this derivative. First the stress-strain data could be regressed with a polynomial, which is very easy to differentiate, and secondly the central difference approximation (or linear regression of a small region about the point of interest) can be used. Both methods have advantages and disadvantages.

The polynomial method is quite easy, several programs such as Excel, Cricket Graph, Passage and Lotus 123 offer good polynomial regression functions.

This method needs several words of caution. First the slopes that we are dealing with are often in the 1,000's or 100,000's. It is very difficult to see the difference between a section of a curve with a slope of 100,000 and a slope of 150,000. A regression may look like it goes through all the points, but may have sections with slopes that are

very different from the actual data. For this reason higher order polynomials provide more degrees of freedom and better fits as shown in Figure 45. Higher order polynomials should never be used to extrapolate, only use the regression inside the limits of your data.

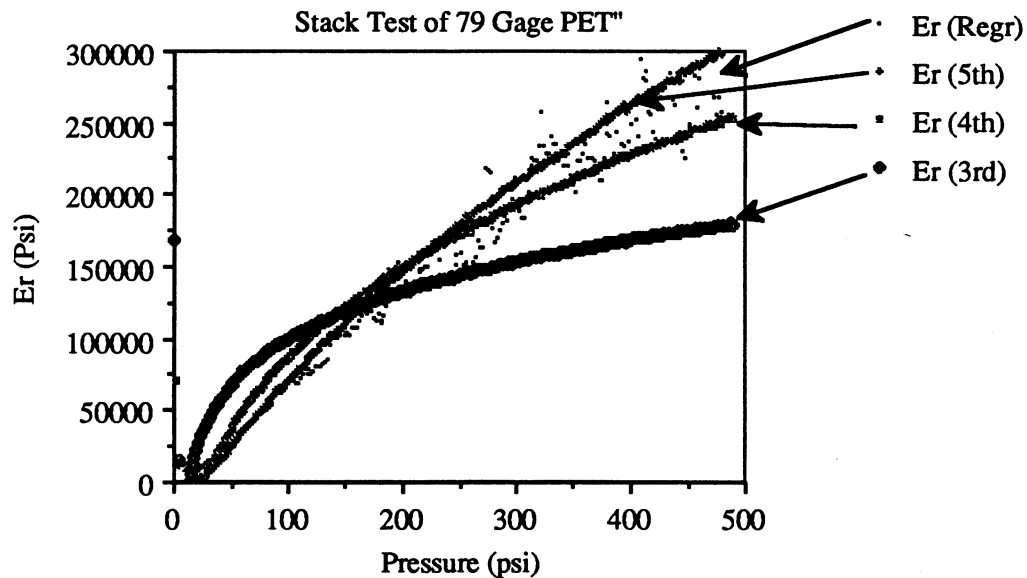


Figure 45. Derivative Plot of Different Order Polynomials

The central difference technique simply takes the difference of two stress values and divides by the difference in the corresponding strain values. This method is very noisy, especially with the very small change in strain which occurs in load control at high pressures. The problem can be avoided by taking large quantities of data and using the Linest() function in a Microsoft Excel. This function finds the slope of a set of x-y pairs around the desired point. The number of x-y pairs can be adjusted to achieve the appropriate "filtering." This procedure can easily be done using the Instron data in a spreadsheet as shown in Figure 46. Column "F" in the slope using the Linest() function on several points from columns "E" and "D".

The last step is to plot the modulus (Column F) versus radial pressure (Column E) and regress the data to find the relationship between E_r and radial pressure, as shown in Figure 47.

	A	B	C	D	E	F
1	POSITION (IN)	PSI	Strain	Strain abs()	Psi	$E_r = ds/de$
2	0.6539756	0.04279043	0	0	0.04279043	0
3	0.6528914	0.04279043	0.00118292	0.00180881	0.04279043	77.7678183
4	0.6498892	0.12567402	0.00419856	0.00642006	0.12567402	83.3394122
5	0.644302	0.29144517	0.00966336	0.01477633	0.29144517	85.8900515
6	0.636463	0.9545298	0.01752736	0.02680124	0.9545298	88.3922999
7	0.6293748	2.56043689	0.02460828	0.03762874	2.56043689	91.3122432
8	0.6266228	3.59650662	0.02741564	0.0419215	3.59650662	101.18952

Figure 46. Spread Sheet Setup to Calculate E_r with Linear Regression

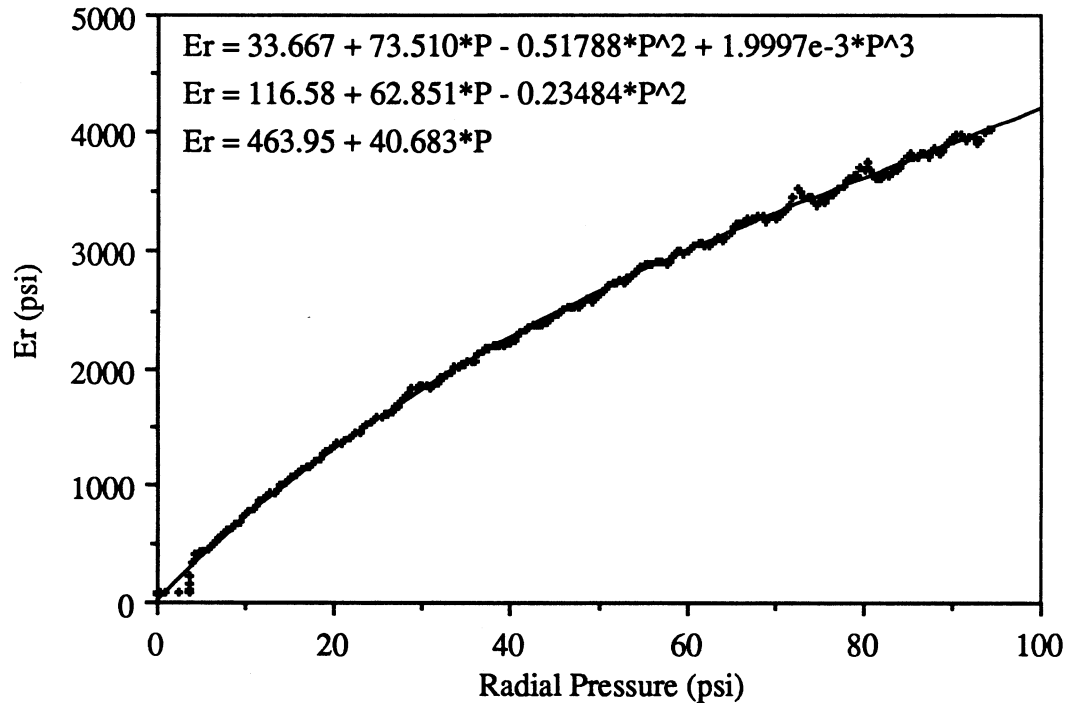


Figure 47. Example of E_r vs Psi with Linear Regression

APPENDIX B

MATERIAL PROPERTY DATA

TABLE II
MATERIAL PROPERTY DATA

Material	C0	C1	C2	C3	K1	K2	Et (psi)	RANGE (PSI)
Bond Paper	0	47.8					554,000	0 - 100
	464	40.5			11.5	40.5		0 - 100
	0	67.5	-0.273					0 - 100
	115	62.7	-0.232					0 - 100
	0	76.2	-0.573	0.0023				0 - 100
	27	74.0	-0.529	0.0020				0 - 100
Newsprint	0	24.3					489,000	0 - 100
	335	19.0			17.6	19.0		0 - 100
	0	36.6	-0.168					0 - 100
	135	31.2	-0.122					0 - 100
	0	50.6	-0.664	0.0050				0 - 100
	92	35.9	-0.239	0.0008				0 - 100
Coated Creape	0	23.9						0 - 100
	210	20.6			10.2	20.6		0 - 100
	0	31.8	-0.111					0 - 100
	94	27.9	-0.077					0 - 100
	0	37.2	-0.297	0.0015				0 - 100
	55	32.9	-0.207	0.0009				0 - 100
79 gage PET	0	636.7						0 - 500
	5540	619.4			8.9	619.4		0 - 500
	0	729.3	-0.257					0 - 500
	-8993	804.2	-0.387					0 - 500
	0	635.5	0.394	-0.0010				0 - 500
	-6232	732.8	-0.011	-0.0005				0 - 500
92 gage PET	0	384.0						0 - 500
	6136	430.8			14.2	430.8	445,000	0 - 500
	0	512.5	-0.173					0 - 500
	-840	519.5	-0.185					0 - 500
	0	572.3	-0.588	0.0006				0 - 500
	-7279	685.9	-1.061	0.0012				0 - 500
Cast PP	0	39.7						0 - 100
	335	34.5			9.7	34.5		0 - 100
	0	52.8	-0.182					0 - 100
	133	47.3	-0.134					0 - 100
	0	62.5	-0.519	0.0026				0 - 100
	36	59.7	-0.461	0.0023				0 - 100
Adhesive PP	0	83.8						0 - 100
	-1393	105.1			-13.3	105.1		0 - 100
	0	16.7	0.912					0 - 100
	611	-7.9	1.119					0 - 100
	0	57.1	-0.460	0.0105				0 - 100
	58	52.9	-0.377	0.0100				0 - 100

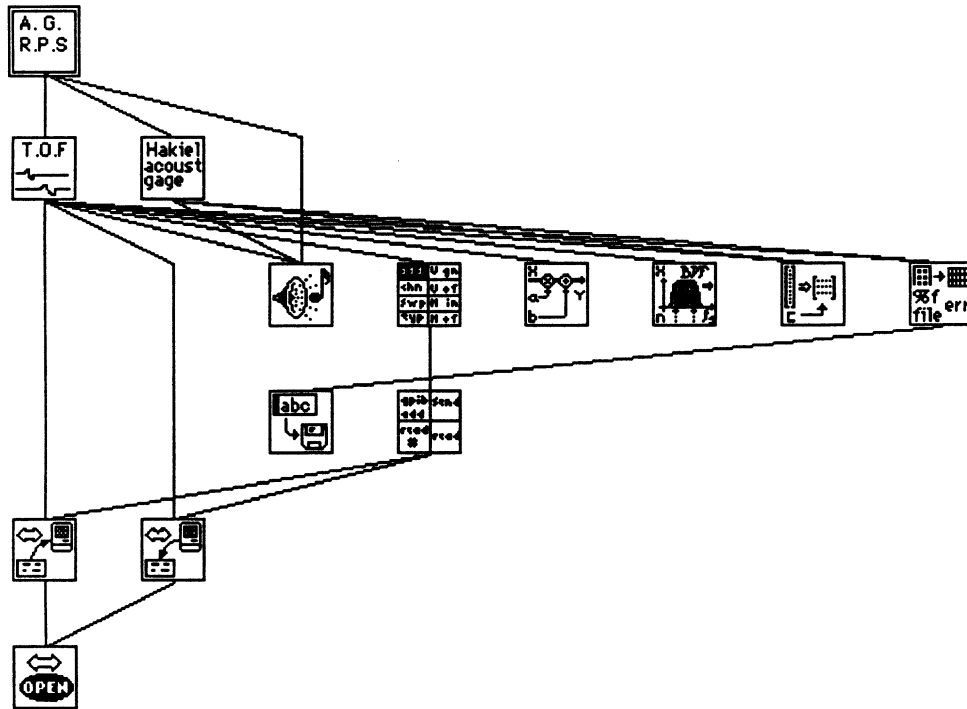
APPENDIX C

ACOUSTIC GAGE PROGRAM (LabVIEW 2)

Acoustic Gage
Wednesday, July 17, 1991 9:06 AM

Page 1 A.G.
R.P.S.

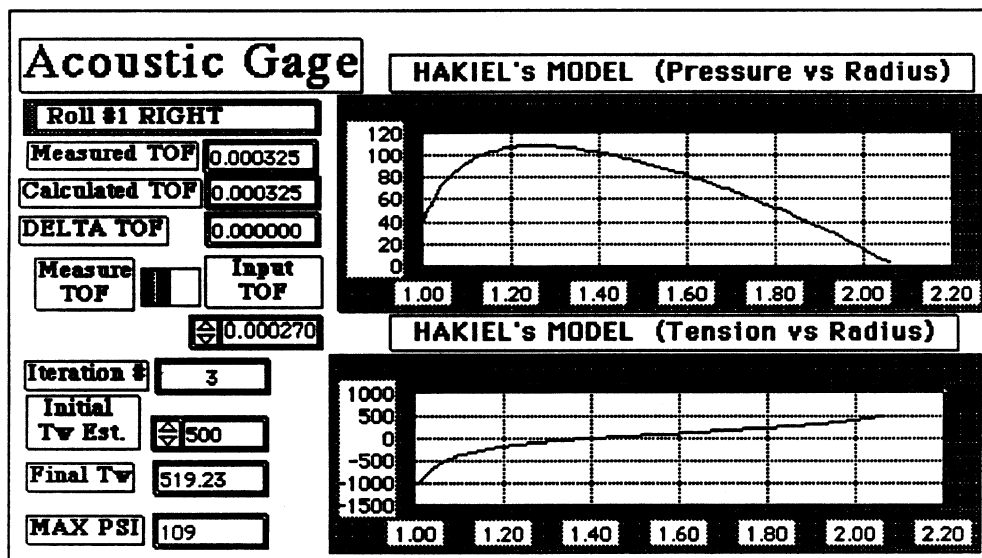
Position in hierarchy



Acoustic Gage
Wednesday, July 17, 1991 9:06 AM

Page 2 A.G.
R.P.S.

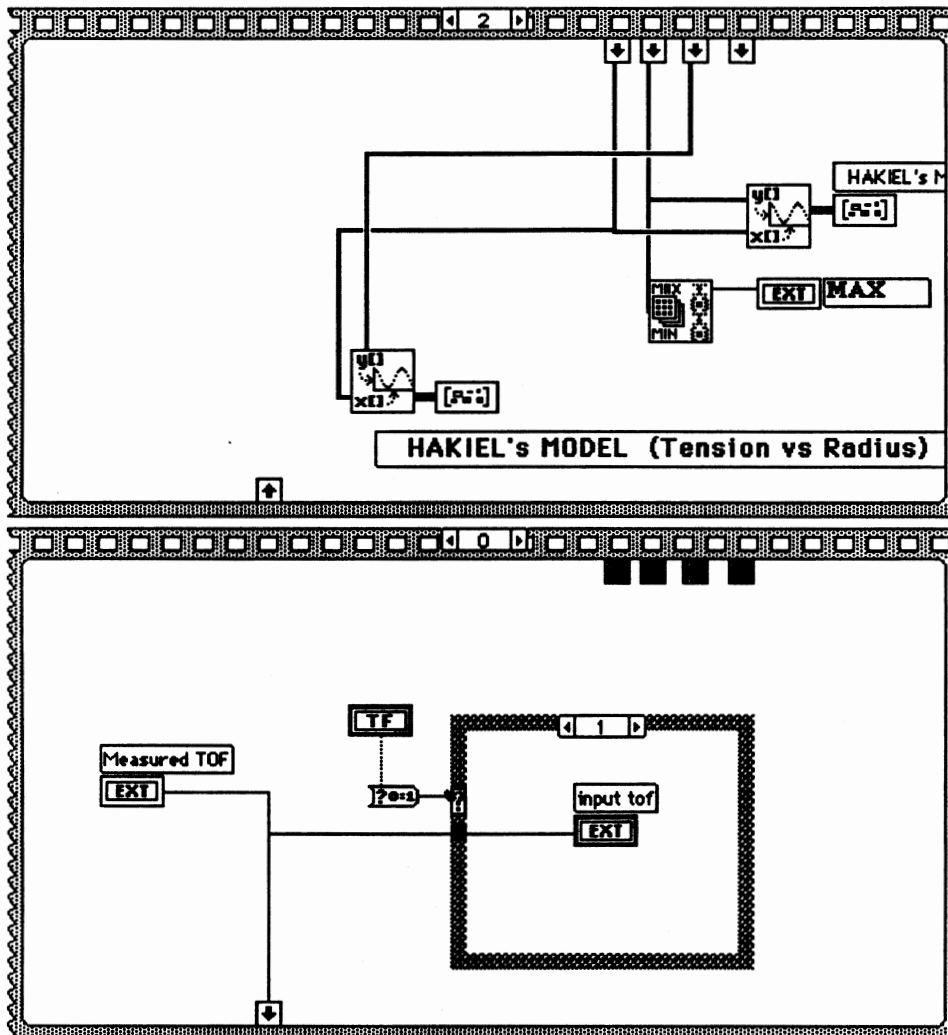
Front Panel



Acoustic Gage
Wednesday, July 17, 1991 9:06 AM

Page 3 A.G.
R.P.S

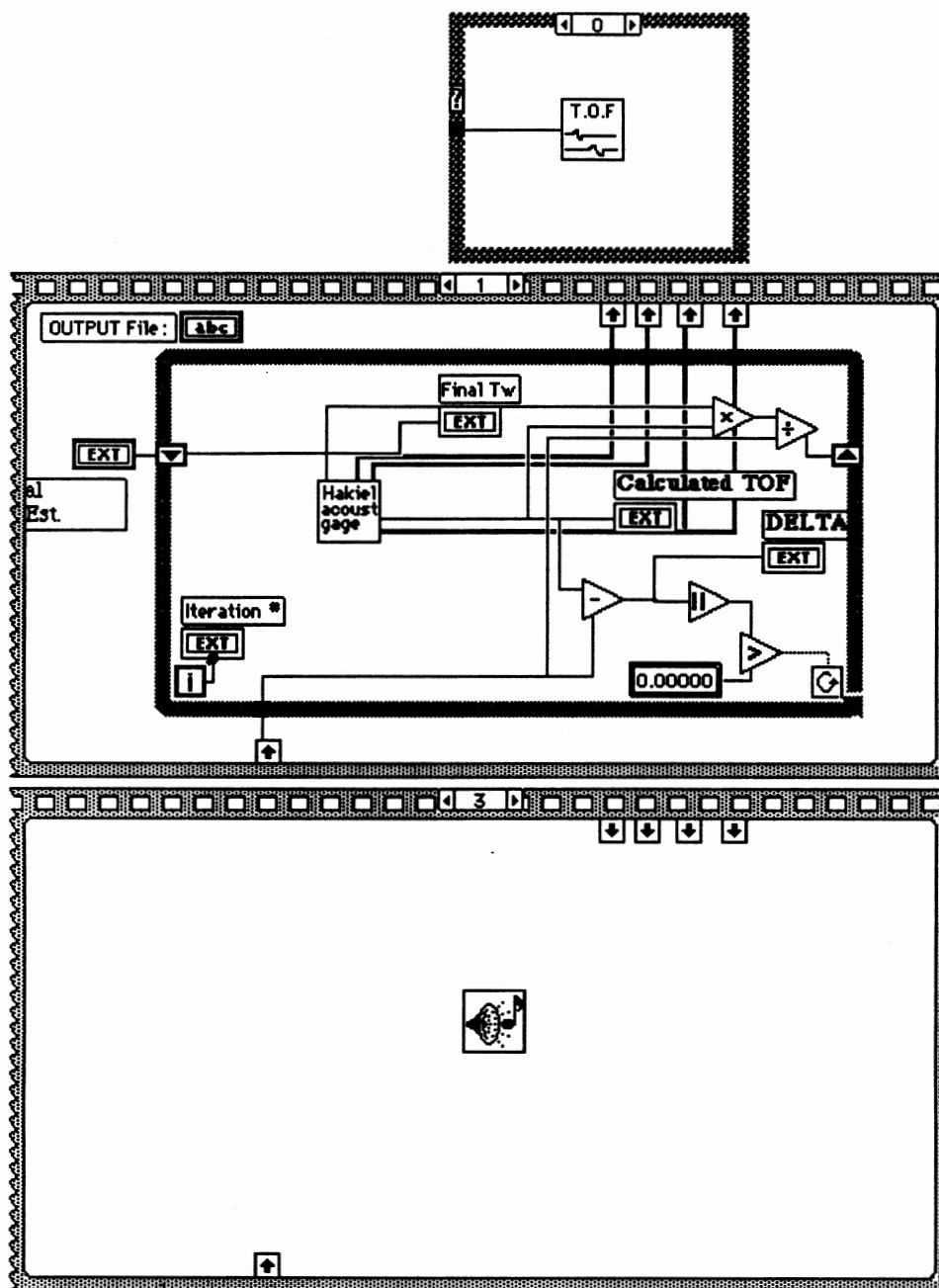
Block Diagram




Acoustic Gage
Wednesday, July 17, 1991 9:06 AM

Page 4

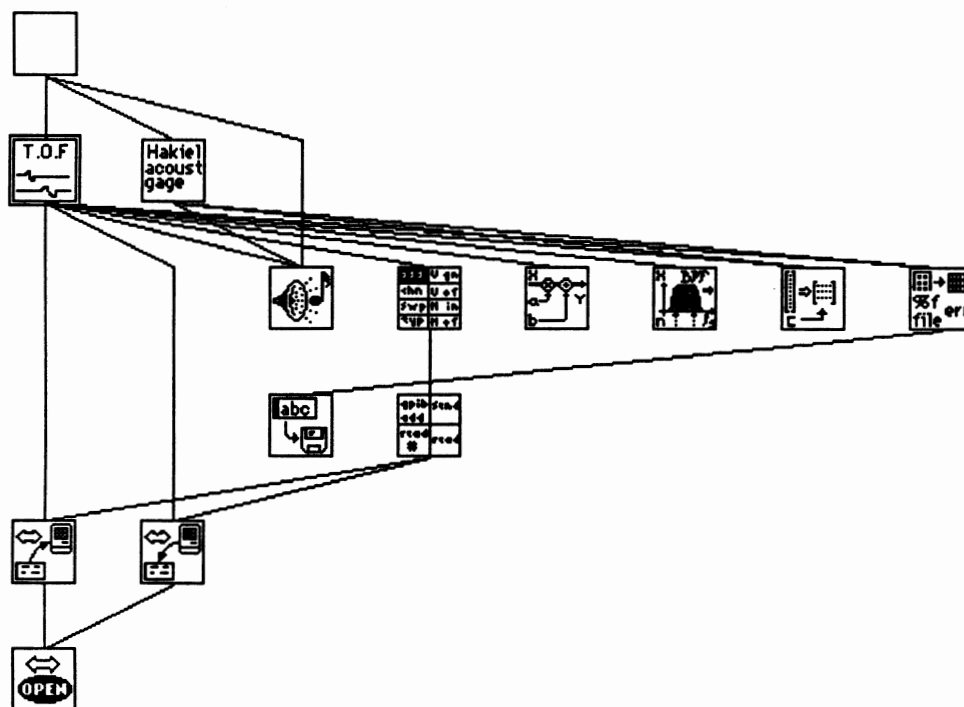
A.G.
R.P.S




TOF Icon
Wednesday, July 10, 1991 8:22 AM

Page 1 

Position in hierarchy



Connector Pane

 — Time of Flight

TOF Icon

TDF Icon
Wednesday, July 10, 1991 8:22 AM
Front Panel

Page 3 TDF Icon
Wednesday, July 10, 1991 8:22 AM

Page 4 TDF Icon

Amplitude Array #1 (volts)

Amplitude Array #2 (volts)

OP18 addr

Output Array (volts)

L0 (sec)

At (sec)

#1 Filter Order #2 Filter Order

Sampling Hz Sampling Hz

HP Filter Hfc HP Filter Hfc

LP Filter Lfc LP Filter Lfc

* Points

Sparsing

Core TDF

Time of Flight

Wave 1 Wave 2

Expand A - Expand A -

Expand B - Expand B -

Memory C - Memory C -

Memory D - Memory D -

Function E - Function E -

Function F - Function F -

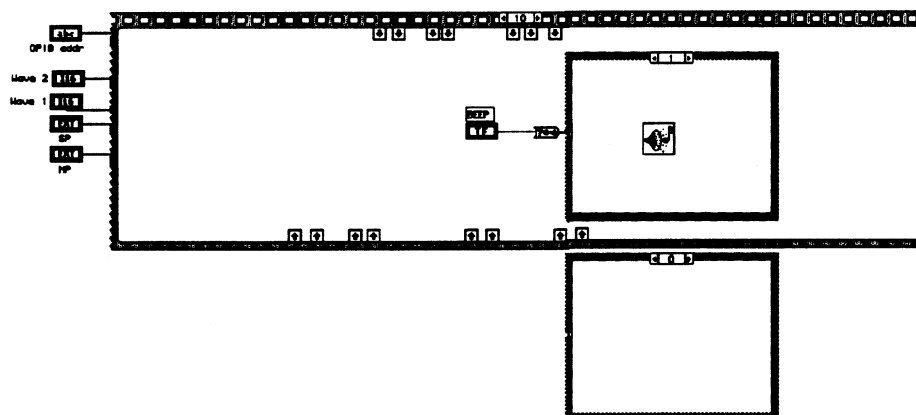
Channel 1 - Channel 1 -

Channel 2 - Channel 2 -

TDF Icon
Wednesday, July 10, 1991 8:22 AM
Block Diagram

Page 5 TDF Icon
Wednesday, July 10, 1991 8:22 AM

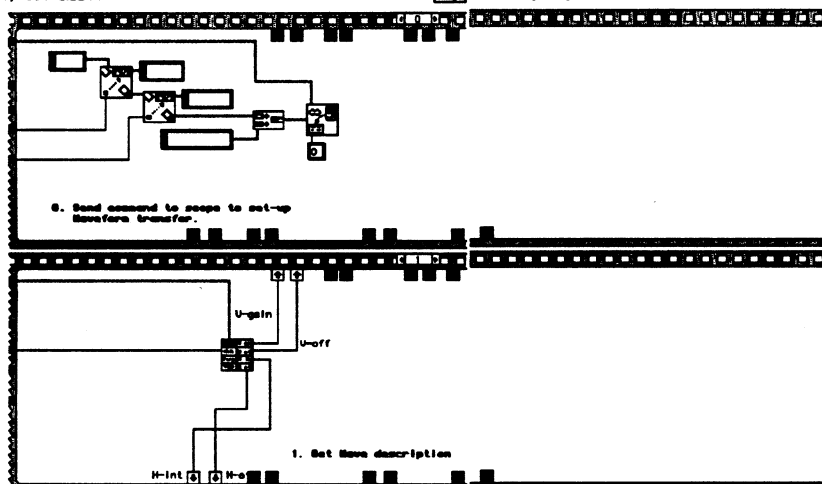
Page 6 TDF Icon



TDF Icon
Wednesday, July 10, 1991 8:22 AM

Page 7 TDF Icon
Wednesday, July 10, 1991 8:22 AM

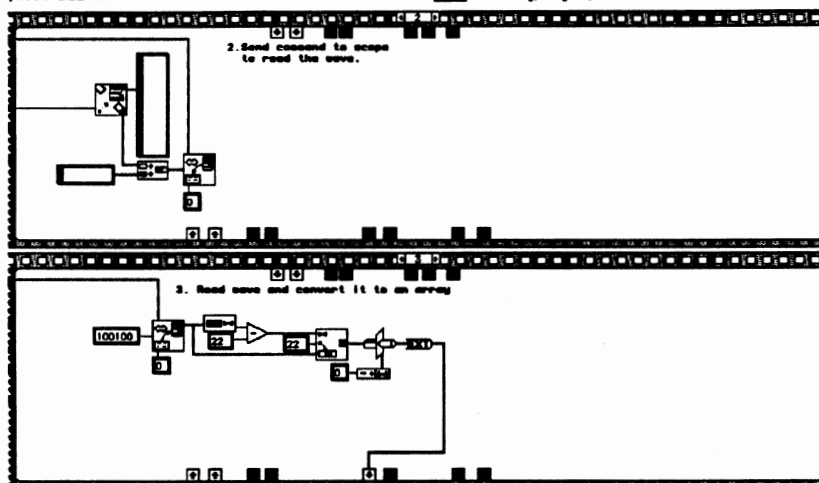
Page 8 TDF Icon



T0F Icon
Wednesday, July 10, 1991 8:22 AM

Page 9 T0F Icon
Wednesday, July 10, 1991 8:22 AM

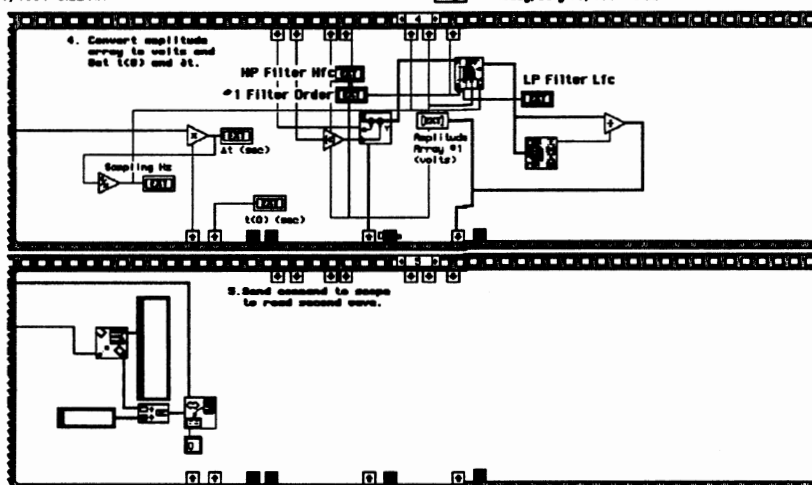
Page 10 T0F Icon



T0F Icon
Wednesday, July 10, 1991 8:22 AM

Page 11 T0F Icon
Wednesday, July 10, 1991 8:22 AM

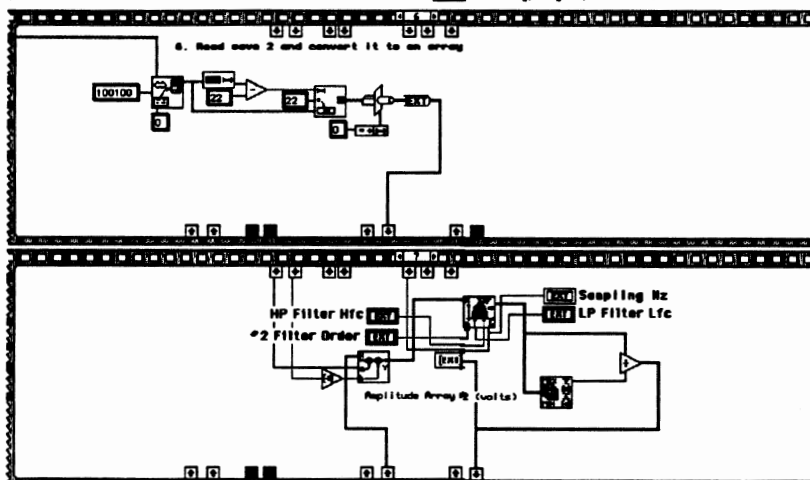
Page 12 T0F Icon



TDF Icon
Wednesday, July 10, 1991 8:22 AM

Page 13 TDF Icon
Wednesday, July 10, 1991 8:22 AM

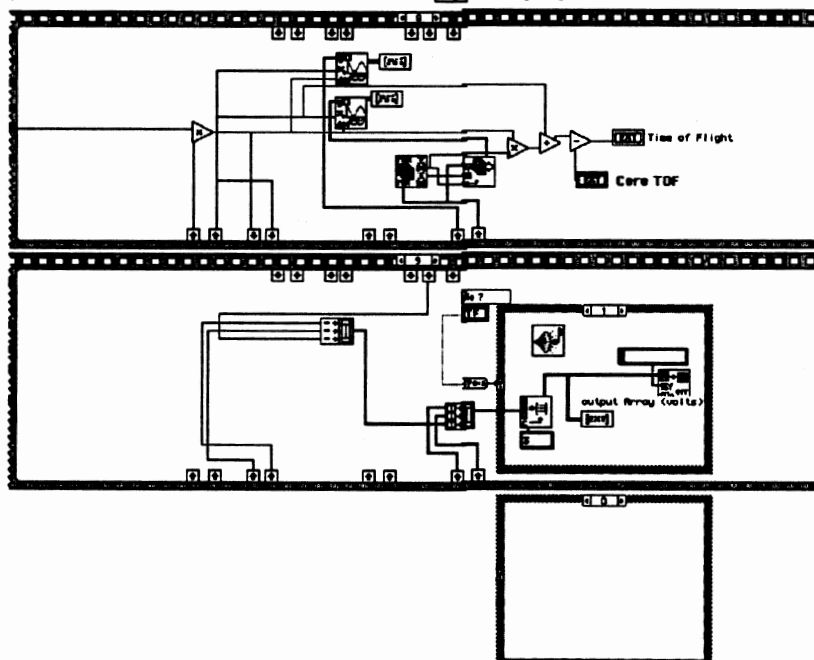
Page 14 TDF Icon




TDF Icon
Wednesday, July 10, 1991 8:22 AM

Page 15 TDF Icon
Wednesday, July 10, 1991 8:22 AM

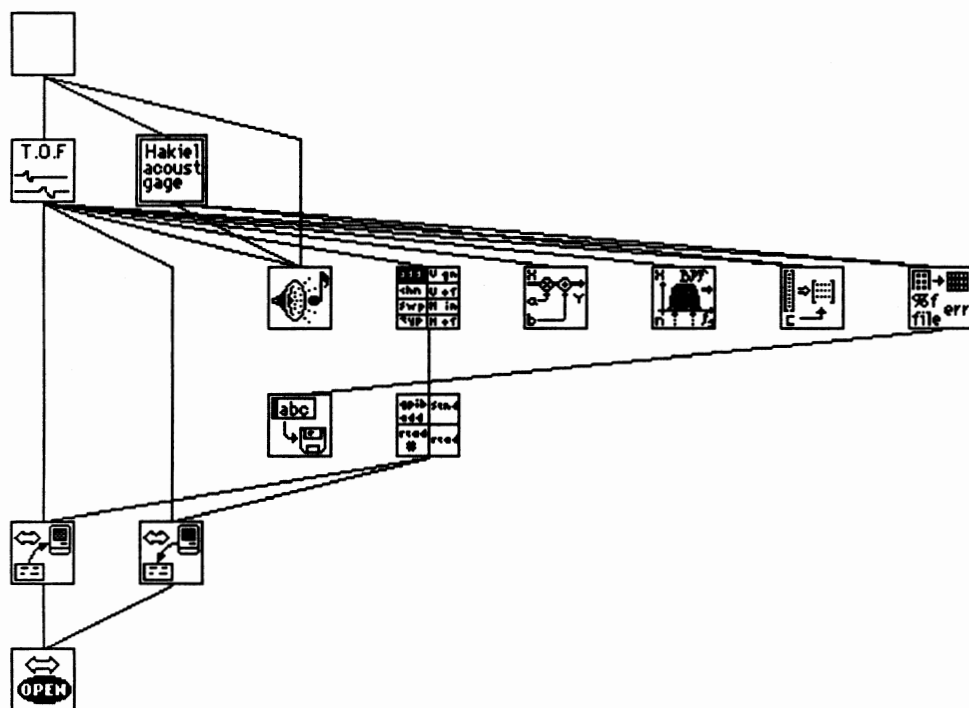
Page 16 TDF Icon



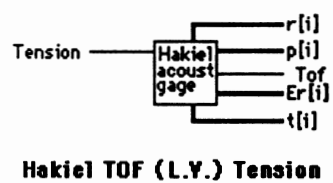
Hakiel TOF (L.V.) Tension
Tuesday, July 2, 1991 3:53 PM

Page 1 

Position in hierarchy



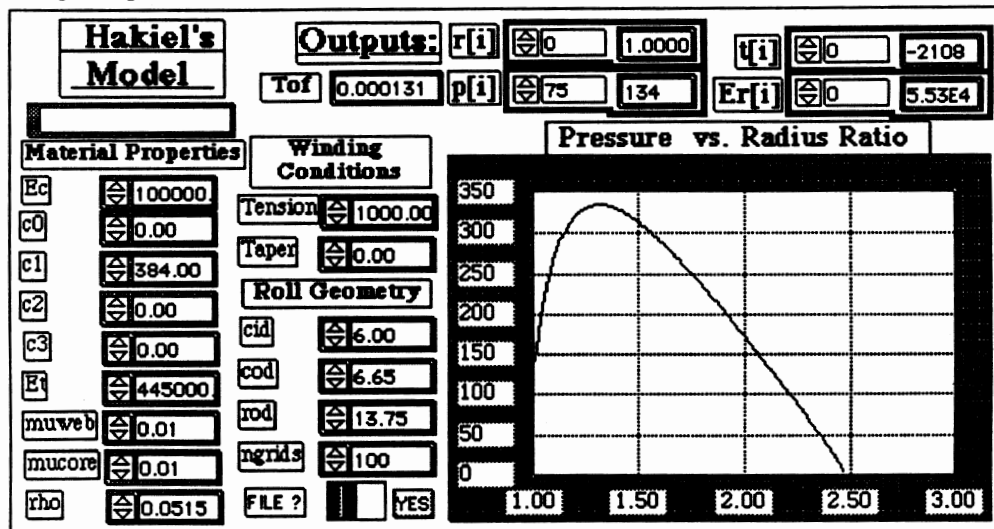
Connector Pane



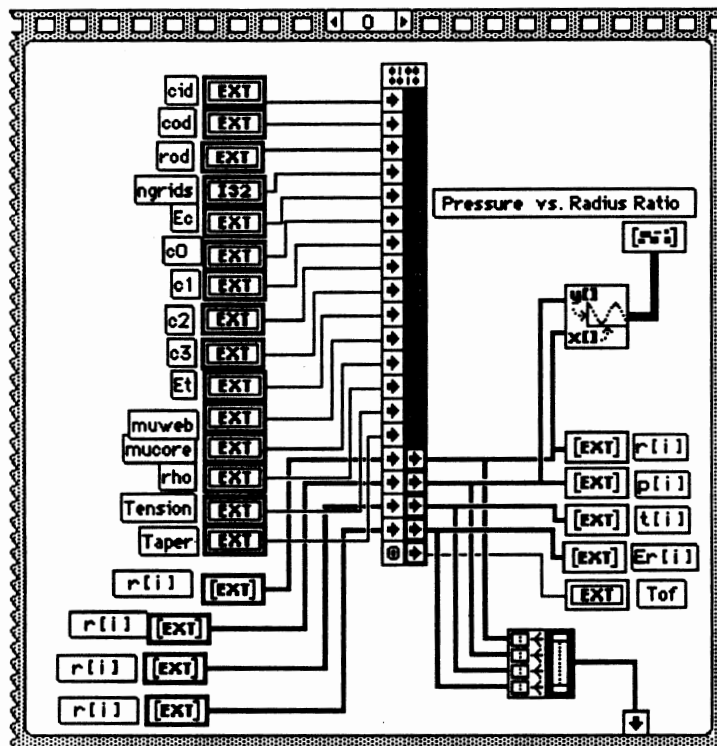
Front Panel

Hakiel TOF (L.V.) Tension
Tuesday, July 2, 1991 3:53 PM

Page 2 Hakiel
acoust
gage



Block Diagram




```

/*
 * Code Interface Node header file
 */

/*
 * typedefs
 */

typedef struct {
    int32 dimSize;
    float96 arg1[];
} TD2;
typedef TD2 **TD2Hdl;

/*
 * Code Interface Node prototypes:
 */

pascal void CINInit(void);
pascal void CINDispose(void);
pascal void CINAbort(void);
pascal void CINRun(float96 *input1, float96 *input2, float96 *input3, int32 *input4,
float96 *input5, float96 *input6, float96 *input7, float96 *input8, float96 *input9,
float96 *input10, float96 *input11, float96 *input12, float96 *input13, float96 *input14,
float96 *input15, TD2Hdl output1, TD2Hdl output2, TD2Hdl output3, TD2Hdl output4,
float96 *output5);
pascal void CINLoad(void);
pascal void CINSave(void);

/*****
*****
*
*      HAKIEL WINDING MODEL                      By R.P. Swanson 2-5-91
*
*      This program uses Z. Hakiels Finite Difference approach
*      (1986 Tappi Finishing and Converting Conference) to solve
*      for stresses in a wound roll. The code is written in "C" for
*      use with a "Think C" compiler on a Macintosh computer.
*
*      Rev 1.0      2-5-91 New Program
*
*****
*****/

```



```

c2=*in8;          /* Er(p) ploy fit curvature*/
c3=*in9;          /* Er(p) ploy fit cubic*/
et=*in10;         /* Tangential modulus of web */
muweb=*in11;      /* Poisson's ratio of web stack */
mucore=*in12;     /* Poisson's ratio of core */
rho=*in13;        /* density of web */
sten=*in14;       /* Starting web stress */
taper=*in15;      /* Winding tension taper % */

```

```

initialize();
n=ngrids;

```

```

/* Add lap #1 */
p[1]=tw[1]*h/r[1];

```

```

/* Add lap #2 */
p[2]=tw[2]*h/r[2];
p[1] += p[2]/rk;
er[2]=calc_er(p[2]);

```

```

/* Add lap #3 */
p[3]=tw[3]*h/r[3];
aa2=1.0-(3.0*h)/(2.0*r[2]);
bb2=(h*h/(r[2]*r[2]))*(1.0-et/er[2]) - 2.0;
cc2=1.0+(3.0*h)/(2.0*r[2]);
dp[1]=cc2*p[3]/(-rk*bb2-aa2);
dp[2]=rk*dp[1];
p[1] += dp[1];
p[2] += dp[2];

```

```

/* Add lap #4 thru n using Tri-diagonal by B.E. LEE */
for(i=4;i<=n;++i)
{
    tri_diag(i);

    /* Add dp[] to p[] */
    for(jj=1;jj<=i;++jj)
    {
        p[jj] += dp[jj];
    }
}
/*end of lap 4 thru n loop */

```

```

/* Calculate t[] and er[]*/

```

[illegible]

```

/*****/
void initialize() /* START OF initialize */
/*****/
{
  int j,jj;
  double r02,rc2;

  /* zero matrix*/
  for(j=0;j<ngrids+1;j++)
  {
    p[j]=0.0;
    t[j]=0.0;
    dp[j]=0.0;
    a[j]=0.0;
    b[j]=0.0;
    c[j]=0.0;
    d[j]=0.0;
    er[j]=0.0;
    r[j]=0.0;
    tw[j]=0.0;
    beta[j]=0.0;
    gama[j]=0.0;
  }

  /* calculate "h" the normalized grid spacing */
  h=((rod-cod)/2.0)/ngrids)/(cod/2.0);

  /* calculate r[i] the normalized radius array */
  for(j=0;j<ngrids+1;j++)
    r[j]=1.0 + h*(j - 1.0);

  /* calculate tw[i] the winding tension array */
  for(j=0;j<ngrids+1;j++)
    tw[j]= sten * (1.0 - (taper/100.0)*((r[j] - r[0]) / r[j]));

  /* calculate ecm the core stiffness from Roisum p-25*/
  r02=(cod/2.0)*(cod/2.0);
  rc2=(cid/2.0)*(cid/2.0);
  ec=ecm*( r02 - rc2 )/(r02 + rc2 - mucore * (r02 - rc2));

  /* calculate cc the core constant */

```

```

cc = et/ec - 1.0 + muweb;
rk=1.0+h*cc;

}

/*****
double calc_er(press)          /* START OF calc_er();
*/
/*****
double press;
{
double erl;
erl=c0+c1*press+c2*press*press+c3*press*press*press;
return(erl);
}

/*****
void tri_diag(int k)           /* START OF tri_diag(press);
*/
/*****
{
int iii;
double gi2,h_r;
k=k-1;
    dp[k+1]=tw[k+1]*h/r[k+1];
    a[1] = 0.0;
    b[1] = -rk;
    c[1] = 1.0;
    d[1] = 0.0;
    for (iii=2; iii <= k; iii++) {
        h_r = h/r[iii];
        gi2 = et/calc_er(p[iii]);
        a[iii] = 1.0-1.5*h_r;
        b[iii] = h_r*h_r*(1.0-gi2)-2.0;
        c[iii] = 1.0+1.5*h_r;
        d[iii] = 0.0;
    }
    d[k] = -dp[k+1]*c[k];
    c[k] = 0.0;

    beta[1] = b[1];
    gama[1] = d[1]/b[1];
    for (iii=2; iii <= k; iii++) {

```



```

        beta[iii] = b[iii]-a[iii]*c[iii-1]/beta[iii-1];
        gama[iii] = (d[iii]-a[iii]*gama[iii-1])/beta[iii];
    }
    dp[k] = gama[k];
    for (iii=k-1; iii >= 1; iii--)
        dp[iii] = gama[iii]-c[iii]*dp[iii+1]/beta[iii];
}

```

APPENDIX D

ACOUSTIC GAGE PROGRAM (Quick BASIC)

```

'
' |
' | Acoustic Gage Program , REVISION 06-14-91
' | This program solves for wound roll internal pressure
' | From Time of Flight, Material Property and Geometry Data
' |
' | Special version for the Quick Basic for Mac   R.P.Swanson 6-14-91
' |
'
Asize =100

```

```

gx1=200      ' Abs graph coords in Pixels
gy1=45
gx2=500
gy2=335

```

```

OPTION BASE 0
DIM r(Asize), p(Asize), t(Asize), er(Asize)
DIM tw(102),a(102),b(102),c(102),d(102),dp(102),beta(102),gama(102)

```

```

' Set up Windows
WINDOW 1,"HAKIEL'S Model - Roll Pressure vs Radius",(1,40)-(512,342),1
WINDOW 2,"graph",(gx1,gy1)-(gx2,gy2),3
WINDOW 3,"command window",(10,315)-(195,330),4
GOSUB defaults
1 'start of main loop
GOSUB MENU1
GOTO 1

```

```

'GOSUB iorollpara

```

```

*****
END          '          End of Main
*****

```

```

501 LOCATE 1, 1 :PRINT "          "
    LOCATE 1, 1: INPUT "1) Tension (psi) ="; sten
    RETURN
502 LOCATE 1, 1 :PRINT "          "
    LOCATE 1, 1: INPUT "2) Taper (%) ="; taper

```

```

RETURN
503 LOCATE 1, 1 :PRINT “                                     “
    LOCATE 1, 1: INPUT “3) Pack (pli) =”; pack
    RETURN
504 LOCATE 1, 1 :PRINT “                                     “
    LOCATE 1, 1: INPUT “4) Core ID (in.) =”; cid
    RETURN
505 LOCATE 1, 1 :PRINT “                                     “
    LOCATE 1, 1: INPUT “5) Core OD (in.) =”; cod
    RETURN
506 LOCATE 1, 1 :PRINT “                                     “
    LOCATE 1, 1: INPUT “6) Roll OD (in.) =”; rod
    RETURN
507 LOCATE 1, 1 :PRINT “                                     “
    LOCATE 1, 1: INPUT “7) Core Mod (psi)=”; ecm
    RETURN
508 LOCATE 1, 1 :PRINT “                                     “
    LOCATE 1, 1: INPUT “8) Er ->    C0 =”; c0
    RETURN
509 LOCATE 1, 1 :PRINT “                                     “
    LOCATE 1, 1: INPUT “9)                C1 =”; c1
    RETURN
510 LOCATE 1, 1 :PRINT “                                     “
    LOCATE 1, 1: INPUT “10)             C2 =”; c2
    RETURN
511 LOCATE 1, 1 :PRINT “                                     “
    LOCATE 1, 1: INPUT “11)            C3 =”; c3
    RETURN
512 LOCATE 1, 1 :PRINT “                                     “
    LOCATE 1, 1: INPUT “12) Et (psi) =”; et
    RETURN
513 LOCATE 1, 1 :PRINT “                                     “
    LOCATE 1, 1: INPUT “13) Web Pois. Ratio=”; muweb
    RETURN
514 LOCATE 1, 1 :PRINT “                                     “
    LOCATE 1, 1: INPUT “14) Core Pois. Ratio=”; mucore
    RETURN
515 LOCATE 1, 1 :PRINT “                                     “
    LOCATE 1, 1: INPUT “15) Density(lbs/in^3) =”; rho
    RETURN
516 LOCATE 1, 1 :PRINT “                                     “
    LOCATE 1, 1: INPUT “16) Web Friction Coef=”; mu
    RETURN

```

‘ _____sub compute roll structure

compute:

WINDOW OUTPUT 3

LOCATE 1, 1: PRINT “ ”

LOCATE 1, 1: PRINT “ *** COMPUTING ***”;

CALL

hakiel(sten,taper,pack,cid,cod,rod,ecm,c0,c1,c2,c3,et,muweb,mucore,rho,mu,r(),p(),t(),er(),tof)

WINDOW OUTPUT 3

LOCATE 1, 1: PRINT “ ”

RETURN

‘ _____MENU1:_____

MENU1:

WINDOW OUTPUT 1

GOSUB clearit

LOCATE 1, 2: PRINT “_____ Main Menu _____”

LOCATE 3, 2: PRINT “I->Input roll data”

LOCATE 4, 2: PRINT “R->Read roll data from file”

LOCATE 5, 2: PRINT “M->Model roll”

LOCATE 6, 2: PRINT “T->Tension plot toggle”

LOCATE 7, 2: PRINT “S->auto Scale”

LOCATE 8, 2: PRINT “Y->manual Y scale”

LOCATE 9, 2: PRINT “X->manual X scale”

LOCATE 10, 2: PRINT “C->Clear plot screen”

LOCATE 11, 2: PRINT “F->File output data”

LOCATE 12, 2: PRINT “D->file roll modeling Data”

LOCATE 13, 2:PRINT “A->Acoustic gage menu”

LOCATE 14, 2 :PRINT “E->Exit program”

WINDOW OUTPUT 3

LOCATE 1, 1: PRINT “Select Main Menu item ? ”;

44 SELECT CASE UCASE\$(INKEY\$)

‘ ***I->Input roll data***

CASE “I”

GOSUB iorollpara:

‘ ***R->Read roll data from file***

CASE “R”

GOSUB Readfile

‘ ***M->Model roll***

CASE “M”

```

GOSUB compute
IF autoscaleflag=1 THEN GOSUB autoscale
WINDOW OUTPUT 2
IF autoscaleflag=1 THEN CLS
CALL MacGraph(r(),p(),xtitle$,ytitle$,gridflag,xmin,xmax,ymin,
ymax,gx1,gy1,gx2,gy2)
IF tenplotflag=1 THEN CALL MacGraph(r(),t(),xtitle$,ytitle$,gridflag,xmin,xmax,ymin,
ymax,gx1,gy1,gx2,gy2)

'***T->Tension plot toggle ***
CASE "T"
IF tenplotflag=1 THEN tenplotflag=0 ELSE tenplotflag=1
WINDOW OUTPUT 3
LOCATE 1,1
IF tenplotflag=1 THEN PRINT "Plot Tension";
IF tenplotflag=0 THEN PRINT "No Tension Plot";

'***S->auto Scale ***
CASE "S"
autoscaleflag=1
WINDOW OUTPUT 3
LOCATE 1, 1 :PRINT "autoscale"

' ***Y->manual Y scale***
CASE "Y"
autoscaleflag=0
WINDOW OUTPUT 2:CLS
WINDOW OUTPUT 3
LOCATE 1, 1 :PRINT "
LOCATE 1, 1: INPUT; "Y min, Y max";ymin,ymax

'*** X->manual X scale ***
CASE "X"
autoscaleflag=0
WINDOW OUTPUT 2:CLS
WINDOW OUTPUT 3
LOCATE 1, 1 :PRINT "
LOCATE 1, 1: INPUT; "X min, X max";xmin,xmax

'*** C->Clear plot screen ***
CASE "C"
WINDOW OUTPUT 2
CLS

```

*** F->File output ***

CASE "F"

GOSUB Fileit

*** D->file roll Data Setup ***

CASE "D"

GOSUB Filessetup

*** A->Acoustic gage menu ***

CASE "A"

GOSUB acoustic

***E->Exit program ***

CASE "E"

END

CASE ELSE

GOTO 44

END SELECT

RETURN

' _____sub defaults: _____
defaults:

*** Roll Parameters *****

cid=3! ' Core inside diameter '

cod=3.62 ' Core outside diameter '

rod=9! ' Roll outside diameter '

ngrids%=100 ' number of grid points '

ecm=100000! ' Core modulus of material'

c0=0! ' Er(p) ploy fit constant'

c1=384! ' Er(p) ploy fit slope'

c2=0! ' Er(p) ploy fit curvature'

c3=0! ' Er(p) ploy fit cubic'

et=445000! ' Tangential modulus of web '

muweb=0! ' Poisson's ratio of web stack '

mucore=0! ' Poisson's ratio of core '

rho=.0515 ' density of web '

sten=1000! ' Starting web stress '

taper=0! ' Winding tension taper % '

pack=0! 'pack force in pli'

mu=0! 'web coef of friction'

***** plot parameters *****

xtitle\$="R/R0"

ytitle\$="Psi"

xmin=1

```

xmax=3
ymin=0
ymax=500
gridflag=1
tenplotflag=0
autoscaleflag=1
ngrid=100

```

```

RETURN

```

```

' _____sub iorollpara: input roll parameters_____
iorollpara:
199 GOSUB clearit
WINDOW OUTPUT 1
LOCATE 1 , 2: PRINT "1) Tension (psi) =":LOCATE 1 , 19: PRINT USING
"#####."; sten
LOCATE 2 , 2: PRINT "2) Taper (%) =": LOCATE 2 , 19: PRINT USING "#####.";
taper
LOCATE 3 , 2: PRINT "3) Pack (pli) =": LOCATE 3 , 19: PRINT USING "###.##";
pack
LOCATE 4 , 2: PRINT "4) Core ID (in.) =": LOCATE 4 , 19: PRINT USING"##.###";
cid
LOCATE 5, 2: PRINT "5) Core OD (in.) =": LOCATE 5, 19 :PRINT USING
"##.###"; cod
LOCATE 6, 2: PRINT "6) Roll OD (in.) =": LOCATE 6, 19: PRINT USING"##.###";
rod
LOCATE 7, 2: PRINT "7) Core Mod (psi)=": LOCATE 7, 17: PRINT US-
ING"##.#####"; ecm
LOCATE 8, 2: PRINT "8) Er ->    C0 =": LOCATE 8, 18: PRINT USING"#####.";
c0
LOCATE 9, 2: PRINT "9)          C1 =": LOCATE 9, 18: PRINT USING "#####.";
c1
LOCATE 10, 2: PRINT "10)         C2 =": LOCATE 10, 18: PRINT US-
ING"#####."; c2
LOCATE 11, 2: PRINT "11)         C3 =": LOCATE 11, 18: PRINT US-
ING"#####."; c3
LOCATE 12, 2: PRINT "12) Et (psi) =": LOCATE 12, 17: PRINT USING"##.#####";
et
LOCATE 13, 2: PRINT "13) Web Pois. Ratio=": LOCATE 13, 19: PRINT US-
ING"#####."; muweb
LOCATE 14, 2: PRINT "14) Core Pois. Ratio=": LOCATE 14, 19: PRINT US-
ING"#####."; mucore
LOCATE 15, 2: PRINT "15) Density(lbs/in^3) =": LOCATE 15, 20: PRINT US-
ING"#####."; rho
LOCATE 16, 2: PRINT "16) Web Friction Coef=": LOCATE 16, 20: PRINT US-
ING"#####."; mu

```


WINDOW OUTPUT 3

311 LOCATE 1,1:PRINT “

LOCATE 1,1:INPUT”Change number or 99”; NUM:

```

IF NUM = 1 THEN GOSUB 501
IF NUM = 2 THEN GOSUB 502
IF NUM = 3 THEN GOSUB 503
IF NUM = 4 THEN GOSUB 504
IF NUM = 5 THEN GOSUB 505
IF NUM = 6 THEN GOSUB 506
IF NUM = 7 THEN GOSUB 507
IF NUM = 8 THEN GOSUB 508
IF NUM = 9 THEN GOSUB 509
IF NUM = 10 THEN GOSUB 510
IF NUM = 11 THEN GOSUB 511
IF NUM = 12 THEN GOSUB 512
IF NUM = 13 THEN GOSUB 513
IF NUM = 14 THEN GOSUB 514
IF NUM = 15 THEN GOSUB 515
IF NUM = 16 THEN GOSUB 516
IF NUM = 99 THEN RETURN
GOTO 199

```

‘ _____sub autoscale_____

autoscale:

‘find xmin:

xmin=1

ymin=p(0)

xmax=r(0)

ymax=p(0)

FOR i=0 TO ngrids-1

IF r(i)>xmax THEN xmax=r(i)

IF p(i)<ymin THEN ymin=p(i)

IF p(i)>ymax THEN ymax=p(i)

NEXT i

IF tenplotflag=0 GOTO 38

FOR i=0 TO ngrids-1

IF t(i)<ymin THEN ymin=t(i)

IF t(i)>ymax THEN ymax=t(i)

NEXT i

38 RETURN

‘

clearit:

WINDOW OUTPUT 1

```

LOCATE 1 , 2: PRINT “
LOCATE 2 , 2: PRINT “
LOCATE 3 , 2: PRINT “
LOCATE 4 , 2: PRINT “
LOCATE 5 , 2: PRINT “
LOCATE 6, 2: PRINT “
LOCATE 7, 2: PRINT “
LOCATE 8, 2: PRINT “
LOCATE 9, 2: PRINT “
LOCATE 10, 2: PRINT “
LOCATE 11, 2: PRINT “
LOCATE 12, 2: PRINT “
LOCATE 13, 2: PRINT “
LOCATE 14, 2: PRINT “
LOCATE 15, 2: PRINT “
LOCATE 16, 2: PRINT “
LOCATE 17, 2: PRINT “
RETURN

```

Fileit:

WINDOW OUTPUT 3

```

LOCATE 1,1:PRINT”
LOCATE 1,1:INPUT”File Name ?”;FILE$
OPEN FILE$ FOR OUTPUT AS #1
PRINT #1, “Tension = “; sten
PRINT #1 , “Taper = “; taper
PRINT #1, “Pack = “; pack
PRINT #1 ,”Core ID = “; cid
PRINT #1, “Core OD = “; cod
PRINT #1, “Roll OD = “; rod
PRINT #1, “Modulus of core material = “; ecm
PRINT #1 ,”Er (c0) = “; c0
PRINT #1, “Er (c1) = “; c1
PRINT #1, “Er (c2) = “; c2
PRINT #1, “Er (c3) = “; c3
PRINT #1, “Et = “; et
PRINT #1, “Pos ratio of web = “; muweb
PRINT #1, “Pos ratio of web = “; mucore
PRINT #1, “Density = “; rho
PRINT #1, “Coef of Friction = “; mu
PRINT #1, “TOF = “; tof
PRINT #1, “ “

```

FOR ii=1 TO 99

```

PRINT #1, r(ii) CHR$(9)p(ii)CHR$(9)t(ii)CHR$(9)er(ii)
NEXT ii
CLOSE #1
RETURN

```

Filesetup:

```

WINDOW OUTPUT 3
LOCATE 1,1:PRINT"
LOCATE 1,1:INPUT"File Name ?";FILE$
OPEN FILE$ FOR OUTPUT AS #1
PRINT #1 , sten
PRINT #1 , taper
PRINT #1 , pack
PRINT #1 , cid
PRINT #1 , cod
PRINT #1 , rod
PRINT #1 , ecm
PRINT #1 , c0
PRINT #1 , c1
PRINT #1 , c2
PRINT #1 , c3
PRINT #1 , et
PRINT #1 , muweb
PRINT #1 , mucore
PRINT #1 , rho
PRINT #1 , mu

```

```

CLOSE #1
RETURN

```

Readfile:

```

WINDOW OUTPUT 3
LOCATE 1,1:PRINT"
LOCATE 1,1:INPUT"File Name ?";FILE$
OPEN FILE$ FOR INPUT AS #1
INPUT #1 ,sten
INPUT #1 , taper
INPUT #1 , pack
INPUT #1 , cid
INPUT #1 , cod
INPUT #1 , rod
INPUT #1 , ecm
INPUT #1 , c0
INPUT #1 , c1
INPUT #1 , c2

```

```

INPUT #1 , c3
INPUT #1 , et
INPUT #1 , muweb
INPUT #1 , mucore
INPUT #1 , rho
INPUT #1 , mu

```

```

CLOSE #1
RETURN

```

```

acoustic: ' _____ acous-
tic _____

```

```

WINDOW OUTPUT 1

```

```

GOSUB clearit

```

```

gain = 1

```

```

i=0

```

```

LOCATE 1, 2: PRINT "____ Acoustic Gage ____"
LOCATE 3, 2: PRINT "Iteration # _____>": LOCATE 3, 18: PRINT USING "##";i
LOCATE 4, 2: PRINT "Calculated T.O.F. —>": LOCATE 4, 18: PRINT USING
".#####";tof
LOCATE 5, 2: PRINT "Measured T.O.F.—>": LOCATE 5, 18: PRINT USING
".#####";mtof
LOCATE 6, 2: PRINT "Tension Guess —>": LOCATE 6, 18: PRINT USING
"#####.";sten

```

```

WINDOW OUTPUT 3

```

```

LOCATE 1,1 :PRINT "
LOCATE 1,1 : INPUT "Measured T.O.F. = ";intemp
IF intemp <> 0 THEN mtof=intemp
LOCATE 1,1 :PRINT "
LOCATE 1,1:: INPUT "Tension Guess = ";intemp
IF intemp <> 0 THEN sten=intemp

```

```

GOSUB clearit

```

```

WINDOW OUTPUT 1

```

```

LOCATE 1, 2: PRINT "____ Acoustic Gage ____"
LOCATE 3, 2: PRINT "Iteration # _____>": LOCATE 3, 18: PRINT USING "##";i
LOCATE 4, 2: PRINT "Calculated T.O.F. —>": LOCATE 4, 18: PRINT USING
".#####";tof
LOCATE 5, 2: PRINT "Measured T.O.F.—>": LOCATE 5, 18: PRINT USING
".#####";mtof
LOCATE 6, 2: PRINT "Tension Guess —>": LOCATE 6, 18: PRINT USING
"#####.";sten

```

```

deltatof=1000
'*** acoustic gage iteration loop *****
WHILE ABS(deltatof)>.000001
i=i+1
GOSUB compute
deltatof=tof-mtof
WINDOW OUTPUT 1
LOCATE 3, 18: PRINT USING "##";i
LOCATE 4, 18: PRINT USING "#####";tof
LOCATE 6, 18: PRINT USING "####.";sten
consta=sten*tof 'assume inverse fcn of form sten=consta/tof
sten=consta/mtof
WEND
'plot acoustic gage output
IF autoscaleflag=1 THEN GOSUB autoscale
WINDOW OUTPUT 2
IF autoscaleflag=1 THEN CLS
CALL MacGraph(r(),p(),xtitle$,ytitle$,gridflag,xmin,xmax,ymin,
ymax,gx1,gx2,gy2)
IF tenplotflag=1 THEN CALL MacGraph(r(),t(),xtitle$,ytitle$,gridflag,xmin,xmax,ymin,
ymax,gx1,gx2,gy2)
BEEP
FOR ii=1 TO 10000:NEXT ii
RETURN
'
SUB
hakiel(sten,taper,pack,cid,cod,rod,ecm,c0,c1,c2,c3,et,muweb,mucore,rho,mu,r(),p(),t(),er(),tof)
STATIC
'*****
'*****
'*
'*      HAKIEL WINDING MODEL                      By R.P. Swanson 6-13-91
'*
'*      This program uses Z. Hakiels Finite Difference approach
'*      (1986 Tappi Finishing and Converting Conference) to solve
'*      for stresses in a wound roll. The code is written in "QB" for
'*      use with a "QB" compiler on a Macintosh computer.
'*
'*      Rev 1.0      6-13-91      New Program
'*
'*****
'*****

```

```
' declare global variables '
```

```
'DEFDBL a-z
```

```
IF redimflag=0 THEN DIM
```

```
tw(100),a(100),b(100),c(100),d(100),dp(100),beta(100),gama(100)
```

```
redimflag=1
```

```
FOR i=0 TO ngrids%-1
```

```
tw(i)=0:a(i)=0:b(i)=0:c(i)=0:d(i)=0:dp(i)=0:beta(i)=0:gama(i)=0:r(i)=0:p(i)=0:t(i)=0:er(i)=0
```

```
NEXT i
```

```
ngrids%=100
```

```
GOSUB initialize
```

```
n%=ngrids%
```

```
' Add lap #1 '
```

```
p(1)=tw(1)*h/r(1)
```

```
' Add lap #2 '
```

```
p(2)=tw(2)*h/r(2)
```

```
p(1) = p(1) + p(2)/rk
```

```
press=p(2)
```

```
GOSUB calcer
```

```
er(2)=er11
```

```
' Add lap #3 '
```

```
p(3)=tw(3)*h/r(3)
```

```
aa2=1!-(3!*h)/(2!*r(2))
```

```
bb2=(h*h/(r(2)*r(2)))*(1!-et/er(2)) - 2!
```

```
cc2=1!+(3!*h)/(2!*r(2))
```

```
dp(1)=cc2*p(3)/(-rk*bb2-aa2)
```

```
dp(2)=rk*dp(1)
```

```
p(1) = p(1) + dp(1)
```

```
p(2) = p(2) + dp(2)
```

```
' Add lap #4 thru n% using Tri-diagonal by B.E. LEE '
```

```
FOR i%=4 TO n%
```

```
GOSUB tridiag
```

```
' Add dp() to p() '
```

```
FOR jj%=1 TO i%
```

```
p(jj%) = p(jj%) + dp(jj%)
```

```

NEXT jj%
NEXT i%'end of lap 4 thru n loop '

' Calculate t() and er()'
FOR jj%=2 TO n%-1
  t(jj%)=-p(jj%)-r(jj%)*((p(jj%+1)-p(jj%-1))/(2*h))
  press=p(jj%)
  GOSUB calcer
  er(jj%)=er11
NEXT jj%

t(1)=-p(1)-r(1)*((p(2)-p(1))/h)
t(n%-1)=sten
press=p(n%-1)
GOSUB calcer
er(n%)=er11
press=p(1)
GOSUB calcer
er(1)=er11
' calc tof '
tof=0!
dist=((rod-cod)/2!)/ngrid%
FOR i%=1 TO n%-1
  tof = tof + dist/SQR(er(i%)*12!*32.17/rho)
NEXT i%

'*****'
GOTO 999      ' END OF MAIN '
'*****'

'*****'
initialize:   ' START OF initialize '
'*****'
' calculate "h" the normalized grid spacing '
h=((rod-cod)/2!)/ngrid%/(cod/2!)

' calculate r(j%) the normalized radius array '
FOR j%=0 TO ngrid%
  r(j%)=1! + h*(j% - 1!)
NEXT j%

```

```

' calculate tw(j%) the winding tension array '
FOR j%=0 TO ngrids%
  tw(j%)= sten * (1! - (taper/100!)*((r(j%) - r(0)) / r(j%)))
NEXT j%

' calculate ecm the core stiffness from Roisum p-25'
r02=(cod/2!)*(cod/2!)
rc2=(cid/2!)*(cid/2!)
ec=ecm*( r02 - rc2 )/(r02 + rc2 - mucore * (r02 - rc2))

' calculate cc the core constant '
cc = et/ec - 1! + muweb
rk=1!+h*cc

RETURN

'*****'
tridiag: ' START OF tridiag
'*****'
k%=i%
k%=k%-1
dp(k%+1)=tw(k%+1)*h/r(k%+1)
a(1) = 0!
b(1) = -rk
c(1) = 1!
d(1) = 0!
FOR iii%=2 TO k%
  hr = h/r(iii%)

  press=p(iii%)
  GOSUB calcer
  gi2 = et/er11
  a(iii%) = 1!-1.5*hr
  b(iii%) = hr*hr*(1!-gi2)-2!
  c(iii%) = 1!+1.5*hr
  d(iii%) = 0!
NEXT iii%

d(k%) = -dp(k%+1)*c(k%)
c(k%) = 0!

beta(1) = b(1)
gama(1) = d(1)/b(1)

```



```

FOR iii%=2 TO k%
  beta(iii%) = b(iii%)-a(iii%)*c(iii%-1)/beta(iii%-1)
  gama(iii%) = (d(iii%)-a(iii%)*gama(iii%-1))/beta(iii%)
NEXT iii%

dp(k%) = gama(k%)
FOR iii%=(k%-1) TO 1 STEP -1
  dp(iii%) = gama(iii%)-c(iii%)*dp(iii%+1)/beta(iii%)
NEXT iii%
RETURN
'*****'
calcer: ' START OF calcer
'*****'
er11=c0+c1*press+c2*press*press+c3*press*press*press
RETURN

999 END SUB
'
'
' SUB PROGRAM MACGRAPH, REVISION 06-17-91
' This sub program takes two matrix x() and y() and makes a line plot
'
' Special version for the Mac R.P.Swanson 6-17-91
'
SUB MacGraph(x(),y(),xtitle$,ytitle$,gridflag,xmin,xmax,ymin, ymax,gx1,gy1,gx2,gy2)
STATIC
'x(), x matrix to be plotted
'y(), y matrix to be plotted
'xtitle$, title of x axis
'ytitle$, title of y axis
'xmin>manual scale min x
'xmax>manual scale max x
'ymin>manual scale min y
'ymax>manual scale max y
'gridflag,0=no grid, 1=grid
'gx1,x coord. of Upper left corner Abs graph coords in pixels
'gy1,y coord. of Upper left corner Abs graph coords in pixels
'gx2,x coord. of Upper left corner Abs graph coords in pixels
'gy2,y coord. of Upper left corner Abs graph coords in pixels

GOSUB graph:
GOSUB box:
IF gridflag=1 THEN GOSUB grid:
GOSUB plots:

```

```

*****
GOTO 9999 'end of main
*****

graph: ' _____ sub that sets up graph and lables _____
'print lables
ppchry=16 'pixels per char y
ppchrx=8 'pixels per char x
ly=INT((gy2-gy1)/ppchry)
LOCATE 1,1:PRINT USING "#####.#";ymax;
LOCATE (ly-2),1:PRINT USING "#####.#";ymin;
lx=INT((gx2-gx1)/ppchrx)
LOCATE ly-1,3:PRINT USING "#####.##";xmin;
LOCATE ly-1,(lx-6):PRINT USING "#####.##";xmax;
LOCATE ly,((lx-6+7)/2):PRINT xtitle$;
LOCATE (INT(ly/2)),1:PRINT ytitle$;
RETURN

box: ' _____ sub that draws box _____
'find pixel pos. of lower left corner
llcx=7*ppchrx
llcy=(ly-2)*ppchry
'find pixel pos. of upper right corner
urcx=(gx2-gx1)-3*ppchrx
urcy=INT(ppchry/2)
deltapx=urcx-llcx
deltapy=llcy-urcy
deltax=xmax-xmin
deltay=ymax-ymin
'draw box
LINE (llcx,llcy)-(llcx,urcy)
LINE -(urcx,urcy)
LINE -(urcx,llcy)
LINE -(llcx,llcy)
RETURN

grid:
' _____ sub plot grid _____
FOR d=.1 TO 1! STEP .1
LINE (INT(llcx+d*deltapx),llcy)-(INT(llcx+d*deltapx),urcy)
LINE (llcx,INT(llcy-d*deltapy))-(urcx,INT(llcy-d*deltapy))
NEXT d
RETURN

' _____ sub plot graph pressures _____

plots:
xmult=deltapx/deltax
ymult=deltapy/deltay

```

```

px=llcx-xmin*xmult+x(LBOUND(x)+1)*xmult
py=llcy+ymin*ymult-y(LBOUND(y)+1)*ymult
PSET(px,py)
FOR i = LBOUND(x)+1 TO UBOUND(x)-1
px=llcx-xmin*xmult+x(i)*xmult
py=llcy+ymin*ymult-y(i)*ymult
'IF px<llcx OR px>urcx THEN GOTO 37
'IF py>llcy OR py<urcy THEN GOTO 37
LINE -(px,py)
37 NEXT i
RETURN
*****
9999 END SUB                'end of MacGraph
*****

```

APPENDIX E

**DETERMINATION OF WOUND ROLL STRUCTURE
USING ACOUSTIC TIME OF FLIGHT
MEASUREMENTS**

**Presented at
The First International Conference on Web Handling
Stillwater, Oklahoma
May 1991**

DETERMINATION OF WOUND ROLL STRUCTURE USING ACOUSTIC TIME OF FLIGHT MEASUREMENTS

Ronald P. Swanson
3M Company
St. Paul, Mn

ABSTRACT

Roll structure measurement is presently done with destructive and intrusive measuring devices, such as FSRs or with specially instrumented winders. These methods are generally limited to research and development applications. Prior to this paper, there was no method of non-destructively determining the structure of a roll with unknown winding conditions.

This paper presents a measurement technique, the Acoustic Roll Structure Gage, that uses through thickness acoustic time of flight measurements to determine roll structure, an extension of the work done by J. David Pfeiffer [1] and alluded to by L. Eriksson [2] and D. R. Roisum [3]. A measurement is made of the time required for an acoustic wave to travel through the roll. This time of flight measurement is used as an extra degree of freedom in a winding model such as Z. Hakiel's [4] to replace an unknown or questionable model input, such as radial modulus or winding tension. The roll structure is determined by adjusting the model input until the calculated time of flight matches the measured time of flight.

The measurement technique was verified by comparison with two other independent methods. Each method was used to map the radial pressures in the left and right sides of six different wound rolls. Excellent results were obtained with the Acoustic Gage, when winding tension was used as the adjustable parameter. The Acoustic Gage agreed with two other independent roll structure measurement tools, all of which were much lower than predicted by winding models. The results cast doubt on the validity of the hoop stress equation as an outer boundary condition for wound roll models.

NOMENCLATURE

E_r = radial modulus, Pa (1 psi = 6.895×10^3 Pa)
 C_1 = slope of the E_r vs. P curve, dimensionless
 P = pressure, Pa (1 psi = 6.895×10^3 Pa)
 c = wave propagation speed, m/s
 E = modulus, Pa (1 psi = 6.895×10^3 Pa)
 ρ = density Kg/m³, (1 lb/in.³ = 3.613×10^{-5} Kg/m³)
 V = velocity, m/s
 t = time, s
 l = length, m
 T_w = winding stress, Pa (1 psi = 6.895×10^3 Pa)
 T = stress, Pa (1 psi = 6.895×10^3 Pa)
 h = web thickness, m (1 in. = .0254 m)
 r = radius, m (1 in. = .0254 m)

BACKGROUND

Many common roll structure measurement techniques are qualitative not quantitative (capable of producing stress profiles in engineering units such as kPa or psi). Examples include the Rhometer, Schmidt Hammer or even a calibrated thumb. Most quantitative measurements are intrusive and destructive, such as FSRs and pull tabs. The remaining quantitative techniques, such as the density analyzer, require the rolls to be wound on special winders, with high precision measurement equipment. A comprehensive discussion of roll structure measurement techniques is given by D.R. Roisum [3]. The roll structure measurement technique presented in this paper can be used to non-intrusively and non-destructively measure roll stresses.

STACK TESTS

When this work began, there were many questions about wave propagation and material properties that could best be answered in a flat rather than cylindrical geometry. These questions include: Can solid body wave mechanics be used with paper and plastic laminate structures? Can a transducer be coupled to paper and plastic laminates? Is the attenuation in paper and plastic laminate prohibitive for time of flight measurements? What are the material properties of a laminate structure?

Effect of Radial Pressure on Modulus and Density

Stack tests were performed, using an Instron 8502, on an assortment of materials including papers and plastic films. The tests showed that the material density changed very little with pressure and therefore can be considered constant. The tests also showed that the radial modulus of a laminate could be modeled as a polynomial function of pressure. Most materials could be modeled using equation (1).

$$E_r = C_1 * P \quad (1)$$

Speed of Sound

The theoretical speed of sound in a solid is given by equation (2), where E is Young's modulus for a bar (one dimensional longitudinal wave) or the bulk modulus for multi-dimensional waves [5]. The stack test data was used to determine the theoretical speed of sound, by replacing E with E_r and using a constant density ρ in equation (2).

$$c = \sqrt{\frac{E}{\rho}} \quad (2)$$

The next step was to determine if this theory, based on solid body mechanics, would be valid for a laminate structure with variable modulus. An apparatus was made that allowed a wave to be initiated and observed as it passed two positions in the test stack under a known pressure. Two Kynar film strips were used as sensors, an oscilloscope, analog amplifiers, filters and analytical techniques were used for signal processing. Initially the leading edges of the signals were used to determine the time of flight between the two sensors. This technique produced wave velocities well in excess of those predicted by equation (2). It was later determined that this technique is not valid due to the existence of forerunners [6]. Forerunners are small waves that travel ahead of the main energy packet, at speeds in excess of the group velocity. The best technique to measure wave speed was to place the two sensors relatively close together and to use cross correlation to determine the time of flight. The sensors were placed relatively close to minimize the wave shape change due to frequency dependent velocity and attenuation. The decrease in accuracy caused by close spacing was more than offset by the accuracy increase from cross correlation. The results of this test showed that equation (2) is valid for a laminate structure with variable modulus. The test also gave insight, and forewarning, into the difficulties involved in time of flight measurements with low frequency, small bandwidth, waves traveling through highly attenuating non-linear materials.

Wave Generation and Reception

Initial efforts into wave generation and reception concentrated on commercial ultrasonic equipment typically used for non-destructive testing. This equipment is high frequency and wide bandwidth, which is advantageous for time of flight measurements. This equipment works very well on steel and composites, where coupling fluids and high contact pressures are not considered destructive or intrusive, but this is not the case with wound rolls. A test of a pair of Panametrics 13mm (.5 inch) 1 Mhz transducers showed that 175 kPa (25 psi) was required to dry couple a signal through a 10 mm (.38 inch) stack of polyester film. A frequency analysis of the received signal revealed that all the frequency components above 300 kHz had been completely attenuated. This test showed that excessive intrusive coupling pressure was required to transmit a signal through a web stack that is a

small fraction of the stack heights encountered in most wound rolls. The test also revealed that the bandwidth advantage of the commercial systems is nullified by the high frequency attenuation of the material. An attempt was then made to build a piezo pulsar that had approximately 100 times the energy of the commercial systems, but lacked the commercial systems bandwidth. This system was only a marginal improvement over the commercial systems. A pulsar with perhaps 10,000 times the energy of the commercial equipment is needed to initiate a wave capable of coupling to and traveling through a large roll. This pulsar must not only have very high energy, but also bandwidth that will fully exploit the frequency transmission capability of the wound roll.

A mechanical pulsar was developed that released about 1 joule of energy in 3.3 μ s (300 kHz), which translates to 300 kW of peak power. This was done by using a form of the Hopkinson pressure bar. A short bar (projectile) is shot, at known velocity, into a longer bar (pressure bar). A pressure wave, of magnitude described by equation (3), and duration equal to the time required for the wave to travel from the point of impact to the other end of the short bar and back, as described by equation (4), travels down the pressure bar and into the roll. Figure 1 is a cross sectional view of the mechanical pulsar. The mechanical pulsar produces high frequency, wide bandwidth waves capable of traveling through very large rolls. The air vents allow the projectile to travel at high velocity and prevents the pressure bar from acting as a pneumatic cylinder. The spring allows the pressure bar to be coupled to the roll with light contact pressure.

To use the pulsar, tip the pulsar back allowing the projectile to slide to the inlet end of the tube. Press the pressure bar against the roll with very light spring pressure. Fire the pneumatic valve, causing the projectile to be shot into the pressure bar, initiating the wave.

$$P = \rho c V \quad (3)$$

$$t = \frac{2 \cdot l}{c} \quad (4)$$

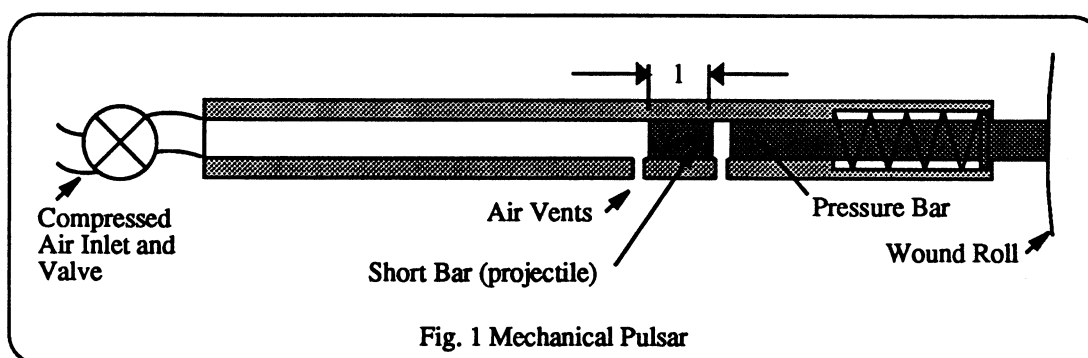


Fig. 1 Mechanical Pulsar

Coupling and Attenuation

The attenuation in a laminate is very important to this project. A test was performed to determine the signal attenuation through both film and paper. The signal attenuation was determined by placing two sensors in a stack at several different pressures and distances and recording a wave as it passed. The attenuation, expressed in dB, was calculated as ten times the common logarithm of the ratio of peak signal strengths. The results of these tests were fit with a simple regression in equations (4) and (5).

$$\text{Paper dB / 2.54 cm (1 in.)} = -4.5 + .000002 * P \quad (4)$$

$$\text{Film dB / 2.54 cm (1 in.)} = -8.0 + .000003 * P \quad (5)$$

This attenuation is very high. At pressures commonly found in wound rolls the signal will lose more than half its strength for every 2.5 cm (1 inch) of travel.

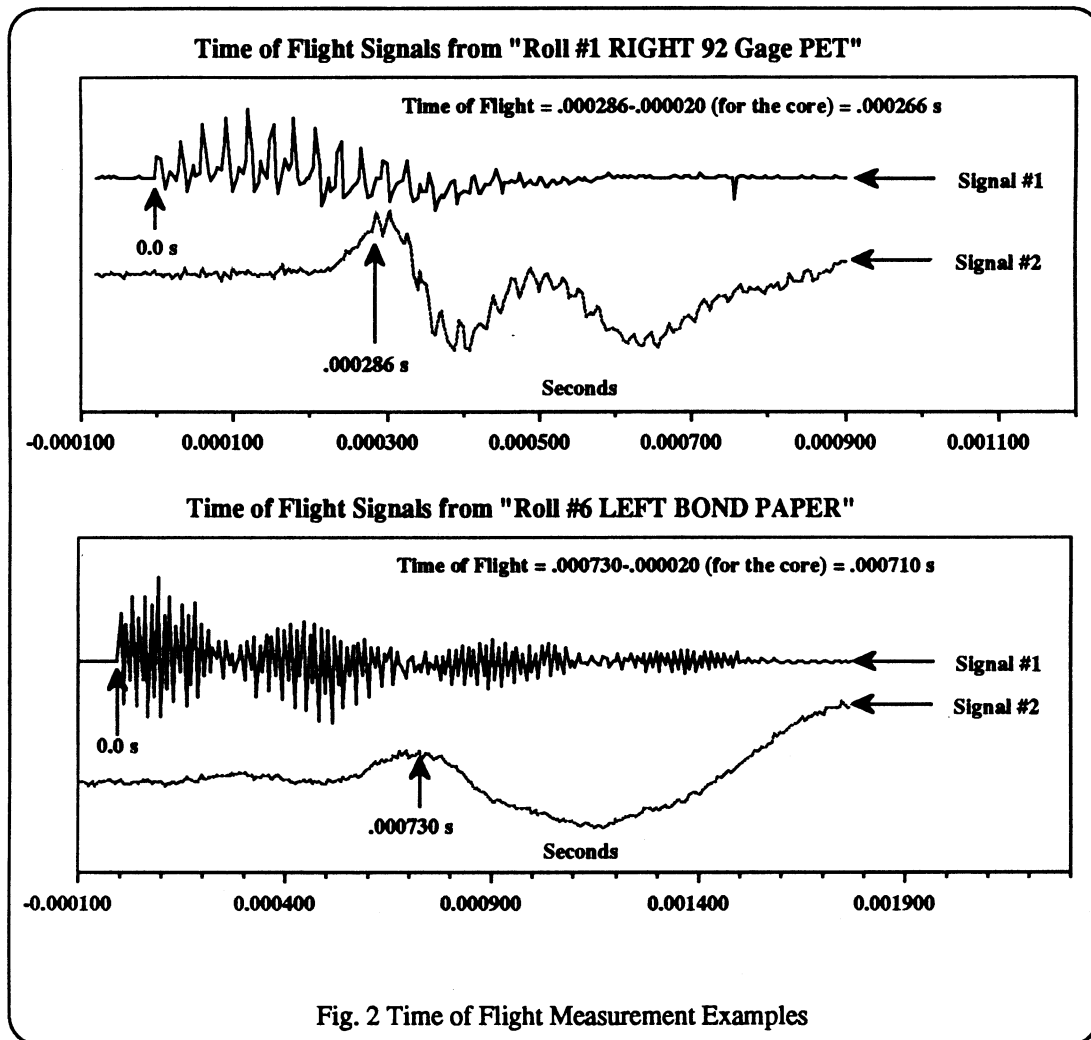
ACOUSTIC ROLL STRUCTURE MEASUREMENT

The stack tests answered many questions about wave propagation through laminate structures. The tests also provided valuable information about wave generation, reception and signal processing. With these questions answered, the emphasis was then shifted from the stack to roll geometry.

Time of Flight Measurement

To determine the time of flight through the roll, the wave must be initiated and received at known times. Unlike the stack test, cross correlation cannot be used because of the extreme differences in wave shape between initiation and reception. A simple technique to determine the initiation time of the wave is to place a Kynar film sensor between the pulsar pressure bar and the roll. When the pulsar is fired, the Kynar produces a voltage signal as the wave travels from the pressure bar through the Kynar and into the roll. The signal from the Kynar sensor can go directly into an oscilloscope. This signal is very clean and has an amplitude of several volts. The scope is dc coupled and triggered at a level above the noise, but well below the peak amplitude of the signal. The actual trigger level is not important because of the extremely fast rise time of the signal. Recall that the total theoretical pulse duration is only $3.3 \mu\text{s}$ as compared to time of flights ranging from hundreds to thousands of microseconds.

The signal is received with a simple accelerometer or Kynar sensor hand held against the inside of the core. Again, this signal often requires very little amplification or filtering. The determination of the exact time the wave has been received is very difficult because of the low frequency and small bandwidth of the wave. Many references were consulted about this problem. There are several references discussing the problem, but a satisfactory solution was not found in the literature. The stack tests showed that the leading edge of the wave cannot be used because of the forerunners. The technique that worked best was to pick the first peak that was at least 5 standard deviations above the signal noise. In all the cases tested, this algorithm produced very reasonable time of flight values. Figure 2 shows several examples of normalized signals and time of flight measurements used in the Appendix.



Determination of Roll Structure

The time of flight measurement is an extra degree of freedom (redundant or indeterminate constraint) that can be used in a winding model such as Hakiel's to replace an unknown or questionable model input, such as winding tension, or radial modulus. An example of its use is the determination of the roll structure of an arbitrary roll from the warehouse. All the input needed to model this roll could be determined except for the winding tension. A guess could be made of the winding tension, and the roll modeled. The model will produce a pressure profile that can be used with equations (1) and (2) to determine the speed of sound as a function of radius. The speed of sound as a function of radius can be integrated from the core to the outside of the roll to calculate the time of flight resulting from the initial guess. The difference between the calculated time of flight and the actual measured time of flight is then used to make a better guess at the winding tension. This iteration process is continued until the calculated time of flight converges with the actual measured time of flight. The data from the last iteration is the roll structure. This method is called the Acoustic Roll Structure Gage.

Another potential unknown or questionable model input is radial modulus. The time of flight measurement can be used with equation (2) to determine the average radial modulus. This constant modulus can be used in a model such as Altmann [7], Yagoda [8] or Hakiel to determine roll structure. This method is called the Constant E_r Roll Structure Gage.

A computer program was written that reads the two signals from an oscilloscope. These two signals are processed, according to the criterion discussed earlier, to determine the measured time of flight. The program has two options: Constant E_r and Acoustic Gage. If the Constant E_r option is selected, the time of flight measurement is used to calculate and average E_r , which is used in the model to replace the stack test E_r function. The remaining model inputs, including T_w , remain unchanged. The program then calculates the roll structure, plots the radial pressure distribution and files the data. If the Acoustic Gage option is invoked, an initial guess of T_w and the stack test E_r function is used to calculate the roll structure. This radial pressure and equations (1) and (2) are integrated to determine the calculated time of flight. The error between the measured time of flight and the calculated time of flight is used to make a better guess at T_w . This iteration process continues until the difference between the measured and calculated time of flight is less than 1 μ s. The roll structure data from the last iteration is plotted and the data written to a file. Figure 3 is a screen dump of the Acoustic Gage program used to determine the roll structure of "Roll #1 RIGHT" in the Appendix.

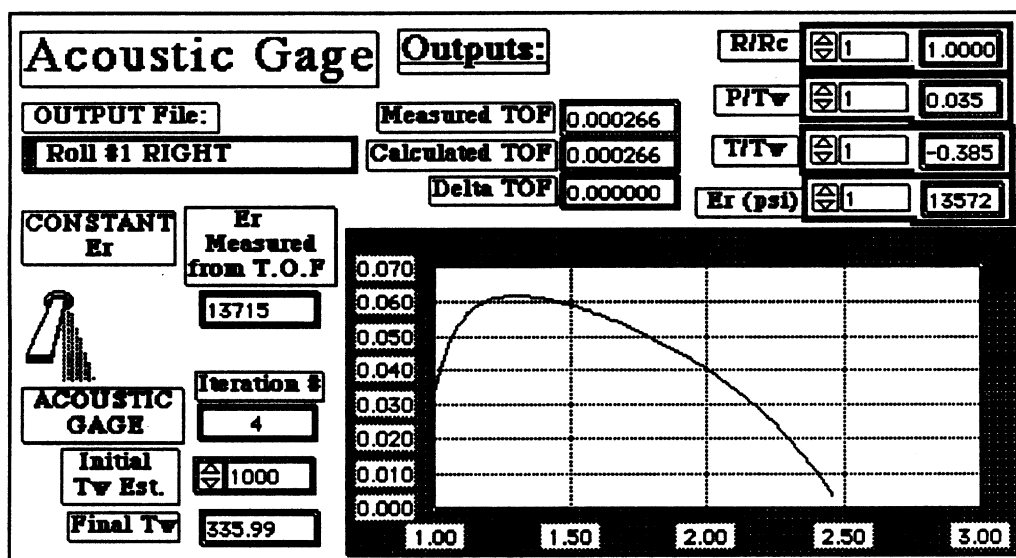


Fig. 3 Acoustic Gage Program Screen

Verification

The acoustic measurement techniques were verified by comparison with two independent measurement methods: FSRs and pull tabs. The two direct pressure measurement methods and the two acoustic techniques were used to map the radial pressures in the left and right sides of six different wound rolls. The results of these measurements, along with Hakiel's model output, are given in the Appendix. Excellent results were obtained with the Acoustic Gage when winding tension was used as the adjustable parameter. When the average radial modulus, determined with time of flight measurements, was substituted for the stack test data the resulting radial pressure profile was often very similar to the original Hakiel's model output. This suggests that the radial modulus determined with stack tests is probably accurate. The excessive pressures predicted by winding models, the excellent results obtained by adjusting winding tension in the Acoustic Gage and the indication that stack tests produce accurate radial modulus data, cast doubt on the validity of the hoop stress boundary condition.

Hoop Stress Boundary Condition

Four different models were used to calculate the expected radial pressure for these rolls. The model input parameters were carefully measured and independently verified. Except for the core area, all the models predicted very similar results. The pressures predicted by all the models were considerably higher than the actual pressure measured with three independent techniques: FSRs, pull tabs and the Acoustic Gage. These models all use the same outer boundary condition, the hoop stress equation (6).

$$P = \frac{T_w * h}{r} \quad (6)$$

This equation assumes no shear stresses and does not account for such factors as air entrainment. A simple modification, to make this boundary condition more realistic, is to use some value T in place of T_w , such that $T < T_w$. The Acoustic Gage uses the extra degree of freedom from the time of flight measurement in place of T_w and iterates to find a value T that is more reasonable.

RESULTS AND CONCLUSION

A new roll structure evaluation tool has been developed. This measurement technique uses time of flight measurements and existing winding models to determine roll structure. This method has several advantages over existing roll structure evaluation tools. These advantages include being non-destructive and non-intrusive and not requiring knowledge of the winding conditions.

Stack tests were done to determine material properties and confirm that solid body wave mechanics could be used to describe waves in laminates. A mechanical pulsar was developed that can generate a high energy, wide bandwidth wave in a wound roll. A time of flight measurement method was also developed. These components, including an existing winding model, were integrated into an algorithm to determine roll structure. This system is called the Acoustic Roll Structure Gage.

The Acoustic Gage results agreed with two other independent roll structure measurement tools, all of which were much lower than predicted by winding models. The results cast doubt on the validity of the hoop stress equation as an outer boundary condition for wound roll models.

ACKNOWLEDGMENTS

I would like to thank Dr. J. Keith Good and Dr. Richard Lowery for their guidance and assistance. I also would like to thank everyone involved with the Web Handling Research Center, which provided a unique opportunity to research this project and broaden my knowledge of web handling and engineering. I also would like to thank J. David Pfeiffer for initiating this work in 1966 and for his insights and assistance.

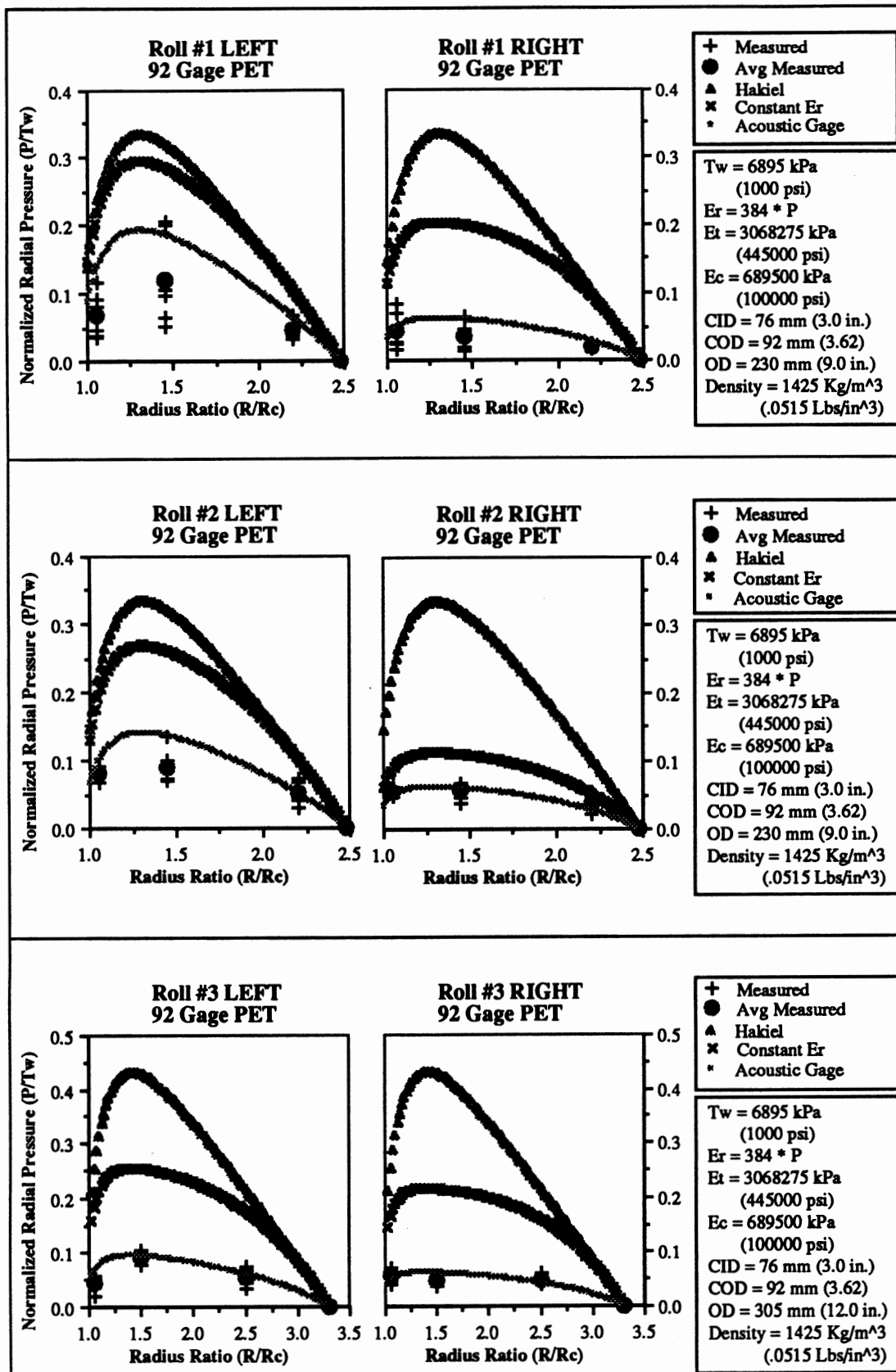
I also would like to express my thanks to 3M Company, especially my supervisor Yvonne Cadwallader and managers Robert Nelson and Shuzo Fuchigami who provided the opportunity and support required to complete this project.

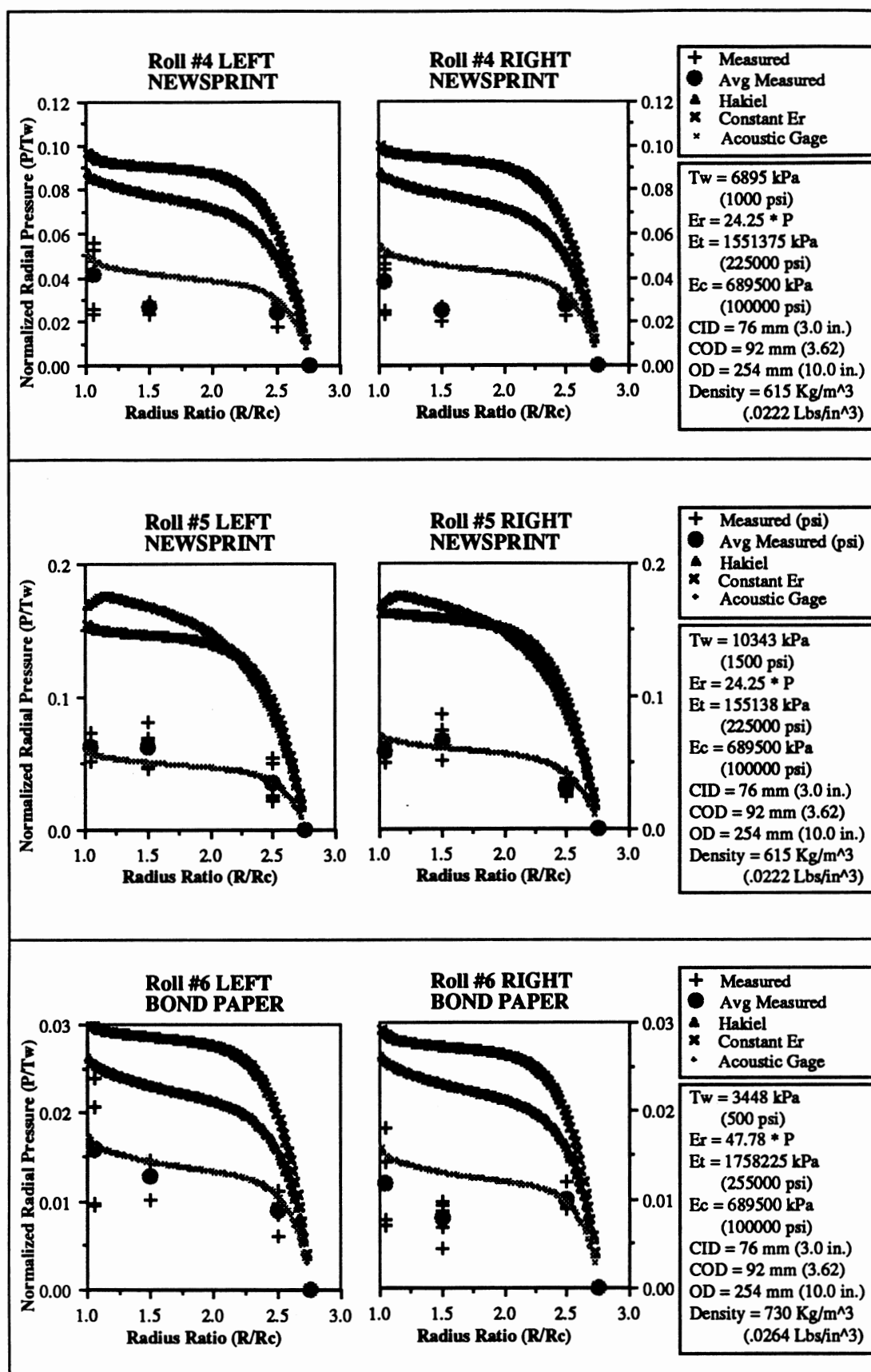
REFERENCES

1. Pfeiffer, J. D. "Internal Pressures in a Wound Roll of Paper." Tappi Journal, Vol. 49, No. 8, August 1966, pp. 342 - 347.
2. Eriksson, L., "Deformations in Paper Rolls," Proceedings of the first Winding Technology Conference, Stockholm Sweden, March 1987, pp. 195 - 212
3. Roisum, D.R. "The Measurement of Web Stresses During Roll Winding." Ph.D Thesis, Department of Mechanical and Aerospace Engineering, Oklahoma State University, May 1990.

4. Hakiel, Z. "Nonlinear Model for Wound Roll Stresses." Tappi Journal, Vol. 70, No. 5, May 1987, pp. 113 - 117.
5. Kinsler, L. E., Frey, A. R., Coppens A. B., Sanders, J. V., Fundamentals of Acoustics, Third Edition, John Wiley & Sons, 1982.
6. Brillouin, Leon, Wave Propagation and Group Velocity, Academic Press, New York, 1960.
7. Altmann, H. C. "Formulas for Computing the Stresses in Center-Wound Rolls." Tappi Journal, Vol. 51, No. 4, April 1968, pp. 176 - 179.
8. Yagoda, H. P., "Generalized Formulas for Stresses in Wound Rolls," Tappi Journal, Vol. 64, No. 2, February 1981, pp. 91 - 93.

APPENDIX





APPENDIX F

**DETERMINATION OF WOUND ROLL STRUCTURE
USING ACOUSTIC TIME OF FLIGHT
MEASUREMENTS**

(Visuals)

**Presented at
The First International Conference on Web Handling
Stillwater, Oklahoma
May 1991**

**Determination of
Wound Roll
Structure using
Acoustic
Time of Flight
Measurements**

**By
Ronald P. Swanson**

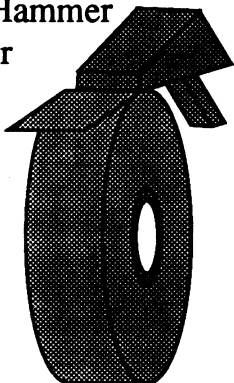
**3M Company
St Paul, Mn**

Roll Structure Measurement Tools

Surface Measurements:

Schmidt Hammer

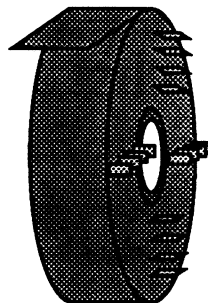
Rho Meter



Intrusive and Destructive:

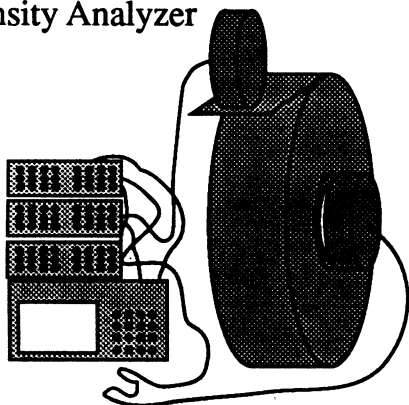
FSRs

Pull Tabs



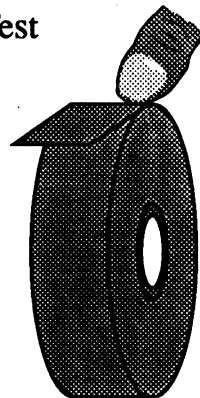
Instrumented Winders:

Density Analyzer



Qualitative:

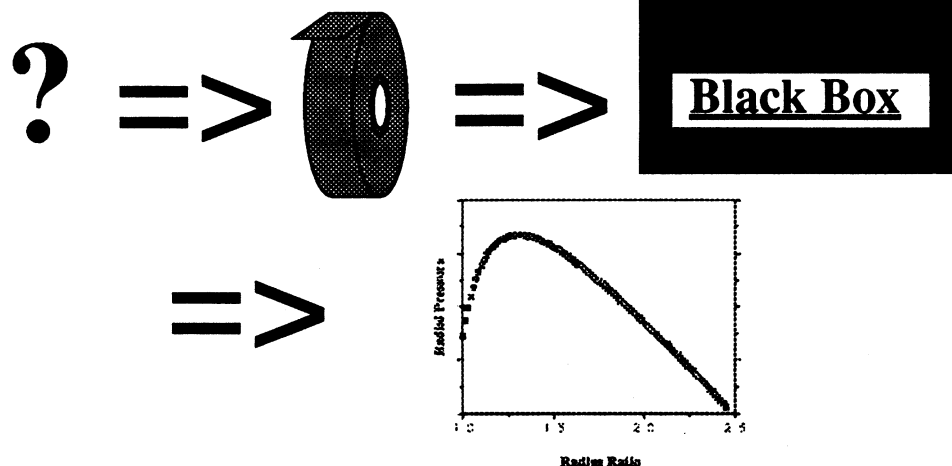
Thumb Test



Black Box Roll Structure Measurement

Objective:

- * Post Process
- * Non-destructive
- * Non-intrusive
- * Quantitative (P vs. r)

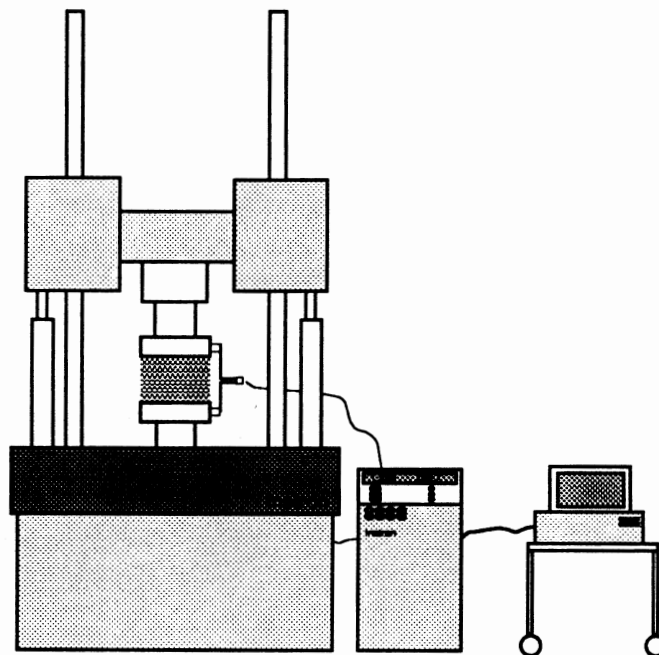


Acoustic Time of Flight Measurement

Stack Tests

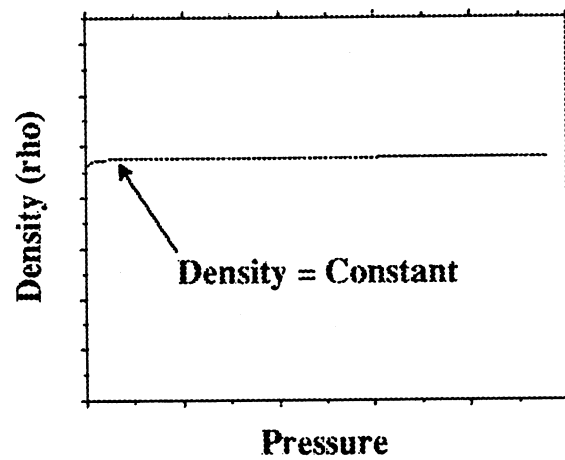
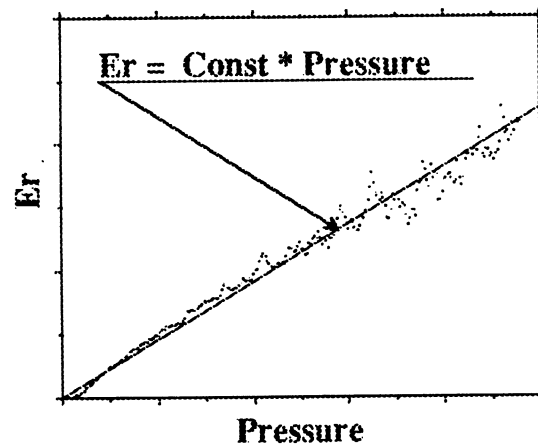
Questions:

1. What are the material properties of a laminate structure?
2. Can solid body wave mechanics be used on laminates?
3. Can a transducer be coupled to a stack?
4. Is attenuation prohibitive for T.O.F. measurements?



Instron 8502

Material Properties



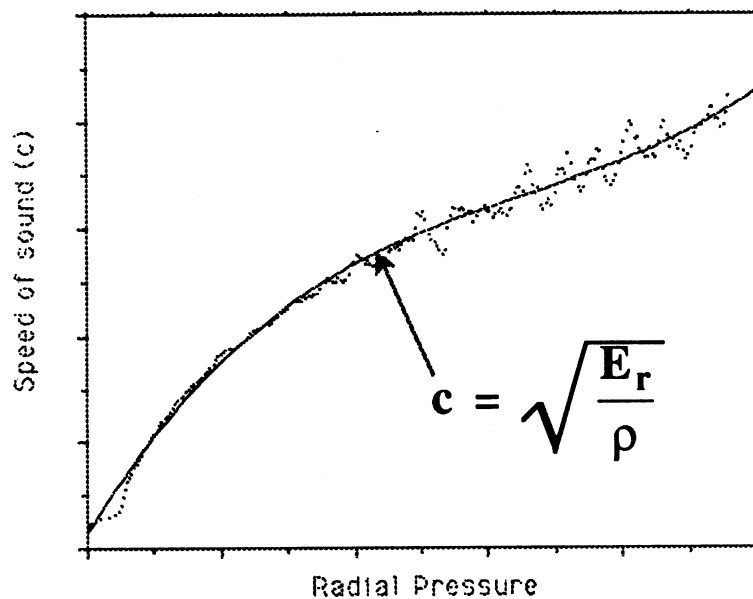
Theoretical Speed of Sound

$$c = \sqrt{\frac{E}{\rho}}$$

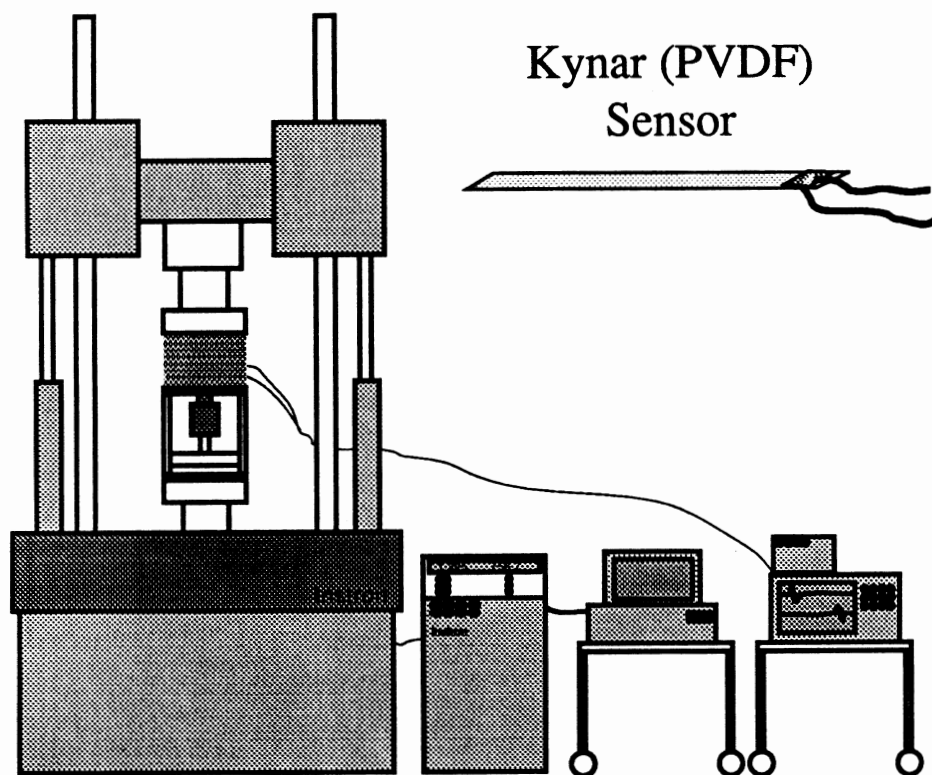
c = speed of sound

E = modulus (E_r ?)

ρ = density

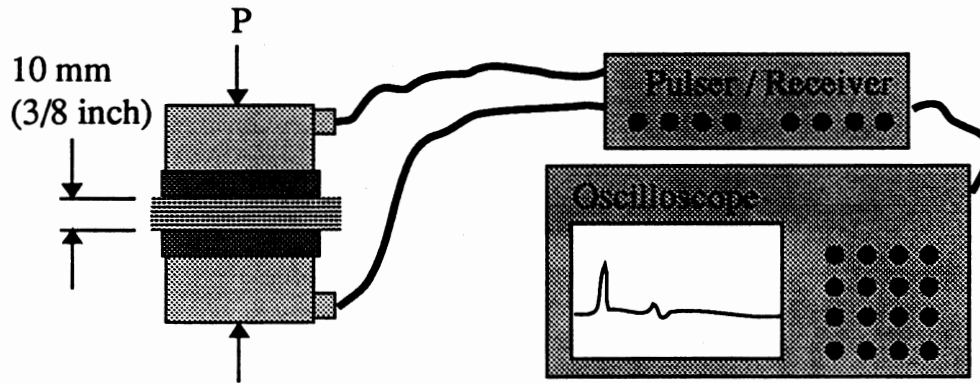


Measured Speed of Sound

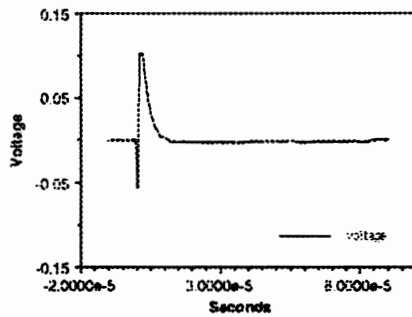


Inston 8502
Setup for Time of Flight Measurements

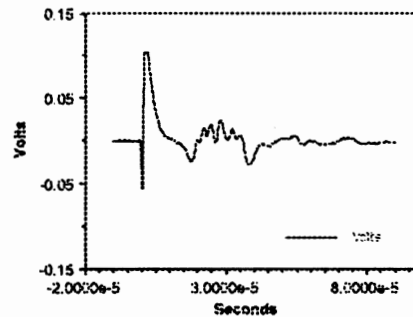
Wave Generation



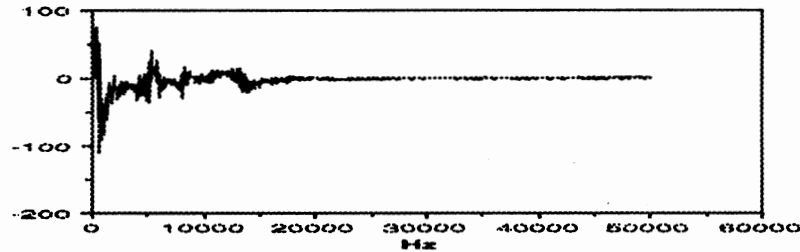
Data from "1 Mhz 5 psi .38" pet"



Data from "1 Mhz 25 psi .38" pet"



Data from "79G2.443"25psi =19 s+ss=10"



Attenuation:

$$\text{Paper dB} / 2.54 \text{ cm (1 in.)} = -4.5 + .000002 * P$$

$$\text{Film dB} / 2.54 \text{ cm (1 in.)} = -8.0 + .000003 * P$$

Mechanical Pulsar

$$P = \rho c V$$

$$t = \frac{2 * l}{c}$$

P = pressure

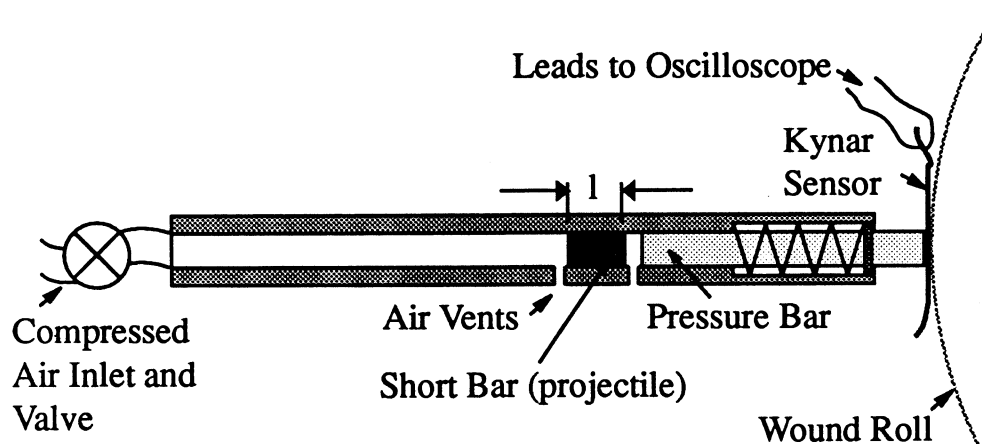
ρ = density

c = speed of sound

V = velocity

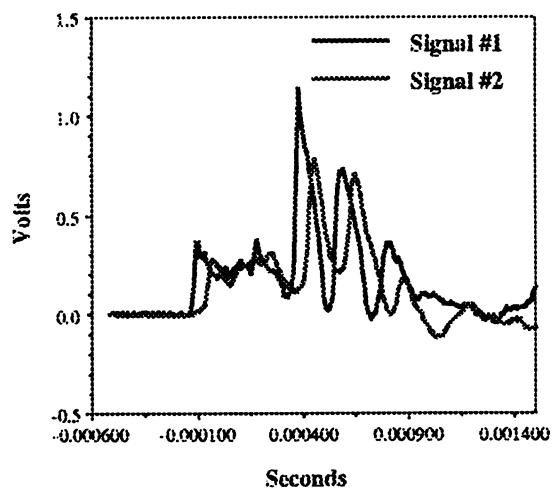
t = time

l = length

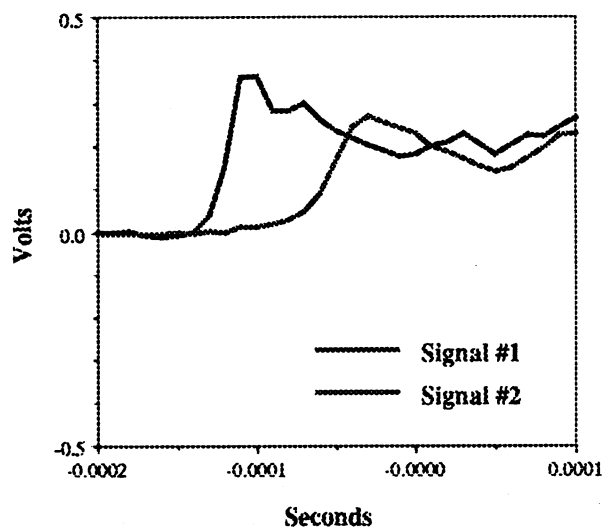


Measured Speed of Sound

Signals from "79 Gage PET 50 PSI"



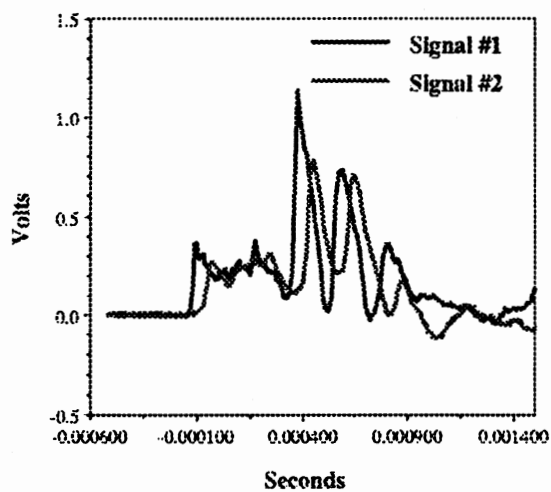
Signals from "79 Gage PET 50 PSI"



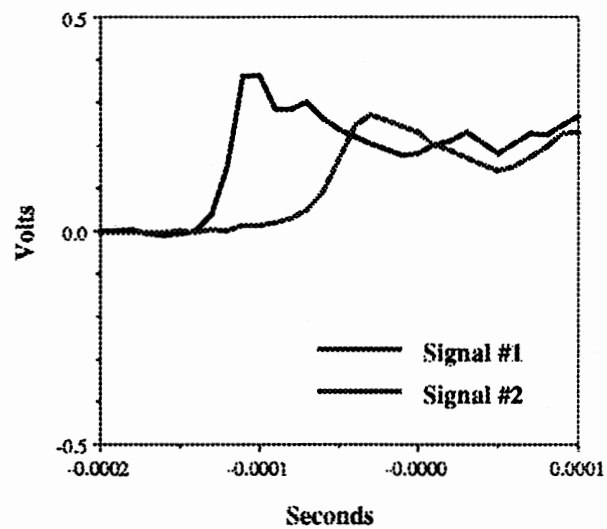
10.0

Measured Speed of Sound

Signals from "79 Gage PET 50 PSI"



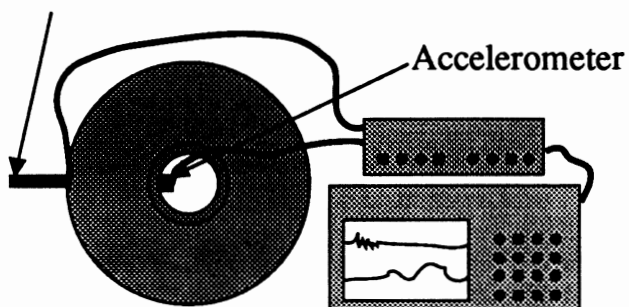
Signals from "79 Gage PET 50 PSI"



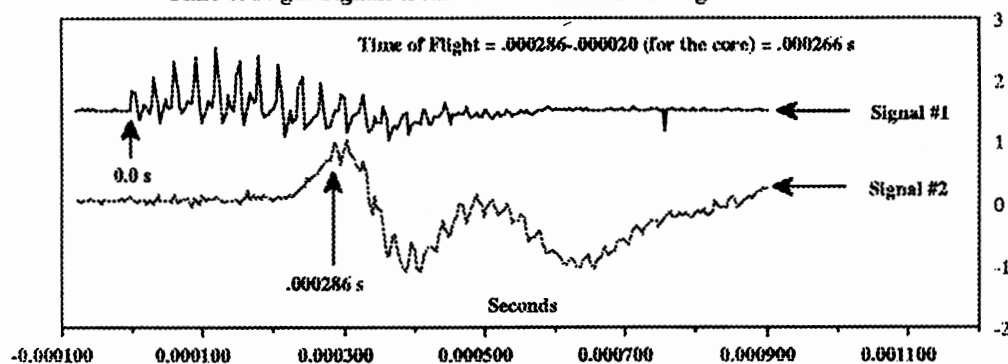
10.0

Wave Reception

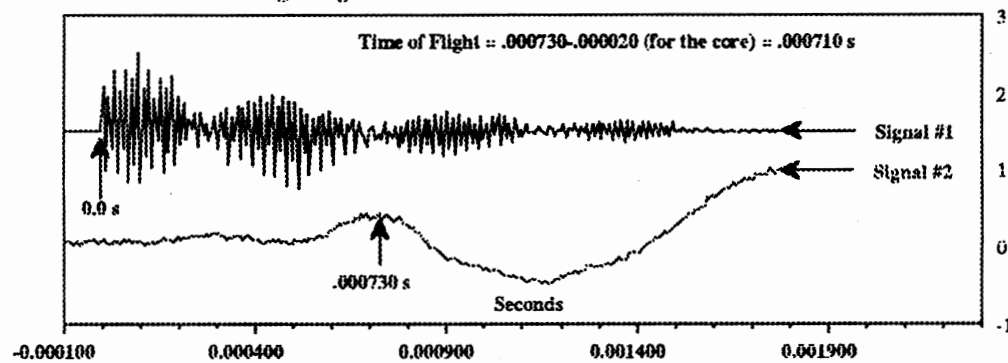
Mechanical Pulser



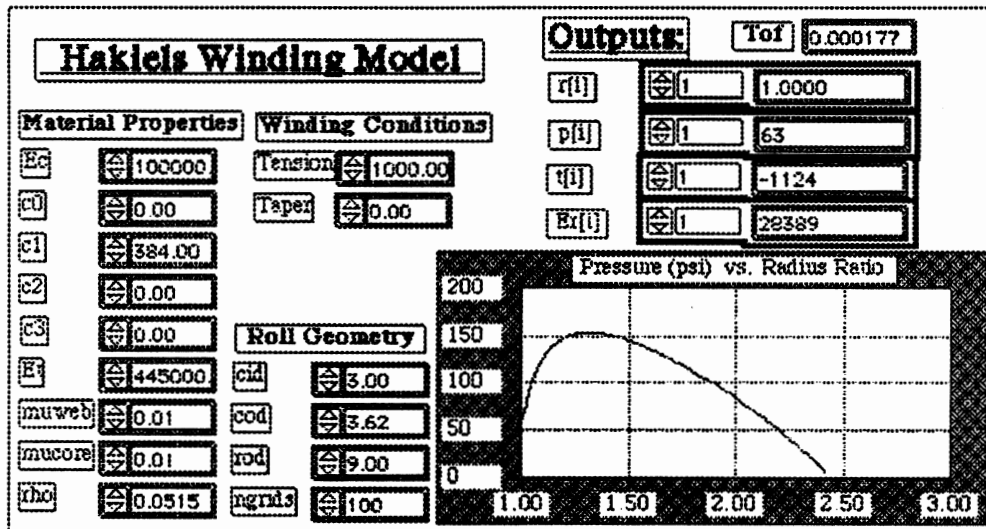
Time of Flight Signals from "Roll #1 RIGHT 92 Gage PET"



Time of Flight Signals from "Roll #6 LEFT BOND PAPER"



Determination of Roll Structure



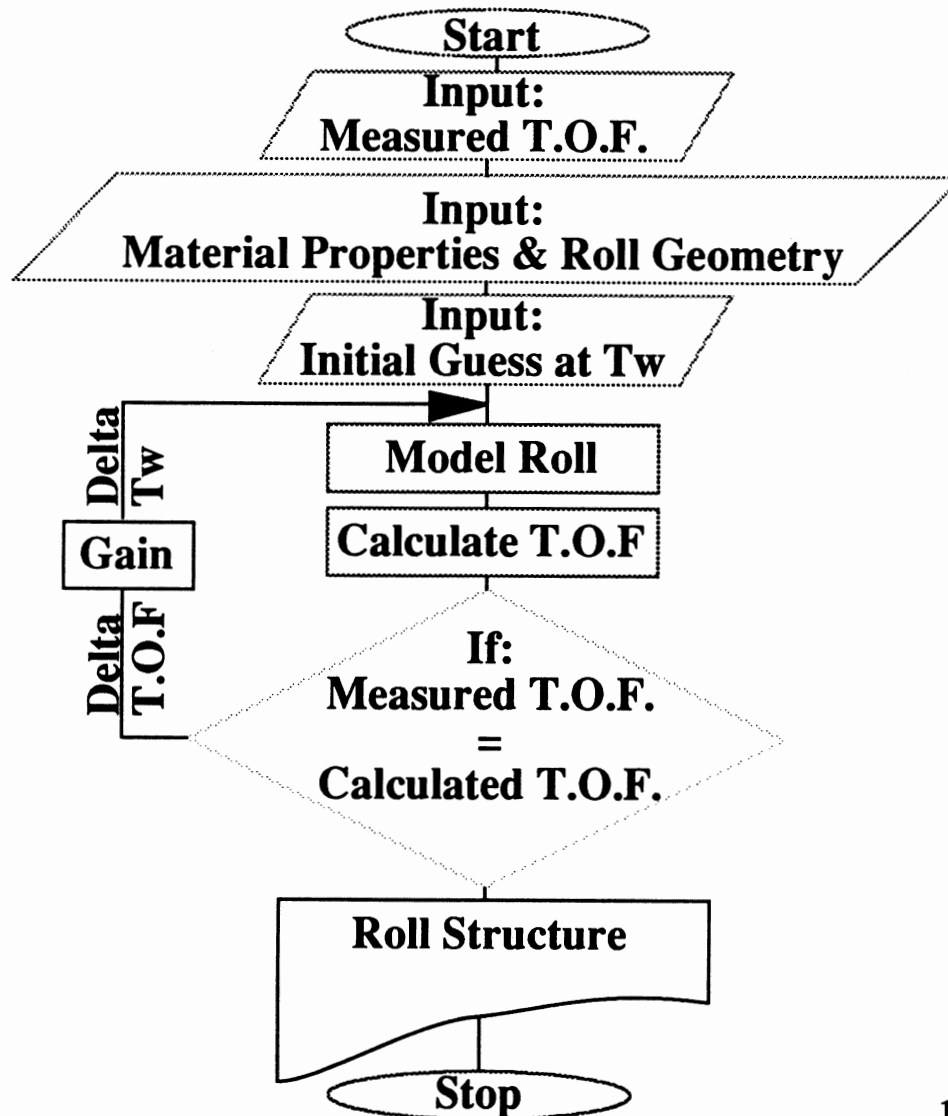
13 Model Inputs => Roll Structure

Equation #14:
Calculated T.O.F = Measured T.O.F

$$\text{T.O.F} = \int_{R_i}^{R_o} \frac{1}{c(r)} dr$$

12.0

Program Schematic




Program

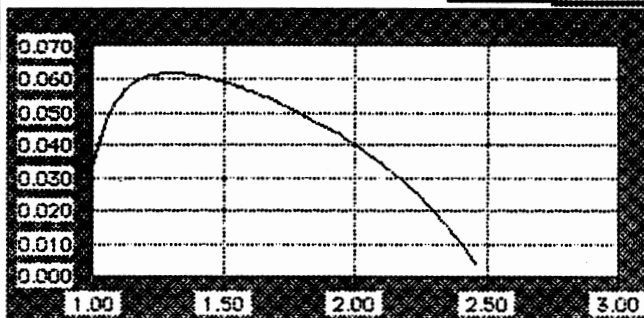
Wave 1		Wave 2		Time of Flight
Expand A -	Expand A -	Expand B -	Expand B -	
Expand B -	Expand B -	Memory C -	Memory C -	
Memory D -	Memory D -	Function E -	Function E -	
Function F -	Function F -	Function F -	Function F -	
Channel 1	Channel 1	Channel 2	Channel 2	
Channel 2	Channel 2			
#1 Filter Order	2			
Sampling Hz	1.0E6			
HP Filter Hfc	1.0E6			
LP Filter Lfc	0			
#2 Filter Order	2			File ? <input type="checkbox"/> YES File Name <input type="text"/> Core TOF <input type="text"/> 0.000020
Sampling Hz	1.0E6			
HP Filter Hfc	1.0E6			
LP Filter Lfc	0			

Time of Flight: 0.000266

Hakiels Winding Model		Outputs		Tof			
Test Roll #1:		I	0	1.0000	t	0	-2.109
Material Properties		P	0	0.144	Er	0	55.347
Winding Conditions		Pressure Ratio vs. Radius Ratio					
Ec	100000	Tension	1000				
c0	0.00	Taper	0.00				
c1	384.00	Roll Geometry					
c2	0.00	cid	3.00				
c3	0.00	cod	5.62				
E	445000	rod	9				
muweb	0.01	ngrid	100				
mucore	0.01	FILE Data ?					
rho	0.0515	<input type="checkbox"/> YES					

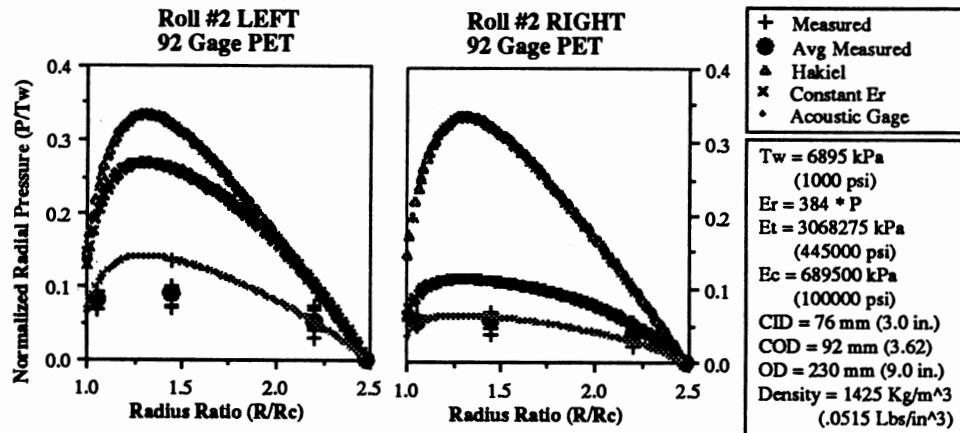
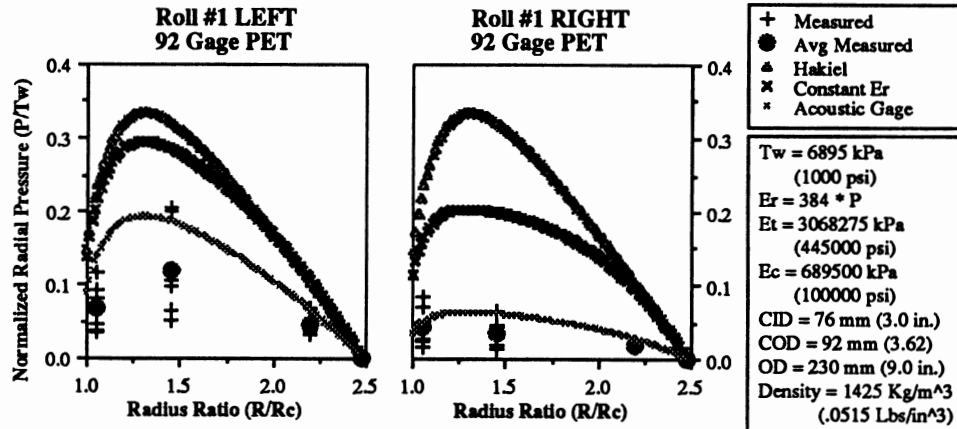
Acoustic Gage

Acoustic Gage		Outputs:	
OUTPUT File:		Measured TOF	0.000266
Roll #1 RIGHT		Calculated TOF	0.000266
		Delta TOF	0.000000
CONSTANT Er	Er Measured from T.O.F	R/Rc	1 1.0000
	13715	P/Tw	1 0.035
ACOUSTIC GAGE	Iteration #	T/Tw	1 -0.385
Initial Tw Est.	1000	Er (psi)	1 13572
Final Tw	335.99		

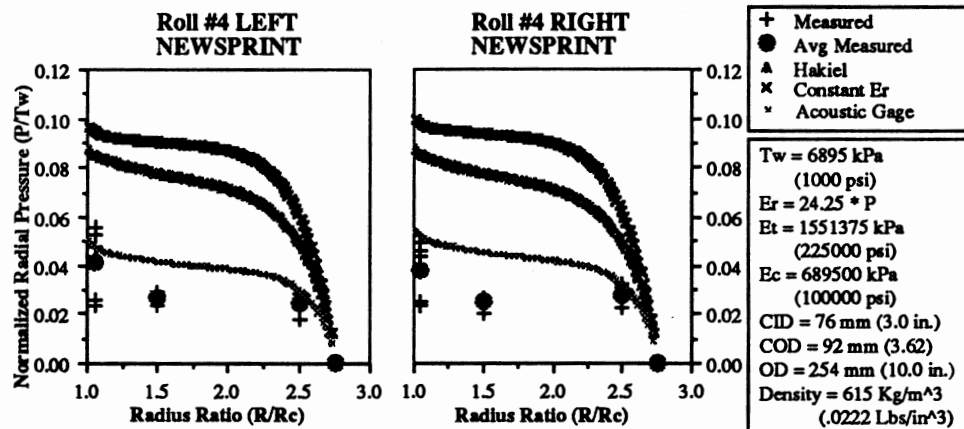
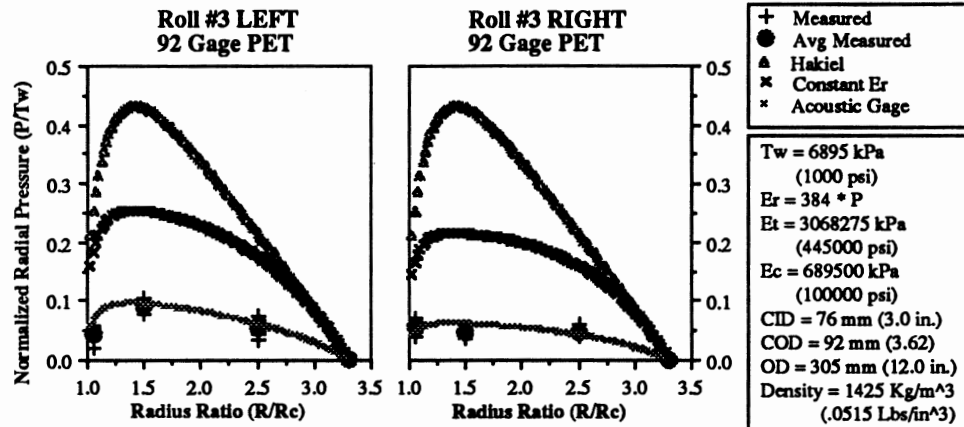


15.0

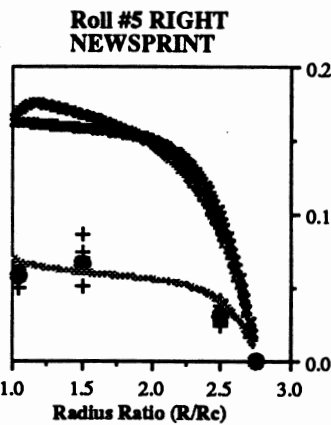
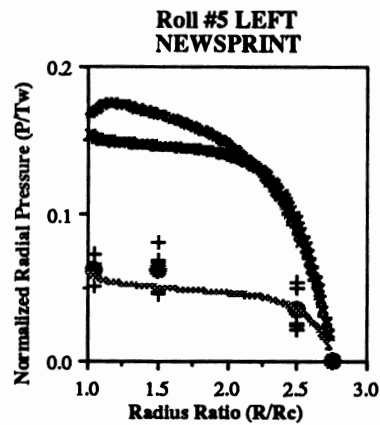
Verification



Verification

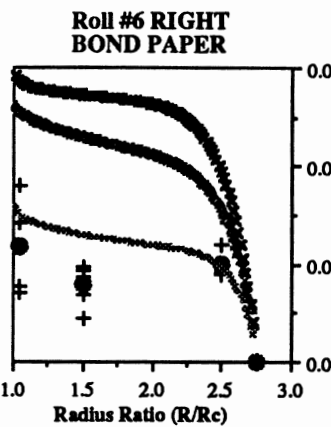
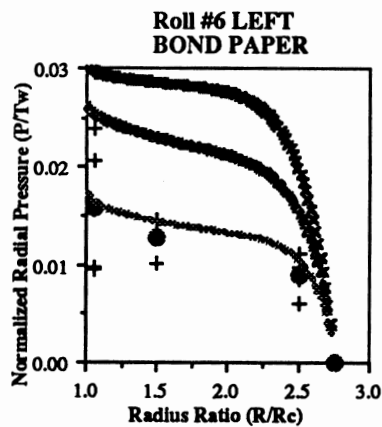


Verification



+ Measured (psi)
 • Avg Measured (psi)
 ▲ Hakiel
 x Constant E_r
 • Acoustic Gage

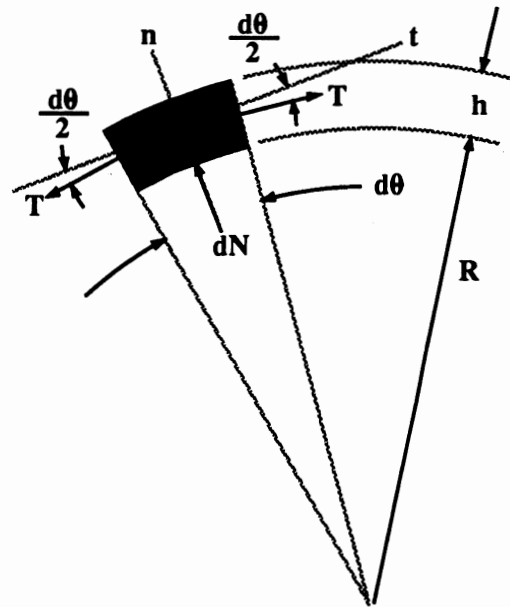
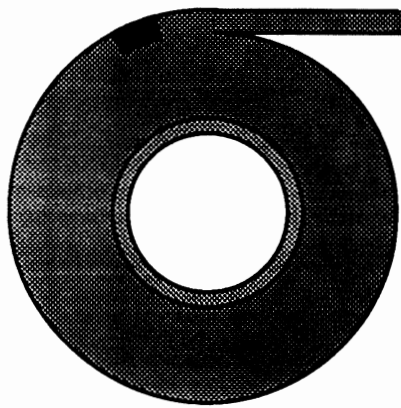
$T_w = 10343 \text{ kPa}$
 (1500 psi)
 $E_r = 24.25 \cdot P$
 $E_t = 155138 \text{ kPa}$
 (225000 psi)
 $E_c = 689500 \text{ kPa}$
 (100000 psi)
 $CID = 76 \text{ mm (3.0 in.)}$
 $COD = 92 \text{ mm (3.62)}$
 $OD = 254 \text{ mm (10.0 in.)}$
 $Density = 615 \text{ Kg/m}^3$
 (.0222 Lbs/in³)



+ Measured
 • Avg Measured
 ▲ Hakiel
 x Constant E_r
 • Acoustic Gage

$T_w = 3448 \text{ kPa}$
 (500 psi)
 $E_r = 47.78 \cdot P$
 $E_t = 1758225 \text{ kPa}$
 (255000 psi)
 $E_c = 689500 \text{ kPa}$
 (100000 psi)
 $CID = 76 \text{ mm (3.0 in.)}$
 $COD = 92 \text{ mm (3.62)}$
 $OD = 254 \text{ mm (10.0 in.)}$
 $Density = 730 \text{ Kg/m}^3$
 (.0264 Lbs/in³)

Hoop Stress Boundary Condition



$$\text{Radial Pressure} = \frac{T_w * h}{R}$$

VITA |

Ronald Paul Swanson

Candidate for the Degree of

Master of Science

Thesis: DETERMINATION OF WOUND ROLL STRUCTURE USING ACOUSTIC TIME OF FLIGHT MEASUREMENTS

Major Field: Mechanical Engineering

Biographical:

Personal Data: Born in Pasco, Washington, April 23, 1960, the son of Harold R. and Lora L. Swanson.

Education: Graduated from Glenwood High School, Glenwood, Iowa, in May 1978; received Associated of Applied Science Degree in Mechanical Technology from Iowa Western Community College at Clarinda, May, 1980; Part time math courses at University of Northern Iowa at Cedar Falls, 1980 and 1981; received Bachelor of Science Degree in Mechanical Engineering from University of Nebraska at Lincoln, May 1985; Part time engineering and math courses at University of Minnesota at Minneapolis between 1985 and 1990; completed requirements for the Master of Science Degree at Oklahoma State University in December 1991.

Work Experience: Senior Development Engineer, 3M Company - Engineering Systems and Technology, St Paul, Minnesota, 1990 to present.

Advanced Development Engineer, 3M Company - Engineering Systems and Technology, St Paul, Minnesota, 1987 to 1990.

Development Engineer, 3M Company - Engineering Systems and Technology, St Paul, Minnesota, 1985 to 1987.

Cooperative Student/ Engineer, 3M Company - Magnetic Audio/Video Division, Hutchinson, Minnesota, 1984.

Tool and Die Designer, Schoitz Engineering, Waterloo, Iowa, 1980-1981.

Apprentice Tool Maker (Part Time), Central States Tool and Die, Omaha, Nebraska, 1979-1980.